AN ABSTRACT OF THE THESIS OF

Zachary J. Southworth for the degree of Master of Science in Industrial Engineering presented on December 9, 2013

Title: Bottom-up Cost Modeling for Vanadium Redox Flow Battery Component Manufacturing

Abstract approved:

Karl R. Haapala

In the U.S. there are increasing energy demands that require an ever-increasing need for the large-scale use of new energy resources. Specifically, sporadic renewable energy sources are being incorporated into utility energy portfolios. Thus, supporting stationary energy storage technologies are needed to make these renewable sources reliable and feasible for grid-scale use. Large-scale redox flow battery systems (RFB), such as the vanadium redox flow battery system (VRB), are being investigated to determine if they are capable of meeting these energy storage needs. The U.S. Department of Energy (DOE) released 2015 performance cost targets for grid-scale energy and power needs. Cost models are able to accurately estimate component manufacturing costs, production system costs, and cost targets. There is a need for a new bottom-up cost modeling methodology to assess RFB components produced by continuous web production methods in order to investigate the feasibility of meeting cost targets, as well as to understand the cost drivers and trends that are directing RFB component costs.

An existing bottom-up process-based method for discrete part manufacturing is modified for the development of this new methodology. Cost models are created for three VRB stack components: the bipolar plate, felt electrode, and proton exchange membrane. Key

information used to create the cost models was obtained from equipment suppliers, experts, and the research literature. This involved researching manufacturing methods and determining details for 25 state-of-the-art production operations for each of these components. Over 50 equipment and raw material suppliers are also investigated to produce this work. Additionally, over 30 budgetary quotes are obtained, along with over 50 equipment and raw material cost values from literature, and 40 supplemental equipment costs posted on company websites. Results from the cost models show U.S. DOE performance cost targets can be met for the components and VRB network investigated. The primary cost drivers are found to be the raw material and utility costs. The most sensitive cost parameters for the bipolar plates, felt electrode, and proton exchange membrane are the raw graphite flake costs, web width, and Nafion® ionomer costs, respectively. Identified cost reduction opportunities include increasing the web widths, selecting alternative raw materials, and increasing the production rate of each manufacturing line. Alternative thermal processing operations and equipment should be investigated, as these accounted for over 30% of capital costs. These results indicate that Nafion® ionomer cost is the primary cost driver for the cell stack components investigated, even when speculative future high volume prices are used. Finally, the cost model results can be used to determine competitive cost strategies for the production of these components.

Bottom-up Cost Modeling for Vanadium Redox Flow Battery Component Manufacturing

by
Zachary J. Southworth

A THESIS

submitted to

Oregon State University

in partial fulfillment of
the requirements for the
degree of

Master of Science

Presented December 9, 2013
Commencement June 2014

Master of Science thesis of Zachary J. Southworth presented on December 9, 2013.

APPROVED:

Major Professor, representing Industrial Engineering

Head of the School of Mechanical, Industrial, and Manufacturing Engineering

Dean of the Graduate School

I understand that my thesis will become part of the permanent collection of Oregon State University libraries. My signature below authorizes release of my thesis to any reader upon request.

Zachary J. Southworth, Author

ACKNOWLEDGEMENTS

I would like to acknowledge the continuous support that I received from my major professor Karl R. Haapala and from Professor Brian K. Paul throughout my research. This work would not have been possible without the support of Dr. Scott A. Whalen at PNNL. Also, I would like to thank Dr. Chinweike Eseonu and Dr. Leslie Burns for also serving as my thesis examination committee members. I wish to thank the Pacific Northwest National Laboratory for funding this research and for the continuous assistance they offered with this research. Additionally, I would like to thank all of my friends, family, and God, for all of their love and support, especially Dr. Sarah Song.

CONTRIBUTION OF AUTHORS

Chapter 3

Karl R. Haapala contributed to the design, writing, and interpretation of cost model data throughout the model development. Brian K. Paul contributed by providing a strategy to collect equipment supplier information, along with guidance on how to create the cost model spreadsheets using previously developed equations and spreadsheets. Scott A. Whalen contributed by providing goals, research direction, and showing an operational VRB.

Chapter 4

Karl R. Haapala contributed with the design, writing, and interpretation of cost model data throughout the model development. Brian K. Paul contributed by providing direction on how to interpret the results. Scott A. Whalen contributed by providing insight from his VRB research.

TABLE OF CONTENTS

TABLE OF CONTENTS (Continued)

Page

TABLE OF CONTENTS (Continued)

Page

TABLE OF CONTENTS (Continued)

Page

TABLE OF CONTENTS (Continued)

Page

LIST OF FIGURES

Figure Page

LIST OF FIGURES (Continued)

Figure Page

LIST OF TABLES

LIST OF APPENDICES

LIST OF APPENDIX FIGURES

Figure Page

LIST OF APPENDIX TABLES

LIST OF ABBREVIATIONS

BOM: Bill of Materials

BPP: Bipolar Plate

DOE: (U.S.) Department of Energy

G1: Generation One

MBI: Microproducts Breakthrough Institute

MEA: Membrane Electrode Assembly

MS-Excel: Microsoft Excel 2010

NEG: Naturally Expanded Graphite

OE: Office of Electricity (U.S. Department of Energy)

OSU: Oregon State University

PEM: Proton Exchange Membrane

PEMFC: Proton Exchange Membrane Fuel Cell

PNNL: Pacific Northwest National Laboratory

RAPS: Remote Area Power Systems

RFB: Redox Flow Battery

VRB: Vanadium Redox Flow Battery

DEDICATION

I would like to dedicate this work to my parents James and Jean Southworth for their endless love and support throughout my education. I do not know how I could have made it without their help.

Chapter 1: Introduction

1.1 Motivation

In the U.S. there are increasing energy demands that require an ever-increasing need for the large-scale use of reliable and sustainable renewable energy resources (US DOE, 2011a; Li et al., 2011; Skyllas-Kazacos et al., 2011; Parasuraman et al., 2013). Increasing energy demands and power quality and reliability needs (Divya and Østergaard, 2009; Turker et al., 2013) are contributing towards the growing market for fuel cells, electrical storage systems (Tokuda et al., 2011), and other types of energy storage systems (Skyllas-Kazacos et al., 2011; BTI, 2012; Curtin et al., 2012). These energy systems can also contribute to the emerging smart grid technologies, as they can be used to improve the reliability and sustainability of the distribution of electrical energy (US DOE, 2011a; Skyllas-Kazacos et al., 2011; Weber et al., 2011). Certain states have utilities increase their renewable portfolio to over 20% under their Renewable Portfolio Standards (RPS), either through mandatory government requirements or internal goals (EIA, 2013a). Some countries are targeting RPS goals of 100% by 2050, and at least one is by 2020 (Farooq et al., 2013). Further research is needed to assist with the development of newer technologies for the U.S.'s electric power grid system (US DOE, 2011a; Nexight Group, 2010). There is a need for GW / GWh (as well as MW / MWh) scale battery systems to meet growing power capacity and energy demands (Viswanathan et al., 2012; Parasuraman et al., 2013; Kear et al., 2011). Energy storage systems for renewable energy need to meet certain power and energy capital cost targets in order to

be cost and technically effective technologies that can assist in the optimization of the U.S. electrical grid (US DOE, 2011a; Houchins et al., 2012).

The U.S. Department of Energy (DOE) Office of Electricity (OE) released capital energy storage (performance) cost targets for 2015 for energy at $150/kWh and for power at $1,250/kW for stationary energy storage capacity (US DOE, 2011a). These targets can be applied to assess the costs of large-scale battery systems (Johnson, 2012), they are approximately 30% below energy storage cost capabilities in 2011; and it is posited that this reduction should make the use of renewable resources more viable (US DOE, 2011a; Houchins et al., 2012). The U.S. government has been supporting these storage technologies by various tax incentives and supportive programs (US DOE, 2011a; US DOE, 2012; Parfomak, 2012). The DOE performance cost targets are not met by current production methods, and when considering predictions of component raw material pricing (US DOE, 2011a; Houchins et al., 2012). Capital cost targets have been released in order to drive renewable energy resources, stationary electrochemical battery storage systems, and fuel cell technologies forward (US DOE, 2011a; Houchins et al., 2012).

An increase in renewable resources will likely have positive social, economic, and political impacts both in the USA and worldwide (Kear et al., 2011). The increased use of renewable resources will potentially lower the cost of living worldwide, reduce the reliance on other countries for energy resources, reduce pollution, and promote future energy research and development efforts worldwide (US DOE, 2011a; Kear et al., 2011). There is also a national benefit from the use of renewable energy systems as critical power sources in disasters (BTI, 2013). Two of the major challenges with using

renewable resources are that they sporadically supply energy (Parasuraman et al., 2013; (Turker et al., 2013; Weber et al., 2011) and that current mass production technology incorporation in manufacturing settings are still in the early stages of production and commercialization (Kear et al., 2011; Mohamed, 2012; Harris et al., 2010). Large-scale energy storage systems are needed to increase the reliability of utility grids that use renewable energy (Parasuraman et al., 2013; Turker et al., 2013; Weber et al., 2011).

One promising type of fuel cell that can rise to the challenge of meeting these energy needs is the proton (ion) exchange membrane fuel cell (PEMFC) (Peighambardoust et al., 2010; Hamrock and Yandrasits, 2006). A PEMFC is a type of fuel cell that transfers energy using proton exchange membranes (PEMs); hydrogen fuel cells are well known types of PEMFC (US DOE, 2012; BTI, 2012). PEMs are sometimes referred to as polymer electrolyte membranes in literature (Li and Sabir, 2005), or as ion exchange membranes (Weber et al., 2011). Electrochemical regenerative PEMFCs are devices that do not use fuel, but rather use electrolyte solutions to transfer electrical energy from either two charged electrolyte solutions, or a charged liquid electrolyte and gaseous species (Yufit et al., 2013; Brandon et al., 2012; Skyllas-Kazacos et al., 2011). Flow batteries are a storage system where energy is transferred between electrolyte liquids (that are typically flowing from tanks), the flow battery is a more common name for the regenerative PEMFCs (Li et al., 2011; Eckroad, 2007; Brandon et al., 2012; Skyllas-Kazacos et al., 2011; Weber et al., 2011). Redox flow batteries (RFBs) are a specific type of flow battery that transfers energy using reduction and oxidation reactions (Skyllas-Kazacos et al., 2011; Parasuraman et al., 2013; Weber et al., 2011). Vanadium

redox flow batteries (VRBs) are a specific type of RFB that use vanadium electrolytes, and these VRBs are examined in depth in this research. VRBs store and transfer energy using different ion oxidation states of vanadium in a sulfuric acid electrolyte mixture (Skyllas-Kazacos et al., 2011; Parasuraman et al., 2013; ; Zhang et al., 2012; Yamamura et al., 2011). The all-vanadium redox flow battery (a redox battery that uses only one type of electrolyte in the stack), or generation one (G1) VRB (Viswanathan et al., 2012), was created at the University of New South Wales in 1984 (Skyllas-Kazacos et al., 2011). VRBs are now used in a number of MW-scale facilities (Weber et al., 2011). Throughout this research, the term VRB refers to any type of VRB, while G1 VRBs refers specifically to the all-vanadium redox flow battery.

In this research, a new process-based bottom-up cost model method is used to develop unit cost models for three of the major VRB components. VRBs are an effective and promising technologies because they are modular and can be scaled-up into larger systems (Mohamed, 2012; Blanc and Rufer, 2010; You et al., 2009; Eckroad, 2007). The VRB is being investigated because it is an effective technology that has already been incorporated in a large number of facilities around the world (Li et al., 2011; Skyllas-Kazacos et al., 2011; Parasuraman et al., 2013; Kear et al., 2011; You et al., 2009; Prudent, 2012; IPHE, 2010). New cost models for the VRB are needed as most of the components used in VRB stacks are produced with older technologies and manufacturing methods, or scaled-up laboratory systems (Kear et al., 2011; Zhang et al., 2012; Mohamed, 2012; Harris et al., 2010). In this research, a group of VRB systems are called

a VRB network, a group of stacks are called a system, a group of cells are called a stack, and a cell is composed of two half cells.

Recent cost modeling efforts (in literature available to the public, much of the information used by companies producing these storage systems is proprietary for VRB systems largely focus on finding overall costs from high level cost and performance models) typically are not looking at individual cost drivers for each component, they are instead looking for overall performance costs and what component unit costs are (Kear et al., 2011; Viswanathan et al., 2012; Parasuraman et al., 2013; Eckroad, 2007). The bottom-up cost model method focuses on finding the costs associated with the current technological states of each manufacturing process step, separate from profit and indirect overhead, using capital equipment information as its foundation (Carlson et al., 2005; McFarland et al., 2004; Böhringer and Rutherford, 2008). The cost models are developed to account for all of the individual costs associated with each manufacturing operation, including bulk raw material purchases, capital costs, and labor costs (Carlson et al., 2005; McFarland et al., 2004). For energy technologies, top-down cost models have been constructed from available component prices, rather than costs, that reflect purchases of one or more component types in large volumes from component suppliers, or reflect costs from an even higher level economy-wide or marketing point of view (McFarland et al., 2004; Böhringer and Rutherford, 2008).

Current VRBs are produced in relatively low quantities, research is needed to both identify the cost drivers for VRB components and to identify their costs. The primary objective of this research is to develop a bottom-up cost modeling methodology for RFBs

and apply it to create and analyze models for the primary stack components in a VRB, i.e., the bipolar plate, felt electrode, and proton exchange membrane. These models are to be used to estimate process-based unit costs for RFBs. As a result of this research, the feasibility of VRB component manufacturing, the primary cost drivers for manufacturing the selected components, and manufacturing cost reduction opportunities will be better understood.

The cost models developed in this research will contribute towards the determination of the viability of the VRB system components using various manufacturing technologies.

1.2 Energy Storage Technology Application

There is an increasing need for technology to facilitate the use of renewable energy resources. The major types of renewable resources include solar, biomass, wind, water, etc. (Li et al., 2011; Weber et al., 2011; Zhang et al., 2012; EIA, 2013a). New energy storage methods are needed to make renewable energy more economically feasible for governmental, industrial, and private entities (Houchins et al., 2012). These energy storage methods are needed to increase the reliability of renewable energy sources (Weber et al., 2011; Kear et al., 2011). It is often preferable to store energy and control its release into a power grid if the energy is received intermittently, as is this case with many sources of renewable energy (Li et al., 2011; Weber et al., 2011; Li et al., 2012). Specifically, electrical grids could face problems with a 20% portfolio or higher of renewable energy resources (Weber et al., 2011). These problems exist because the demand of energy does not always meet the supply of renewable energy, which creates both supply and profitability issues for utility grid companies. VRBs and other energy

storage systems can manage grid systems by load leveling and other methods to resolve this problem. Load leveling is one electrical grid method that stores and distributes energy as needed (Tokuda et al., 2011; Kear et al., 2011; Shimada and Mukai, 2007). Shorter term frequency control on utility grid systems can also be done using VRBs, VRBs are also used for a variety of other applications on energy storage grids (Weber et al., 2011).

1.3 Redox Flow Battery Technology Application

Recently, proton exchange membrane fuel cells (PEMFCs) and other proton exchange membrane (PEM) applications have been heavily used in various industries as electrical energy storage (EES) systems (Li et al., 2011). PEMFCs work by transferring energy from fuel (a common fuel is hydrogen (BTI, 2012; US DOE, 2012) into various media through chemical reactions by utilizing a membrane that restricts fluid transfer, while still transferring protons between charged and uncharged electrolytes (Blanc and Rufer, 2010; Eckroad, 2007). Redox flow batteries use PEMs to transfer protons between electrolytic compounds through reduction and oxidation chemical reactions (Skyllas-Kazacos et al., 2011; Parasuraman et al., 2013; Weber et al., 2011). RFBs are less-commonly known as regenerative fuel cells (Brandon et al., 2012; Skyllas-Kazacos et al., 2011; Li et al., 2011), electrochemical energy storage systems (Li et al., 2011; Parasuraman et al., 2013), polymer electrolyte membrane fuel cells (Li and Sabir, 2005), and as a type of PEMFC (EG&G, 2005). RFBs are increasingly used in a variety of technologies because the power and energy delivery of an RFB can be physically separated, where power capacity is determined by the amount and design of cell stacks in a battery, while the energy

capacity is determined by the concentration and amount of electrolyte (Weber et al., 2011; Viswanathan et al., 2012).

1.4 Vanadium Redox Flow Battery Technology Application

The VRB is a promising EES system, as it does not exhibit cross contamination between the electrolytes on each half cell and associated problems (including corrosion), because each half cell only has a vanadium-based electrolyte (Viswanathan et al., 2012; Skyllas-Kazacos et al., 2011; Parasuraman et al., 2013; Liu et al., 2012). The energy storage capacity of the VRB is determined by the overall amount of vanadium used in the electrolyte (Viswanathan et al., 2012; Yamamura et al., 2011). The power is determined by the overall electrode reactive area in the VRB system (Viswanathan et al., 2012; Skyllas-Kazacos et al., 2011). The vanadium redox flow batteries can be produced with a variety of components, but often they use similar components, i.e., felt electrodes, bipolar plates, flow channels, proton exchange membranes, pump systems, PVC frames, tank systems, and electrolytes (Blanc and Rufer, 2010; Eckroad, 2007).

1.5 Cost Modeling in this Research

The bottom-up cost model method in this research focuses on finding the process-based costs associated with the current technological states of each processing step using capital equipment information as its foundation. This methodology is modified from prior work by Microproduct Breakthrough Institute (MBI) researchers at Oregon State University (OSU) and the Pacific Northwest National Laboratory (PNNL) (Lajevardi et al., 2011; Paul, 2013; Lieth et al., 2010).

The resulting unit cost information provided by this method does not include profits, indirect overhead costs, and tax/regulatory costs (Carlson et al., 2005; McFarland et al., 2004; Böhringer and Rutherford, 2008). These bottom-up cost models are able to show the cost drivers for various components, as well as showing what areas should be investigated for potential cost reductions. The models are also set up so that someone familiar with the modeling technique can add or modify processes, input parameters, and equations. Design and process inputs can be altered for comparison purposes, such as evaluating labor rates, annual production volume, raw materials, line speed capability, and capital equipment parameters (see Figure 3). Raw material costs are representative of prices from material suppliers, which includes profit in addition to cost of goods sold (COGS) for the materials.

Throughout this research the raw materials are referred to as both costs (considered a cost category) and prices (raw material price is included). Each of the cost models are composed of seven cost categories: tool depreciation, facility, labor, maintenance, raw materials, consumables, and utilities. A value is needed for each of these categories for each manufacturing operation. In order to find values for these cost categories and other cost model inputs, a method of collecting data and reviewing the energy storage system is developed. Also, manufacturing process steps are selected for each component. In order to find the data to develop the cost models, several steps are taken. A literature review is first conducted, primarily using journal articles and patents. Next, discussions with equipment suppliers are undertaken, followed by obtaining budgetary quotes from these machine equipment suppliers. Finally, company literature and other publications are

used to complete the cost models. Uncertainties and fluctuations in raw material pricing posed challenges for the information gathering portion of cost model development. Long dwell times are needed for various heating operations for each cost model. These posed a challenge with the state of the art line speed capabilities that are being targeted, as very long dryers and ovens are needed. Furthermore, there are challenges in selecting certain manufacturing process steps and with determining what equipment is needed for each step, as some of these components use fairly new technology. Finally, specific component designs are selected for the research in order to limit the scope of model development work. These components were selected in consultation with researchers at the Pacific Northwest National Laboratory (PNNL), and specific assumptions about the components are defined in this work.

1.5.1 Component Selection

The specific components selected to be investigated are as follows: Naturally expanded graphite (NEG) resin impregnated bipolar plates (BPP) that are modeled from SGL's TF6 specifications (SGL Group, 2012), felt electrodes that are modeled from SGL's GFD4.6 polymer precursor impregnated nonwoven porous graphite felt electrode specifications (SGL Group, 2012), and Nafion® perfluorosulfonic acid (PFSA) proton exchange membranes at 1100 equivalent weight (EW) (grams of dry Nafion® per mole of sulfonic acid group (Mauritz and Moore, 2004)) and 5 mil thickness that are modeled from DuPont's Nafion®115 specifications (DuPont, 2009). These specific components are selected because they are the proven and most costly components of the cell stacks in VRB Systems and other flow battery systems (Houchins et al., 2012; Weber et al., 2011;

SGL Group, 2012; DuPont, 2009; Brett, 2005). The size and amount of cells in a stack (stacks combine to form a system) determines the power rating of a VRB (Blanc and Rufer, 2010).

The graphite bipolar plate is selected because it has traditionally been the high cost component in fuel cells, and because bipolar plates are used in a wide variety of PEMFCs (Brett, 2005; Yuan et al., 2005). The graphite felt electrode is selected because it is a major component with regard to the size and function in current VRB systems. The Nafion® PFSA PEM (typically the N115 and N117 (Weber et al., 2011)) type of membranes is selected because it typically accounts for the majority of the cost of a typical RFB cell (Skyllas-Kazacos et al., 2011; SGL Group, 2012; Chen et al., 2013). For each of these components, a bottom-up cost model is developed in an MS-Excel file with the following worksheets: version history, design inputs, process inputs, calculations, results, and references and assumptions. The manufacturing cost models are designed to be incorporated with future performance models with the major assumption that each of the components will move immediately to an assembly step (Greene et al., 2011).

1.6 Research Tasks

Several research tasks are undertaken to achieve the objective of this research. The first task is to create a cost modeling methodology that can be applied to the selected G1 VRB cell components. Three cell stack components of the VRB currently being investigated by PNNL are selected, i.e., bipolar plates, felt electrodes, and proton exchange membranes. Subtasks include selecting state-of-the-art manufacturing methods and gathering equipment information from equipment suppliers.

The second task is to determine the primary cost drivers for the three VRB stack components modeled. Subtasks include identifying capital costs, cost trends, and determining cost reduction strategies. Finally, based on this work, cost reduction opportunities are identified, as well as opportunities for future cost model development.

1.7 Thesis Outline

Chapter 1 provides the motivation and overview for this research, along with the research tasks. Chapter 2 reviews literature on proton exchange membrane fuel cells, redox flow batteries, vanadium redox flow batteries, and current cost models for these types of systems. Chapter 3 is a journal article titled "Chapter 3: A Bottom-up Cost Modeling Method for Vanadium Redox Flow Battery Component Manufacturing." This article develops a cost modeling methodology for RFB components, and the bipolar plate is modeled to demonstrate the method. Chapter 4 is a journal article titled "Chapter 4: Cost Analysis of Gigawatt-Scale Vanadium Redox Flow Battery Component Manufacturing Using Bottom-up Cost Models." This article applies the methodology developed in Chapter 3 to create cost models for the felt electrode and proton exchange membrane. The results of the models created in Chapter 3 and Chapter 4 are analyzed and discussed. Chapter 5 provides the conclusions of this research and proposes several opportunities for future work.

Chapter 2: Literature Review

A literature review is written to present the state of knowledge and application of VRBs, explain gaps in its understanding, and to justify the need for further research. First, the general need for energy storage technologies is presented. This includes fuel cells, proton exchange membrane fuel cells (PEMFCs), flow cells, redox flow batteries (RFBs), and vanadium redox flow batteries (VRBs): VRBs are a type of RFB, RFBs are a type of flow cell, PEMFCs are a type of fuel cell, and fuel cells are a type of energy storage device. Next, the state of knowledge, benefits, and challenges of RFBs and VRBs is presented. Limitations of the current state of research are explained, followed by an explanation of the state of key VRB components that are investigated in this research.

2.1 Technology and Policy for Sustainable Energy

There is an increasing need for the use of renewable energy resources worldwide, as well as in the United States (Li et al., 2011; Kear et al., 2011). Technologies are in development to assist with the integration of renewable energy sources in a variety of applications, ranging from large-scale (GW power capacity and GWh energy capacity (Viswanathan et al., 2012)) utility grids to small-scale vehicle transportation (Parasuraman et al., 2013; Weber et al., 2011). The U.S. DOE has a strategic plan that is funding the research, demonstration, and commercialization of energy storage technologies for applications in both automotive and non-automotive industries, including regenerative PEMFCs for grid-scale energy storage (US DOE, 2011a; Greene et al., 2011; US DOE, 2011b). The Office of Electricity and Energy Reliability (OE)

within the U.S. Department of Energy (DOE) is planning to fund $200 million between 2011 and 2015 (US DOE, 2011a). The U.S. Congress allocated another $136 million in 2012 for the development of hydrogen and fuel cell technologies (US DOE, 2012). Intensive research and development efforts surrounding fuel cells and their related technologies have been recently undertaken, resulting in patents and commercial products (Hamrock and Yandrasits, 2006; US DOE, 2012; Wee, 2007). These development efforts have included proton exchange membranes (PEMs), which are integral to VRBs (and other RFBs).

PEMs have selective ion transport properties that have been enabling their application in commercial fuel cell technologies, particularly DuPont Nafion® PEMs (Peighambardoust et al., 2010; Wu et al., 2013). PEMFCs were first used in the U.S. by NASA (developed by General Electric) in the 1960s for the Gemini Space Flights (Litster and McLean, 2004; Scott, 2009; Paola Costamagna, 2001). A high level of commercial and research activities are currently underway regarding the use of proton exchange membrane fuel cells (PEMFCs) as energy sources for small scale transportation and energy storage solutions (US DOE, 2011a; Houchins et al., 2012; Wee, 2007). The U.S. DOE is actively funding and promoting research for PEMFCs, in the 500,000 fuel cell volume range (annual fuel cell production volume for automobiles) (Houchins et al., 2012; Carlson et al., 2005; US DOE, 2011b). There is a need for energy storage systems that have adequate energy capabilities, power capabilities, durability and efficiencies for use in utility grid systems (Weber et al., 2011). The redox flow battery (RFB) is a potential solution for the needs of these large scale operations (Li et al., 2011). Flow battery

technology was first patented in Germany in 1954 (Kangro, 1954; Shigematsu, 2011). Vanadium redox flow batteries (VRBs) have been identified as the most promising energy storage technology by the Electric Power Research Institute (EPRI) (Eckroad, 2007) and other literature sources (Blanc and Rufer, 2010). VRBs are a specific type of flow batteries that use vanadium electrolyte mixtures. A number of large-scale VRB facilities have already been developed and are under development in Japan, Australia, Thailand, and the U.S. (Eckroad, 2007).

2.2 Redox Flow Battery Technology

RFBs are electrochemical systems that function by transferring energy between charged and uncharged electrolytes through reduction and oxidation reactions (Weber et al., 2011). Grid-scale applications typically use large volume tanks to store the electrolytes (Parasuraman et al., 2013; Weber et al., 2011; Kear et al., 2011). These RFBs are typically composed of a felt electrode, proton exchange membrane (PEM), bipolar plate, frame, electrolytes, tanks, pumps, power system, and other components (Tokuda et al., 2011; (Weber et al., 2011). In RFBs a series of stacks is called a system, while a group of cells is called a stack (Blanc and Rufer, 2010). A PEM is a primary component in RFB systems (Eckroad, 2007; Parfomak, 2012). PEMs serve as the cation exchange components in these batteries (see Figure 2.1), and are where the protons are transferred between the cells (Kear et al., 2011; Carlson et al., 2005). VRBs are a specific type of flow battery. Generation one (G1) VRBs use only one electrolyte mixture, while other RFBs (bromine/polysulfide, zinc/bromine, zinc/cerium, iron/chromium (Skyllas-Kazacos et al., 2011; Weber et al., 2011; Eckroad, 2007)) typically use two electrolyte mixtures.

For G1 VRBs, the electrolyte liquid is comprised of vanadium dissolved within sulfuric acid and other compounds (Parasuraman et al., 2013; Eckroad, 2007; Ma et al., 2012). Flow battery (a type of PEMFC) research has been conducted since the 1970s by NASA, while VRB-related research was initiated at the University of New South Wales in 1984 (Viswanathan et al., 2012; Weber et al., 2011; Kear et al., 2011; Blanc and Rufer, 2010; Eckroad, 2007).

2.2.1 Energy System Challenges and Benefits

The benefits of incorporating new energy storage methods into the U.S. power grid have been recognized by companies and governmental agencies, who are now promoting the technological development and implementation of these storage methods. The U.S. DOE created the Hydrogen and Fuel Cells Program to increase the use of hydrogen and fuel cells throughout the U.S., for which $136 million dollars was allocated for 2012 (US DOE, 2012). Specific applications expected to benefit from reduced energy storage costs include residential, commercial, and industrial backup power systems (US DOE, 2011a; Tokuda et al., 2011; Tang et al., 2011), solar powered homes, hydrogen fuel cells for automobiles, wind energy conversion, and remote area power systems (RAPs) (Skyllas-Kazacos et al., 2011; Weber et al., 2011; Kear et al., 2011). Additionally, electrical energy storage (EES) technologies can be used as portable power systems and secondary power systems, and to increase the practicality of the industrial use of sustainable resources (US DOE, 2011b). RFBs are one type of EES technology being researched as a utility grid-scale solution to these challenges (Weber et al., 2011).

2.2.2 General Redox Flow Battery Challenges and Benefits

RFBs have unique benefits, especially when compared to traditional battery storage technologies. RFBs have several major advantages over other EESs: power and energy storage capacities are independent of each other (allowing for more flexible system design (Eckroad, 2007; Ma et al., 2012)), they have lengthy lifetimes, and they have relatively high performance parameters (Viswanathan et al., 2012; Li et al., 2011; Parasuraman et al., 2013; Eckroad, 2007; Blanc and Rufer, 2010; Li et al., 2012).

Typical challenges with RFBs are associated with the large amount of electrolyte transfer occurring between the tanks and stacks, the degradation of the components, side reactions, cross contamination, and the periodic need to remix the electrolyte (Kear et al., 2011; Eckroad, 2007; Tang et al., 2011; Ma et al., 2012). Poisonous and explosive gasses can sometimes be produced by RFBs (Blanc and Rufer, 2010; Eckroad, 2007). In addition, Nafion® PEMs are costly, but typically used due to their commercial availability and stability (at 10 to 40 ℃) (Houchins et al., 2012; Parasuraman et al., 2013; Weber et al., 2011; Eckroad, 2007). The use of Nafion® is also prevalent in PEMs for VRBs due to its conductive properties (Weber et al., 2011). The Nafion® raw material typically accounts for most of the cost in an RFB cell (Skyllas-Kazacos et al., 2011; Chen et al., 2013). Despite the widespread use of Nafion® membranes, it is theorized that alternatives to the current membranes would be beneficial to VRBs (Parasuraman et al., 2013). PEM cost is driven by the manufacturing process and the raw material pricing at low volumes; the Nafion® ionomer is priced at about $1000/kg (Eckroad, 2007; James and Spisak, 2012). Research is being conducted into various new high temperature

PEMs that do not rely on Nafion®, but it remains the primary commercially available PEM (Houchins et al., 2012; Harris et al., 2010; DuPont, 2009). Although there are significant challenges with the incorporation of RFBs into utility grids and commercial applications, VRBs are able to overcome some of the major problems that exist with RFBs.

2.2.3 Vanadium Redox Flow Battery Challenges and Benefits

The VRB has similar challenges and benefits as most of the other major RFBs (Zhao et al., 2006). The VRB battery, however, has the significant benefit of not suffering from electrolyte cross contamination, and it can operate at up to 90% efficiency (the efficiency is typically in the 80-90% range (Skyllas-Kazacos et al., 2011; Kear et al., 2011)). Additional benefits of VRBs over RFBs include electrolyte recyclability, and lower component corrosion (Kear et al., 2011; Tang et al., 2011; Ma et al., 2012). A major benefit of using VRBs, aside from the potential cost benefits, is the comparatively (to more toxic batteries, such as lead-acid batteries) small environmental impact (although there are toxic elements in the VRB) (Kear et al., 2011). Additionally, the VRB electrolytes in each half cell do not cause contamination, e.g., due to electrolyte leakage through the PEM, when the VRB is in the uncharged state (Eckroad, 2007). The VRB is also promising because it has already been used for high storage power capacity (kW to MW scale) in multiple facilities, including Sumitomo Densetsu (3 MW, 800 kWh VRB in Osaka, Japan) (Skyllas-Kazacos et al., 2011; Doughty et al., 2010), VRB Power Systems Inc. (10 MWh VRB in Canada) (Kear et al., 2011), Pacificorp Castle Valley (250 kW, 2 MWh VRB in Utah) (Kear et al., 2011; Doughty et al., 2010), Prudent Energy

VRB Systems (600 kW, 3.6 MWh Oxnard, California) (Prudent, 2012), the Chinese National Grid (Zhangbei, Hebei, China) (Skyllas-Kazacos et al., 2011), Painesville Municipal Power Station (1 MW, 8 MWh VRB in Ohio) (Skyllas-Kazacos et al., 2011), Pinnacle VRB (250 kW, 1 MWh VRB in Australia) (Skyllas-Kazacos et al., 2011). Due to industrial and academic research efforts to produce large scale-vanadium redox flow batteries, there is potential that recent technological advances can allow U.S. DOE energy storage cost targets to be met.

A major challenge with the use of Nafion® perfluorosulfonic acid (PFSA) PEMs is the limited operating temperature of the current technology (typically 10-40 ℃ for a 2 molar vanadium electrolyte solution) (Skyllas-Kazacos et al., 2011; Parasuraman et al., 2013; Eckroad, 2007). Additional challenges are the high Nafion® membrane (Skyllas-Kazacos et al., 2011; Chen et al., 2013) and the cost prohibitive vanadium in the electrolyte (Kear et al., 2011). VRBs suffer from their reliance on vanadium (Eckroad, 2007), however, which is a scarce natural resource (Perles, 2012). Vanadium is primarily mined in South Africa, Russia, and China (half of all vanadium is produced in China), and it has traditionally been used by the steel industry (Eckroad, 2007; Perles, 2012). Current research is developing high temperature PEMs with improved efficiencies, with an operational target of 120 ℃ or higher proposed by the U.S. DOE (Houchins et al., 2012; Harris, 2006).

2.3 VRB Components and Functions

A high level view of the operation of a single VRB cell can be simplified for illustration purposes, as seen in Figure 2.1. A VRB cell is composed of two half-cells, with each

side having the electrolyte at a different charged state (other RFBs use different electrolyte compounds in each half cell) (Blanc and Rufer, 2010; Eckroad, 2007). Groups of cells make stacks, groups of stacks make systems, and a group of systems is called a network (in this work, a VRB network is typically referring to the entire VRB power and energy capacity throughout the U.S.). The basic components of a cell are a proton exchange membrane, an electrode (felt) on each side of the membrane, a bipolar plate on the outside of each electrode, and flow channels (in a frame around the bipolar plates, or in the bipolar plates) are on each end of the cells (Blanc and Rufer, 2010; Liu et al., 2012). The VRB typically uses bipolar plates with felt electrodes for the anode and cathode, with a PEM separating the two half cells (Parasuraman et al., 2013; Eckroad, 2007).

Electrochemical reactions occur as the charged or discharged electrolytes are pumped through each cell, which then stores or releases energy (Blanc and Rufer, 2010). Electrochemical reactions change the vanadium electrolytes to one of four charged states. The VRB system operates by storing energy with four valence states, with the charged (V^{5+} oxidation state) vanadium electrolytes in large tank reservoirs (Blanc and Rufer, 2010; You et al., 2009). The different oxidation states of the vanadium electrolyte compound are described in a simplified manner as V^{2+} (purple), V^{3+}(green), V^{4+} (blue) and V^{5+} (charged state, yellow) (Yamamura et al., 2011; Blanc and Rufer, 2010; You et al., 2009; Eckroad, 2007), as seen below in Figure 2.1. In the VRB Charging Schematic Diagram, 4 cells, or 8 half cells, are illustrated. The bulleted items represent components as follows, 1: Tank, 2: Pump, 3: Pipe, 4: Frame, 5: Bipolar Plate, 6: Current Conductor,

7: End Frame (an arrow shows where a tab on the copper current conductor is wired to a load / source), 8: Felt Electrode (where the reactions takes place), and 9: Proton Exchange Membrane (which transfers protons between half cells). Figure 2.1 shows a possible piping solution for the VRB, channel design on the flow frames can reduce the amount of piping to get a similar result.

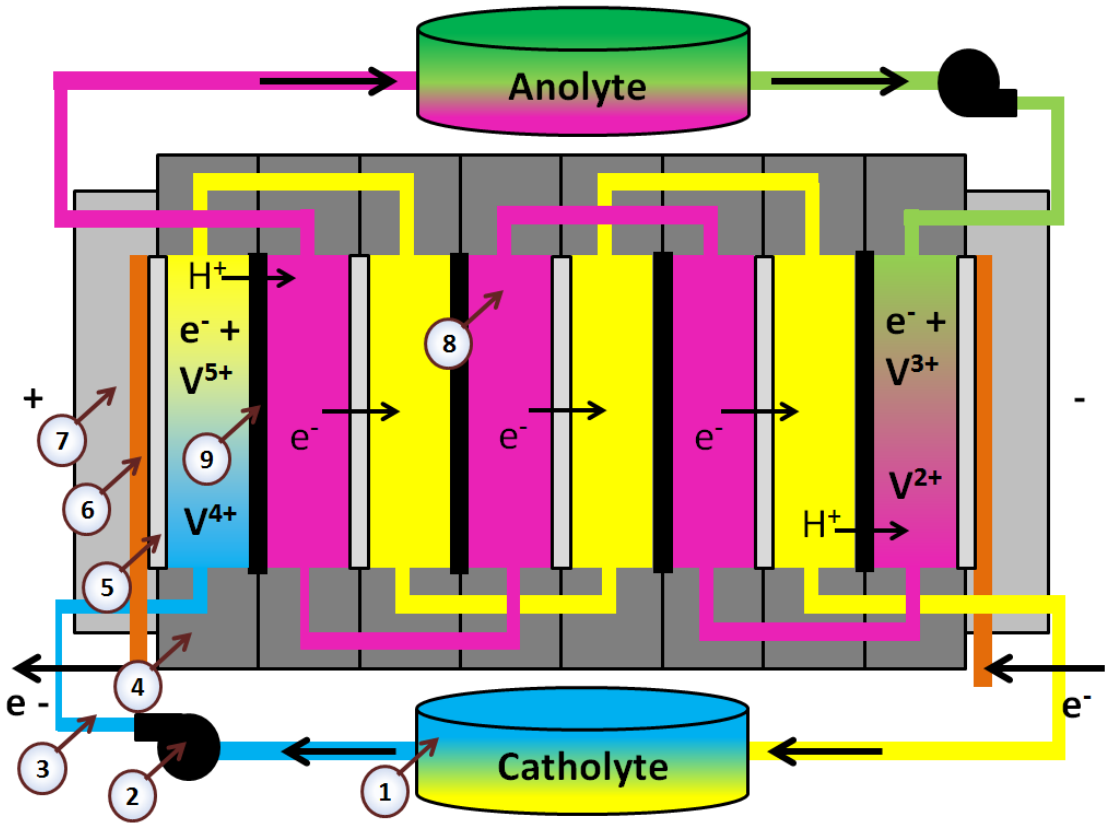

Figure 2.1: VRB Charging Schematic Diagram

(Li et al., 2011; Eckroad, 2007; Weber et al., 2011; Blanc and Rufer, 2010; You et al., 2009)

In the stack charging scenario above, the valence states of the electrolyte are represented by the colors that they will roughly look like when the stack is running. A simplified explanation of the charging electrochemical reaction is discussed, the actual reaction is complex with side reactions and interactions with the non-vanadium compounds in the electrolyte. During charging, electrolyte flows through the stack repeatedly until all of the electricity has been transferred into or out of the stack. First, electrolytes (with electrons supplied to the stack) are pumped to the anode side of the stack (shown with a "-") and valence state 2 electrolytes (or V^{2+}) are pumped into a half cell. Meanwhile, valence state 3 electrolytes (or V^{3+}) are pumped to the other end of the stack. As the valence state 2 and state 3 electrolytes are flowed into each half cell, oxidation and reduction reactions occur (reduction reactions are when valence states decrease). As this redox reaction occurs, the protons pass through the proton exchange membrane, and this transfer of protons results in the redox in each half cell. As the electrolytes are flowed through the system, electrons pass through the bipolar plate from the anode tank electrolytes to the cathode tank electrolytes. As the charging occurs, valence state 4 electrolytes (V^{4+}) in the cathode tank are replaced by the (charged) valence state 5 electrolytes (V^{5+}). (Li et al., 2011; Eckroad, 2007; Weber et al., 2011; Blanc and Rufer, 2010; You et al., 2009; Skyllas-Kazacos et al., 2011). There are a variety of configurations used for the VRB stacks.

A detailed bill of materials (BOM) of a theoretical 1 GW power-scale and 250 MWh energy-scale VRB system (Viswanathan et al., 2012) is presented in Table D. 1 in the Appendix with one such configuration. This 1 GW system this is designed match

PNNL's cost and performance model (Viswanathan et al., 2012). An abbreviated BOM is shown in Table 4.1 in Chapter 4.

2.3.1 Selected VRB Component Detail

As mentioned above, the selected components for this research include the naturally expanded graphite bipolar plate injected with resin, nonwoven graphite felt injected with resin, and the Nafion® PFSA PEM. These components are selected because they are known to work in vanadium redox flow batteries and other flow battery systems, and they are the most costly stack components (Skyllas-Kazacos et al., 2011; Parasuraman et al., 2013; Eckroad, 2007; SGL Group, 2012; DuPont, 2009). DuPont Nafion® membranes are commonly used and have been successfully used in VRBs (Eckroad, 2007; Chen et al., 2013). Graphite bipolar plates impregnated with resins have been used in recent VRB systems (Eckroad, 2007), and these plates have traditionally been made using the method developed by POCO Graphite and SGL Carbon (Brett, 2005). Additionally, graphite felts, specifically soft porous graphite felts manufactured by SGL (SGL Group, 2011), have recently been used in VRBs, in place of other electrode materials (Parasuraman et al., 2013). VRBs with these selected materials are undergoing testing at PNNL. A 0.5 m^2 unit cell area design parameter is selected to be aligned with the component cost breakdown in the paper by Viswanathan et al. describing a VRB cost models (Viswanathan et al., 2012).

2.3.2 Bipolar Plate Detail

One potential manufacturing method for BPPs, with an optimistic demand of 1 GW / 2 GWh puts the component pricing at \$25/m^2 (Viswanathan et al., 2012). The bipolar plate

functions as an electron transfer location (Eckroad, 2007). Typically, it is the heaviest component in a stack, as a physical structure that blocks the electrolyte and proton passage, in addition to being corrosion resistant (Blanc and Rufer, 2010; Eckroad, 2007; Yuan et al., 2005; Brett, 2005). Although BPPs often incorporate machined flow channels machined (Brett, 2005; Yuan et al., 2005), the bipolar plate investigated in this work does not have integrated flow channels (SGL Group, 2012),. The selected manufacturing method and operations are described in Chapter 3.

2.3.3 Felt Electrode Detail

One potential manufacturing method for BPPs, with an optimistic demand of 1 GW / 2 GWh puts the component pricing at $\$20/m^2$ (Viswanathan et al., 2012). Graphite felt electrodes are used in a variety of high temperature battery applications, including the VRB (Parasuraman et al., 2013; Weber et al., 2011; Liu et al., 2012), furnaces, electrodes, and other high temperature applications (SGL Group, 2013a). For the VRB application, the porous graphite felts function as electrochemical reaction sites (Skyllas-Kazacos et al., 2011). The graphite felt selected should not dissolve in vanadium sulfuric electrolytes and should be porous enough for the reactions. The selected system configuration has the graphite felt unattached (it is placed between the bipolar plate and membrane without any adhesive) in the VRB systems. The selected manufacturing method and operations are shown in Chapter 4.

2.3.4 Membrane Detail

One potential manufacturing method for BPPs, with an optimistic demand of 1 GW / 2 GWh, puts the component pricing at \$200 per m^2 (Viswanathan et al., 2012). These

Nafion® membranes are 1100 equivalent weight (EW), or grams of dry Nafion® per mole of sulfonic acid group (Mauritz and Moore, 2004), at 5 mil thickness (DuPont, 2009). Nafion® is the standard product used in the PEMFC industry (Carlson et al., 2005). DuPont originally produced Nafion® membranes using an extrusion casting technique, but recently solution-casting (dispersion) techniques have been employed to create new membranes for RFBs (Harris et al., 2010; Carlson et al., 2005). The membrane selected for cost modeling was the Nafion® PFSA ionomer dispersion at approximately 30% water and isopropanol and 40% solid weight (Carlson et al., 2005; DuPont, 2009). For each 0.5 m^2 of 1 mil Nafion® PFSA PEM, there is an estimated 0.125 kg of Nafion® required for production (DuPont, 2009; James and Kalinoski, 2009; DuPont, 2008). The selected manufacturing method and operations are shown in Chapter 4.

Nafion® PEMs are currently used in a variety of applications. These include medical filtration devices, automobiles, flow batteries, proton passage components in VRBs and hydrogen fuel cells (US DOE, 2011a; BTI, 2012; Houchins et al., 2012). In the all-vanadium redox flow battery (Gen 1), the PFSA PEM Nafion® membrane acts as a separator between the electrolytes, it keeps water permeability low, it provides resistance to prevent shorts in the cell, and it allows protons to pass between the half cells (Houchins et al., 2012). If too thin of a Nafion® membrane is used, the quality may significantly decrease due an increased chance of pinholes and tears (Harris et al., 2010; Grot, 2003). A film backing is used to assist with the following assembly operation (DuPont, 2008).

2.4 Current State of VRB Components

Currently, major components used in VRB systems are produced with emerging manufacturing methods (Weber et al., 2011; Kear et al., 2011; Zhang et al., 2012; Mohamed, 2012; Harris et al., 2010). The systems are also produced as prototypes, with laboratory scaled-up methods, or with low volume production systems (Weber et al., 2011; Kear et al., 2011; Zhang et al., 2012; Mohamed, 2012; Harris et al., 2010). Automotive fuel cell components are currently being mass produced (Harris et al., 2010; Carlson et al., 2005; James and Spisak, 2012; Sinha et al., 2009), and are the same type of components as in the selected VRB system considered in this research. Some companies are producing the components needed for the VRBs, while others are assembling entire VRB systems. Companies creating entire VRB systems include VRB Power Systems, Sumitomo Electric Industries, and Cellenium (Skyllas-Kazacos et al., 2011; Eckroad, 2007). Major companies that produce components for VRBs include GrafTech, DuPont, and SGL (SGL Group, 2012; DuPont, 2009; Orest Adrianowycz et al., 2010). Other suppliers exist that create similar components for alternative solutions and traditional batteries, for instance, Asahi makes PFSA membranes for other PEMFCs (Hamrock and Yandrasits, 2006). Additionally, it is assumed that these cell stack components are produced by web converting processes that (production processes where products are created in continuous widths and thicknesses, they can often be rolled up once they are produced) are assembled continuously after the components are produced (James and Kalinoski, 2009; Mercuri, 2008).

2.4.1 Current State of VRB Component Research

A brief discussion follows on current research and production methods for selected VRB components: graphite felt electrodes, graphite bipolar plates, and Nafion ® PFSA PEM. Current suppliers do have the capability to produce large volumes of felt electrodes and graphite bipolar plates. However, there have been shortages in the suppliers of these felts for other products (Eckroad, 2007). These systems are typically set up for thin web widths, and for components that may not be ideal for large scale stationary energy storage technologies, as current demand for these components comes from non-stationary fuel cell technologies (Houchins et al., 2012). PFSA PEMs for VRBs typically use DuPont's Nafion®, and they are not being produced at high volumes (Eckroad, 2007; Carlson et al., 2005; Chen et al., 2013). There is a considerable amount of research being done by researchers and commercial entities to improve Nafion® membranes, as well as to find alternatives that have similar or improved functionality (Houchins et al., 2012; Chen et al., 2013). DuPont currently has two production methods for Nafion® membranes: extrusion casting and dispersion casting (DuPont, 2009; DuPont, 2008). Membranes made with the extrusion casting method are made with a Nafion® mixture melted through a slot or die onto rolls (Harris, 2006). Membranes made with the dispersion casting method have Nafion® dispersions cast onto a polymer belt (Carlson et al., 2005; Curtin and Howard, 2003). Other methods have been theorized for large-scale production, which are similar to the dispersion casting method (Carlson et al., 2005; Harris et al., 2010). Recent graphite bipolar plate (BPP) production methods produce flow channels by injection or compression molding (or where alternative flow frame

structures are used to support the bipolar plates), while traditional methods use the costly approach of machining flow channels into the plates (Orest Adrianowycz et al., 2010; Cunningham and Baird, 2006; Yuan et al., 2005; Müller et al., 2006; Cunningham et al., 2007), while other methods have flow channels produced by a stamping process (James and Kalinoski, 2009; Orest Adrianowycz et al., 2010). Thin bipolar plates are also known as foils, while naturally expanded graphite plates are also known as flexible graphite sheets (Brett, 2005; Mercuri, 2008; Ottinger et al., 2004). Porous graphite felts in VRBs can be made from woven or nonwoven fiber precursors (Carlson et al., 2005; Trapp et al., 2003; SGL Group, 2013b).

2.4.2 Current State of VRB Component Costs

Current storage systems operate under a range of energy storage costs, energy transfer costs, and capabilities (Skyllas-Kazacos et al., 2011; Kear et al., 2011). The all-vanadium redox flow battery energy capital costs currently exceed U.S. DOE energy storage cost targets (US DOE, 2011a; Viswanathan et al., 2012). The vanadium electrolyte (Kear et al., 2011) and Nafion® PFSA PEMs are known to be major cost drivers of current VRB systems (Skyllas-Kazacos et al., 2011; Chen et al., 2013). Funding and research are currently underway to investigate VRB system designs that can reduce the power and energy capacity costs of large-scale energy storage systems to meet the DOE Office of Electricity's (OE) capacity targets of $150/kWh and $1,250/kW (US DOE, 2011a).

2.4.3 Current VRB and PEM Electrolyte Fuel Cell Cost Models

Top-down and bottom-up cost models have been developed for various types of fuel cells. In general, the bottom-up cost model method focuses on finding the costs associated component specific costs (Carlson et al., 2005; McFarland et al., 2004; Böhringer and Rutherford, 2008). They are developed to account for all of the individual costs associated with each manufacturing operation, including bulk raw material purchases, capital costs, and labor costs (Carlson et al., 2005; McFarland et al., 2004). For energy technologies, top-down cost models have been constructed from available component prices (profit, indirect overhead, taxes / regulatory fees are included), rather than costs, that reflect purchases of one or more component types in large volumes from component suppliers, or reflect costs from an even higher level economy-wide or marketing point of view (McFarland et al., 2004; Böhringer and Rutherford, 2008).

Most of these cost models PEMFC energy storage cost models focus on automotive vehicles, while others look at specific types of components used within the systems. It is beneficial to look at a variety of cost models because different PEM applications use similar components. Recent U.S. DOE-funded PEMFC cost models were developed by NREL (Ernst, 2009), TIAX LLC (Carlson et al., 2005), Directed Technologies Inc. (James and Kalinoski, 2009), and other researchers and groups (Sinha et al., 2009). These cost models look at component cost breakdowns and performance models for energy storage systems that have similar components to those used in VRB cell stacks. VRB specific cost and performance models have been developed by the EPRI (Eckroad, 2007), PNNL (Viswanathan et al., 2012), and other researchers and groups (Parasuraman

et al., 2013; Kear et al., 2011; Zhang et al., 2012; Mouron, 2011). These cost models look at a range of different raw material pricing, component designs, system designs, manufacturing processes, and production speeds. The current literature provides insights into cost drivers, capabilities, and manufacturing process details for the manufacturing of VRB system components and systems (Skyllas-Kazacos et al., 2011). For the VRB systems that are of particular interest, vanadium (in the electrolyte) and Nafion® (in the membrane) have been identified as the primary cost drivers for the all VRB system (Skyllas-Kazacos et al., 2011; Chen et al., 2013). Large-scale manufacturing methods for similar components, such as PEMFCs for automobiles, are done with continuous web converting processes (James and Kalinoski, 2009; Mercuri, 2008). Cost reductions are needed to reduce capital costs for these manufacturing methods to produce components that meet the OE's 2015 cost targets (US DOE, 2011a).

2.5 Limitations of Prior Research

Research is underway to overcome limitations and challenges in the commercialization of large-scale VRB systems (Skyllas-Kazacos et al., 2011). Recent cost modeling efforts (in literature available to the public, much of the information used by commercial companies producing these storage systems is proprietary,) are also typically not looking at individual cost drivers for each component, they are instead looking for overall performance costs and what component unit costs are (Kear et al., 2011; Viswanathan et al., 2012; Parasuraman et al., 2013; Eckroad, 2007). Further research is needed to overcome scale-up and performance problems, temperature range limitations, and lengthening of the life of systems (Skyllas-Kazacos et al., 2011). Recent PEMFC cost

models look at a range of different raw material pricing, component designs, system designs, manufacturing processes, and production speeds. Their transparency is limited. Sources of supplier information are typically not provided, materials choices and designs are often not clear, and it is sometimes not clear if a value provided is a cost or a price, and what types of administrative/indirect-overhead costs are incorporated into the price. Additionally, raw material prices have decreased and are projected to decrease significantly for major components, which limits the relevance/utility of published results from prior cost models. Furthermore, it is often not clear what major assumptions are made and what information is based on estimates. Also, it is not clear what manufacturing process steps and methods are theoretical, and which are proven. Lastly, none of the VRB specific cost models found in literature were purely bottom-up process-based models. Bottom-up process-based models are constructed by investigating unit process costs (profit, indirect overhead, research and development, taxes/regulatory fees are not included in these costs) for the manufacturing operations used to create individual components. As such, bottom-up process models are able to elucidate cost drivers for individual components.

2.5.1 Bipolar Plates: Limitations of Prior Research

Prior modeling research efforts for naturally expanded resin impregnated graphite bipolar were made to estimate the cost of transportation and storage systems (Carlson et al., 2005; Sinha et al., 2009; Orest Adrianowycz et al., 2010) that are designed using different designs, constraints, and assumptions than the system modeled by PNNL (Viswanathan et al., 2012). The bipolar plate cost models reported in the literature are typically made

for smaller web widths (for automotive applications) and different annual production volumes (e.g., 500,000 units for the DOE's fuel cell program) (US DOE, 2012)) (Carlson et al., 2005; Sinha et al., 2009; Orest Adrianowycz et al., 2010). Additionally, raw material prices have recently dropped for graphite flakes and the other materials used in bipolar plate production, which puts the published results from prior cost models out of date. Furthermore, a new cost model is needed that aligns the cycle times for each of the components in the cell stack, including the bipolar plate, as these components will be assembled once they are produced (instead of being packaged). The currently selected components have lengthy dwell times and thermal processing equipment that should be further reviewed to see how they affect the other cost categories in this cost modeling methodology demonstrated in Chapter 3.

2.5.2 Felt Electrodes: Limitations of Prior Research

Prior modeling research efforts for porous nonwoven graphite felt electrodes are made for transportation and storage systems which are designed with assumptions different than the current models, which primarily use woven carbon fiber precursors (Carlson et al., 2005; Sinha et al., 2009). The graphite felt electrodes reviewed are for varying web widths and volumes of components. Felt electrodes are also part of the cell stacks (along with the bipolar plate and membrane), as such they should be produced at cycle times equivalent to those for the other stack components and the primary VRB components. This will facilitate continuous manufacturing and assembly, while reducing work in process inventory and associated costs.

2.5.3 Nafion® Proton Exchange Membranes: Limitations of Prior Research

Prior membrane modeling research has various strengths and limitations. A major limitation of the prior research is that each of the seven cost categories, i.e., tool depreciation, facility, labor, maintenance, raw materials, consumables, and utilities, used in this research are not individually broken down in prior cost models for VRBs and PEMFCs. This reduces the ability to identify manufacturing cost drivers. Also, there was no research found that investigated the same three stack components for assembly alignment, and no research was found that addressed the feasibility of the OE's cost targets being met by VRB systems. Additionally, no prior research was found that that modeled cost of Nafion® membranes at a 0.5 m^2 surface area. Furthermore, it is not clear where all of the cost estimates originated from in prior cost model research, what costs are from real equipment, and what manufacturing methods are selected.

2.5.4 Summary of Prior Research

Due to uncertainties and limited transparencies of previous cost models, there is a need for a new RFB bottom-up cost model that focuses on equipment supplier information to determine separate unit cost categories. This RFB cost model (or a group of component cost models) should be able to determine the feasibility of the RFB system, as well as to identify major cost drivers for the RFB system. This model will allow users to easily input a variety of design and process inputs into a RFB system that is scaled by annual production volume for a selected form factor. A VRB is specifically selected for the modeling in this research. The modeling of these components will be particularly beneficial because it is a cost model estimate of specific components from suppliers

whose commercial components are known to work in various RFBs (SGL Group, 2012) and VRBs (based on work done by PNNL (Viswanathan et al., 2012). The modeling will help determine the feasibility of meeting DOE energy storage cost targets (US DOE, 2011a). An RFB manufacturing cost estimation tool can benefit researchers, developers, and manufacturers, as well as utilities and the energy industry in evaluating the potential for adopting various technology solutions. Such questions are posed and evaluated using the cost model later developed as a part of this research. Cost models are one way to elucidate and communicate cost drivers and technology needs for new and existing energy storage system manufacturers, component manufacturers, and researchers. Thus, this research creates a new cost modeling methodology for novel energy product manufacturing and applies the method to produce cost models for three primary VRB components.

Chapter 3: A Bottom-up Cost Modeling Method for Vanadium Redox Flow Battery Component Manufacturing

by
Zachary J. Southworth, Karl R. Haapala, Brian K. Paul, and Scott A. Whalen

To be submitted to the Journal of Power Sources

http://www.elsevier.com/journals/journal-of-power-sources/

Chapter 3: A Bottom-up Cost Modeling Method for Redox Flow Battery Component Manufacturing

Abstract

Renewable energy resources are increasingly being incorporated into utility grid portfolios throughout the United States. Stationary energy storage solutions are needed to support utility grids that are incorporating renewable energy sources that receive energy intermittently. Research on redox flow batteries technologies (RFB) is underway, as well as commercialization efforts. There is a need for a new bottom-up process-based cost modeling methodology to assess RFB components, in order to assist with the development of RFBs. Of particular interest is the vanadium redox flow battery (VRB). A bottom-up process-based methodology for discrete part manufacturing is modified to assist in VRB cost analysis. A five phase methodology is outlined to create bottom-up cost models for manufacturing individual VRB components. The methodology is then demonstrated for cost analysis of a bipolar plate. The naturally-expanded graphite (NEG) bipolar plate modeled is intended for a GW power-scale VRB network. The model results indicate that a competitive advantage may be gained if there is access to low-cost raw materials and utilities (i.e., electricity, water, and natural gas).

3.1 Introduction

In the U.S., there are increasing energy demands that require an ever-increasing need for the large-scale use of reliable and sustainable renewable energy resources (Li et al., 2011;

Parasuraman et al., 2013; Skyllas-Kazacos et al., 2011; US DOE, 2011a). Energy storage systems for renewable energy need to meet certain power and energy capital cost targets in order to be cost and technically effective technologies that can assist in the optimization of the U.S. electrical grid (Houchins et al., 2012; US DOE, 2011a). Certain states will have utilities increase their renewable energy contribution to their energy portfolio to over 20% under the Renewable Portfolio Standard (RPS), either through mandatory government requirements or internal goals (EIA, 2013a). Some countries are targeting renewable energies to generation 100% of their electrical energy by 2050, and at least one (Scotland) by 2020 (Farooq et al., 2013). These RPS goals are increasing renewable energy demands. Associated power quality and reliability needs (Divya and Østergaard, 2009; Turker et al., 2013) are contributing towards the growing market for fuel cells, large electrical storage systems (Tokuda et al., 2011), and other types of energy storage systems (Skyllas-Kazacos et al., 2011; BTI, 2012; Curtin et al., 2012). These energy systems can also contribute to emerging smart grid technology development, as they can be used to improve the reliability of the distribution of electrical energy (Skyllas-Kazacos et al., 2011; US DOE, 2011a; Weber et al., 2011). Further research is needed to assist with the development of newer technologies for the U.S. electric energy grid (Nexight Group, 2010; US DOE, 2011a). It is estimated that the energy storage industry in the U.S. will grow from $1.5 billion to $35 billion from 2010 to 2020 (US DOE, 2011a).

One promising type of energy storage technology that can rise to the challenge of meeting these energy needs are the proton (ion) exchange membrane battery and fuel cell

systems (PEMFC) (Hamrock and Yandrasits, 2006; Peighambardoust et al., 2010). For large-scale energy storage and transfer systems, variants of proton exchange membrane (PEM) batteries have been investigated (US DOE, 2012). PEMs are sometimes referred to as polymer electrolyte membranes (Li and Sabir, 2005). Regenerative PEMFCs are devices that do not use fuel, but rather electrolyte solutions to transfer energy from electricity to charged electrolyte solutions (Brandon et al., 2012; Skyllas-Kazacos et al., 2011; Yufit et al., 2013). Flow batteries are a PEM system where energy is transferred between electrolyte liquids that typically flow from tanks (Brandon et al., 2012; Eckroad, 2007; Li et al., 2011; Skyllas-Kazacos et al., 2011; Weber et al., 2011). Redox flow batteries (RFBs) are a specific type of flow battery that transfers energy using reduction and oxidation reactions (Parasuraman et al., 2013; Skyllas-Kazacos et al., 2011; Weber et al., 2011). Vanadium redox flow batteries (VRBs) are a specific type of RFB that use vanadium electrolytes, and are discussed more in depth below. VRBs store and transfer energy using different ion oxidation states of vanadium in a sulfuric acid electrolyte mixture (Parasuraman et al., 2013; Skyllas-Kazacos et al., 2011; Weber et al., 2011; Yamamura et al., 2011; Zhang et al., 2012). Herein, the term VRB refers to any type of VRB, while G1 VRBs refers specifically to the all-vanadium redox flow battery. The all-vanadium redox flow battery, or generation one (G1) VRB (Viswanathan et al., 2012), was created at the University of New South Wales in 1984 (Skyllas-Kazacos et al., 2011). VRBs are now used in a number of MW-scale facilities (Weber et al., 2011).

VRBs are an effective and promising technology because they are modular and can be scaled-up into larger systems (Mohamed, 2012; Blanc and Rufer, 2010; You et al., 2009;

Eckroad, 2007). In this research, a bottom-up cost methodology is developed specifically for use with G1 VRBs. Using this methodology, cost models can be made quickly, modularly, and serve as comparison tools for different technologies and manufacturing methods. This methodology will provide guidance in the creation of similar estimation tools to facilitate the development of emerging energy storage system technologies.

Bottom-up models are intended to elucidate unit costs absent of manufacturing profit and administrative costs, and to account for the various technologies necessary to produce components (Carlson et al., 2005; McFarland et al., 2004). These costs are developed by determining the requirements at the manufacturing operation level. For energy technologies, top-down cost models have been constructed from available component prices, which include profit, indirect overhead, and taxes/regulatory fees, for example, which reflect purchases of one or more component types in large volumes from component suppliers, or reflect costs from a higher level economy-wide or marketing point of view (McFarland et al., 2004; Böhringer and Rutherford, 2008).

Bottom-up cost models are needed to assist investigation and decision making for investment and development of VRBs and similar large-scale energy storage systems. Information is needed to assist in the determination of the major manufacturing cost drivers and hurdles presented by this technology. Key components that are used in VRB systems are produced as prototypes or, produced using emerging manufacturing methods, laboratory scaled-up methods, or low volume production systems (Weber et al., 2011; Kear et al., 2011; Zhang et al., 2012; Mohamed, 2012; Harris et al., 2010). Herein, a VRB network refers to a group of VRB systems, where a system is a group of stacks, a

stack is a group of cells, and a cell is comprised of two half-cells. More published research is needed to enable further commercialization of VRB systems; much of the information used by commercial companies producing these storage systems is proprietary.

Cost models for one type of VRB, a modular energy storage system, are typically developed by determining manufacturing methods, bulk raw material purchases, equipment costs, maintenance costs, labor costs, and utility costs (Viswanathan et al., 2012; Parasuraman et al., 2013; Kear et al., 2011; Eckroad, 2007; Mouron, 2011). Bottom-up cost models have been developed for other technologies to account for all of the individual costs associated with each manufacturing operation, this includes bulk raw material purchases, capital costs, and labor costs (Carlson et al., 2005; McFarland et al., 2004). Bottom-up cost models for VRB components and systems will assist with assessing and comparing new technologies to meet cost targets set by the U.S. Department of Energy Office of Electricity Delivery and Energy Reliability (OE) energy storage program (US DOE, 2011a). The OE is providing approximately $200 million dollars of funding from 2011 to 2015 (US DOE, 2011a). Thus, the cost modeling methodology developed herein is used to create bottom-up cost models for three key components of a VRB system: the bipolar plate, described below, and the felt electrode and proton exchange membrane, described by Southworth et al. (Southworth et al., 2013a). This research will contribute towards determination of the viability of the mass production of energy storage components, along with identification of VRB component manufacturing cost drivers. The research objective is to develop and demonstrate a

bottom-up process-based cost modeling methodology that can identify cost drivers for RFB components. This methodology will then be demonstrated for a 1 GW, 250 MWh VRB network; this network is composed of 1,000 1 MW / .25 MWh VRB systems (similar to PNNL's cost model (Viswanathan et al., 2012)). The bottom-up process-based cost model methodology proposed in this research produces VRB component cost models that reveal cost drivers, component feasibility, and other component costs through a five-phase process. This methodology is demonstrated by the development of a bottom-up cost model for bipolar plates, these bipolar plates are key components in the VRB cell stacks (Eckroad, 2007).

3.1.1 Cost Modeling Research and Limitations

Top-down and bottom-up cost models have been developed for various types of fuel cells and stationary flow battery solutions. Most of these cost models focus on components that are produced for automotive PEM systems, while others look at specific types of components used within RFB systems. It is beneficial to review a variety of cost models because the various PEM applications use similar components. Recent U.S. DOE-funded PEMFC cost models for were developed by NREL (Ernst, 2009), TIAX LLC (Carlson et al., 2005), Directed Technologies Inc. (James and Kalinoski, 2009), and other researchers and groups (Sinha et al., 2009). Major cost and performance models for the G1 VRB have been created by the EPRI (Eckroad, 2007), PNNL (Viswanathan et al., 2012), and other researchers and groups (Parasuraman et al., 2013; Kear et al., 2011; Zhang et al., 2012; Mouron, 2011). These cost models consider a range of different raw material pricing, component designs, system designs, manufacturing processes, and production

rates. Their transparency is limited, however. Sources of supplier information are typically not provided, materials and designs are often not clear, and it is sometimes not clear if a value provided is a cost, a price, or what types of administrative/indirect-overhead costs are incorporated into the price. Additionally, raw material pricing has decreased and is projected to decrease significantly for major components, which limits the applicability of published results from prior cost models. Furthermore, it is often not clear what major assumptions are made and what information is based on estimations. Also, it is not clear what manufacturing process steps and methods are theoretical, and what are proven. Lastly, none of the VRB specific cost models found in literature were bottom-up process-based models, which are built by investigating the costs of unit manufacturing operations used to create individual components. Bottom-up cost models do not include profit, indirect overhead, research and development, and taxes/regulatory fees, and are able to reveal cost drivers for individual components and cost categories (Lajevardi et al., 2011; Paul, 2013; Lieth et al., 2010).

The current literature provides insights into cost drivers, capabilities, and manufacturing process details for the manufacturing of VRB components and systems (Skyllas-Kazacos et al., 2011). For the VRB systems that are of particular interest, vanadium (in the electrolyte) and Nafion® (in the membrane) have been identified as the primary cost drivers for the G1 VRB system (Skyllas-Kazacos et al., 2011; Chen et al., 2013). Large-scale manufacturing methods for components used in similar PEM solutions use continuous web converting processes (James and Kalinoski, 2009; Mercuri, 2008). Cost reductions are needed to reduce capital costs for these manufacturing methods to produce

components that meet the DOE OE 2015 cost targets (performance cost targets) and the power and energy capacity needs (US DOE, 2011a). Thus, a cost modeling methodology must be designed so cost drivers can be identified for each of the components in a large-scale system like a grid-scale VRB system. It must also be able to accommodate both discrete and continuous production of components.

3.1.2 Need for Another Cost Model

Bottom-up cost models for VRB component manufacturing require gathering equipment supplier information to quantify individual unit cost categories and manufacturing operation costs. The models should enable users to easily input a variety of global design and process inputs for a large-scale VRB energy storage system. Annual production volumes, production line speeds, raw material costs, and labor rates are example global inputs. In addition to VRB component analysis, the cost modeling methodology would prove particularly beneficial for other modular large-scale energy storage systems. Cost modeling should provide a way to estimate direct costs in accordance with the requirements of U.S. DOE fuel cell program cost targets (US DOE, 2012). A previously reported cost modeling methodology for discrete component manufacturing is modified in this research (Lajevardi et al., 2011). Cost models can elucidate and communicate cost drivers and technology needs for new and existing energy storage system manufacturers, component manufacturers, and researchers. The goal of this research is to create a new cost modeling methodology and to use it to produce three cost models for major VRB components.

No other literature was found that specifically separated the marginal costs into only these seven separate categories, aside from prior work of the MBI researchers (Lajevardi et al., 2011). No literature was found that separated the entire costs into these seven categories for the modeling of VRB components. The literature reviewed for cost models for similar types of components typically groups these categories together. For example, TIAX (Carlson et al., 2005; James and Kalinoski, 2009) groups the transportation PEM components (similar to those in VRBs) into 5 categories: labor cost, equipment and tooling, capital costs, material costs, and "others". VRB specific cost models tend to only show the cost breakdown by the entire VRB system, with only the range costs found for each component presented (not individual component cost drivers) (Kear et al., 2011; Parasuraman et al., 2013; Eckroad, 2007).

3.1.3 Cost Modeling Methodology Overview

Cost modeling equations and cost categories developed by researchers within the Microproduct Breakthrough Institute (MBI), a collaboration of Oregon State University and the Pacific Northwest National Laboratory, for discrete component manufacturing (Lieth et al., 2010) are used as a basis for bottom-up process-based cost models for continuous web converting processes to assess energy storage components, specifically for utility-scale VRBs. An underlying assumption is that processing technologies exist for production of the three large-scale VRB components. Another assumption is that profit, taxes, company administrative costs, and other similar types of costs should not be included in cost estimates, per U.S. DOE cost target requirements of the Hydrogen and Fuel Cells Program (US DOE, 2012). This research aims to develop a cost modeling

methodology that could be used to assess components of large and modular energy storage systems. The cost modeling methodology developed is based on a modeling methodology used by MBI researchers, their methodology is for discrete part processing for micro-scale and nano-scale components (Lajevardi et al., 2011). The discrete part modeling methodology relies on the assumption that bottlenecks can be resolved by adding tools to a particular manufacturing operation, and it is assumed the cost of goods sold can be broken down into seven cost categories. In this prior methodology, if a manufacturing method is selected for a component, as little as five pieces of information from an equipment supplier can be used to model each manufacturing operation. (The sixth category is maintenance and it can be calculated from the assumption that annual maintenance is a certain percent of capital equipment cost. The seventh category is raw material and it can be found from other publications and suppliers). This methodology is then demonstrated by using it to create cost models for the graphite bipolar plates in VRB systems. The graphite bipolar plate is selected to demonstrate this cost modeling methodology because it has traditionally been the high cost component in fuel cells, and because bipolar plates are used in a wide variety of PEMFCs (Brett, 2005; Yuan et al., 2005). Verification of the cost model methodology is performed by developing and validating cost models for key components of a theoretical 1 GW / 250 MWh G1 VRB network (Southworth et al., 2013a), this research validates a cost model developed for bipolar plates.

3.2 Manufacturing Method Strategy

The overarching strategy of the manufacturing method selection is to determine the spreadsheet structure, data acquisition strategy, and input and output requirements to develop effective bottom-up cost models for VRB components. This research is based on prior cost modeling work done by MBI researchers (Lajevardi et al., 2011; Lieth et al., 2010) and a cost and performance VRB model by Viswanathan et al. (Viswanathan et al., 2012). It also draws upon discussions with various machine equipment and raw material suppliers, and on a review of current cost models and VRB component technology publications. The following cost model outputs have been identified (Lajevardi et al., 2011): cost drivers by cost category, cost drivers by process category, capital costs, the effect of production volume on the unit cost, cost trends, and the affect that specific design and process inputs have on unit cost. Each of the cost models are composed of seven cost categories, i.e., tool, facility, labor, maintenance, raw materials, consumables, and utilities. Once the desired cost model outputs are selected, a five phase bottom-up cost modeling methodology is developed.

In order to find the data to develop the bottom-up cost models, several steps are taken for each of the proposed phases of the methodology developed (Figure 3.1). Phase 1 involves selecting a specific component (or starting point) for cost modeling, developing a bill of materials (BOM) of the entire system, and finally identifying the form and function of the components in the BOM. Phase 2 involves reviewing patents and publications, and reviewing state-of-the-art production methods for the selected components and for similar components. Phase 3 starts by determining the

manufacturing method, then determining manufacturing operations, and finally determining machine equipment needs. Phase 4 focuses on discussing capabilities with equipment suppliers, obtaining equipment supplier budgetary quotes, obtaining raw material quotes, and to obtaining equipment supplier information for cost categories. In Phase 5, the cost model is finalized using spreadsheet software (MS-Excel). Spreadsheets created for global production and design inputs, process flow inputs, model calculations, modeling results, and references and assumptions.

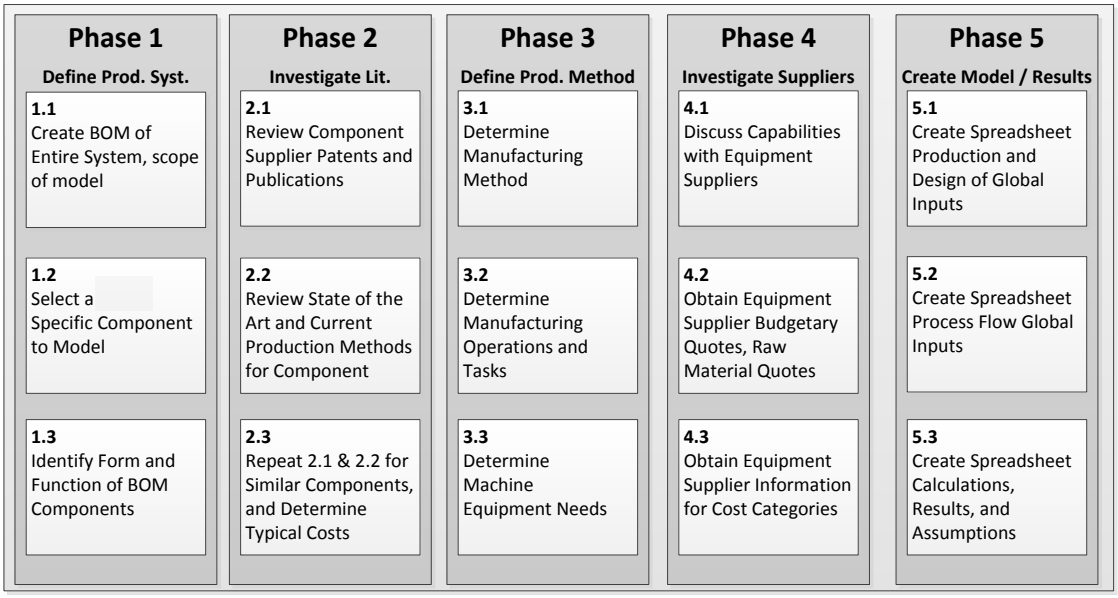

Figure 3.1: Bottom-up Process-Based Cost Modeling Methodology

Each cost category has a specific set of modeling equations to calculate associated unit manufacturing costs ($/part). Individual inputs for each category are as follows: tooling capital ($/tool), laborers per production line (or laborers per piece of equipment), labor rate ($/hour), raw materials ($/tool), consumables (varies depending on equipment), facility (m^2/tool and $/$m^2$), maintenance (percent of total capital cost per year, typically

set at 4%), and utilities (e.g., energy rate, $/kWh). The first phase of this method aims to define the system.

3.2.1 Phase 1: Define the System

The first step of the cost modeling methodology for a system or component is to identify and select a product that is currently in production as a basis for the cost model. The next step in this cost modeling methodology is to develop a bill of materials (BOM) of the desired system and to determine the basic physical properties and functional requirements of each component. The next step is to select a specific component to model. Phase 2 then investigates the component literature.

3.2.2 Phase 2: Investigate Component Literature

Phase 2 begins with an extensive patent and publication search, reviewing technical literature from industry, and discussions with suppliers on current viable production methods to understand the most likely manufacturing method for the desired component. The next steps are to review state-of-the-art production methods and to determine typical costs and information for the seven cost categories, as available. The required raw materials and the number of laborers can be determined by a publication review and assumptions can be drawn, e.g., equipment maintenance cost is assumed to be 4% of tool capital cost for the first iteration of these bottom-up cost models (Paul, 2013)). Later, in Phase 4, information is gathered for the seven cost categories directly from suppliers. Phase 3 then defines the production method.

3.2.3 Phase 3: Define the Production Method

Phase 3 begins with a determination of the manufacturing method for the component that is being modeled, based on the information from Phase 2. The second step is to determine the individual manufacturing operations, tasks, and their respective requirements. The third step is to determine requirements for machine equipment based upon the manufacturing operation needs. Phase 4 then investigates equipment and raw material suppliers.

3.2.4 Phase 4: Equipment and Raw Material Supplier Investigations

Next, equipment suppliers are investigated to determine what types of equipment can feasibly produce the desired components at the target annual production volumes. Raw material suppliers are also investigated to determine raw material costs. Equipment suppliers are then contacted to determine what specific equipment is capable of producing the desired components, and to obtain the associated budgetary prices. Equipment suppliers provide as much utilities, maintenance, consumable, and labor information as possible for their respective equipment. Floor space, utilities, and consumables use rates are particularly important. Information gathered in previous phases (or from additional technical literature gathered in this phase) can be used to supplement any of the information for the seven cost categories. Phase 5 then looks at cost model creation and application.

3.2.5 Phase 5: Cost Model Creation and Application

The final step in the bottom-up cost modeling methodology is to create an interactive tool. The cost model calculates the overall unit cost of a component by combining the

seven cost categories for each manufacturing process step. Global inputs are then selected, such as labor rates, material costs, work hours per year, etc. The cost model results are displayed graphically using the unit costs found for each cost category. An evaluation of the numerical and graphical results can reveal the primary cost drivers by cost category and by manufacturing operation.

The version history worksheet reports the file naming convention, the basic process steps used, and a revision history list. The production and design inputs worksheet is used as an interactive tool to provide users the ability to easily change production and design inputs. The process flow inputs worksheet provides a process flow map, the line speed, critical dwell times, and any scaled-up capital equipment costs. The process calculation worksheet reads in all of the values from the model input worksheets, as well as containing the predetermined cost modeling equations (as shown in the following section) to calculate the total unit costs and unit category costs for each cost model at varying production volume requirements. The general structure of the process calculation worksheet is seen in Figure 3.2. The process results worksheet shows the graphical output of the cost models with a breakdown of the component costs by category, process, and varying production rate. Finally, the references worksheet identifies all of the prior work, technical literature, and supplier feedback used to develop each cost model, along with a clear documentation of the major assumptions and model constraints.

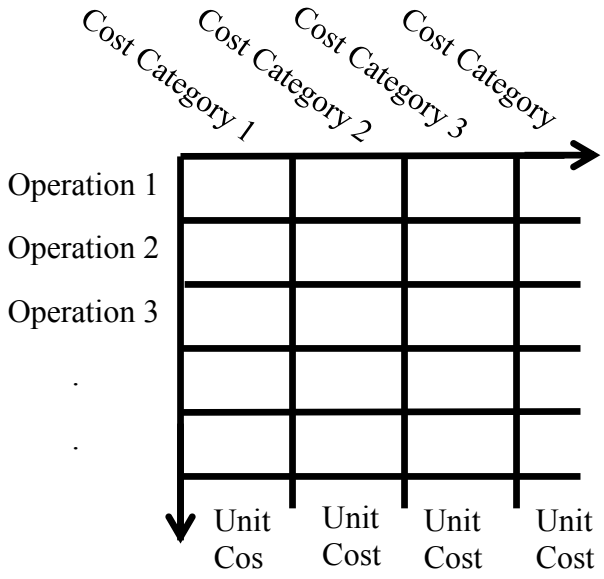

Figure 2.2: Calculation Worksheet

The resulting unit costs can be compiled into unit process costs and unit category costs. Using this information, it is suggested that four major graphical outputs be reported to assist with determining cost drivers and comparisons of components. Suggested graphical outputs include the unit cost breakdown by category and by process. Additional graphical results could be reported for annual production volume, capital costs, scrap cost, and raw material cost, which are provided elsewhere for the bipolar plate modeled in this research (Southworth et al., 2013a). Details about the calculation worksheet equations, differences between modeling discrete and continuous component production, and production, design, and process flow inputs are discussed in the following sections.

3.2.6 Calculations for Cost Categories

General equations for estimating manufacturing costs for the seven categories described above were previously developed for micro-device manufacturing (Paul, 2013), and are

adapted here. These equations were designed to be robust to facilitate cost analysis of diverse systems with various sub-components.

3.2.6.1 Tooling Cost

The calculation of total tooling capital cost T_s and tool count N_t are shown in Equations 3.1 and 3.2, respectively,

$$T_s = \frac{\left(N_t \cdot T\right)\left(1+T_i\right)}{y_t \cdot n_{dy} \cdot K_{sd}} \tag{3.1}$$

$$N_t = Roundup\left[\frac{\left(n_{dy} \cdot \left(K_{sd}/K_{sp}\right)\right)/h_y}{n_p \cdot U_t \cdot Y}\right] \tag{3.2}$$

where T_s is the total tooling capital cost, N_t is the tool count, T is the individual tool cost, and T_i is the tool installation cost as a fraction of tool cost (typically 4%), n_{dy} is the annual demand, i.e., production volume (units/year), h_y is tool utilization time (tool-hours/year, assuming 8,760 hours/year), n_p is the tool capacity (units/tool-hour, estimated based on cycle time), U_t is the tool utilization (%), y_t is the depreciation life of the tool (typically 7 years (Paul, 2013)), K_{sp} is ratio of parts to sub-assembly (e.g. 1 assembly with 4 parts would be 4), K_{sd} is ratio of sub-assembly to assembly, and Y is tool yield (or yield for a process step). Note that to determine yield, it is assumed that inspection and reject removal happen after each part is processed in a continuous system (or at each step in a discrete production system).

3.2.6.2 Facility Capital Cost

The facility capital cost, B_s, is shown in Equation 3.3 (Paul, 2013),

$$B_s = \frac{B_A \cdot N_t \cdot K_{bt} \cdot A_t}{y_b \cdot n_{dy} \cdot K_{sd}} \tag{3.3}$$

where B_A is the unit facility cost ($/m^2) with typical manufacturing space at $1,000/m^2 and cleanroom space at $5,000/m^2 (Paul, 2013), K_{bt} is the ratio of facility footprint to tool footprint, A_t is the tool footprint (m^2/tool), and y_b is the depreciation life of the facility (baseline assumption at 25 years (Paul, 2013)).

3.2.6.3 Labor Cost

The labor cost, L_s, is shown in Equation 3.4 (Paul, 2013),

$$L_s = \frac{L \cdot Roundup\left(N_t \cdot N_{lt}\right)}{n_{dy} \cdot K_{sd}} \tag{3.4}$$

where L is the labor rate ($/person/year) multiplied by one plus the direct overhead (50% typ.), N_{lt} is the labor count per tool (people/tool), n_{dy} is the annual demand, i.e., production volume (units/year), and K_{sd} is the ratio of sub-assembly to assembly (value is set to 1 if there are no sub-assemblies).

3.2.6.4 Maintenance Cost

The maintenance cost, M_s, is shown in Equation 3.5 (Paul, 2013),

$$M_s = \frac{M_t \cdot N_t \cdot T}{n_{dy} \cdot K_{sd}} \tag{3.5}$$

where M_t is the annual maintenance cost as a fraction of tool cost (4% typ.), N_t is tool count (number of tools), T is capital cost of the tool ($/tool), n_{dy} is annual demand, i.e., production volume (units/yr.), K_{sd} is the ratio of sub-assembly to assembly (value is set to 1 if there are no sub-assemblies).

3.2.6.5 Raw Material Cost

The raw material cost, R_s, is shown in Equation 3.6 (Paul, 2013),

$$R_s = \frac{\sum(R \cdot Q_s)}{K_{sp}} \tag{3.6}$$

where R is the supply cost per unit quantity ($/unit) and Q_s is the supply quantity per sub-assembly (unit). The sum of individual raw material costs is divided by the ratio of parts to sub-assembly, K_{sp}.

3.2.6.6 Consumable Cost

The consumable cost, S_s, is shown in Equation 3.7 (Paul, 2013),

$$S_s = \frac{\sum(S \cdot Q_s)}{K_{sp}} \tag{3.7}$$

where S is the supply cost per unit quantity ($/unit) and Q_s is the supply quantity per sub-assembly (unit). The sum of consumable costs is divided by the ratio of parts to sub-assembly (K_{sp}).

3.2.6.7 Utility Cost

The utility cost, U_s, is shown in Equation 3.8 (Paul, 2013).

$$U_s = \frac{\sum (U_c \cdot Q_u)}{K_{sp}} \tag{3.8}$$

where U_c is the utility cost per unit quantity ($/quantity), with deionized and process cooling water at $0.004/gal and wastewater at $0.009/gal (Paul, 2013), electricity at $0.051/kWh (EIA, 2012), and natural gas at $0.24/kg (EIA, 2013b), and Q_u is the utility quantity per component (unit).

3.2.7 Cost Modeling for Discrete and Continuous Part Processing

The prior bottom-up cost modeling methodology was designed so it could be used for discrete part production (Lajevardi et al., 2011; Leith et al., 2010). The cost modeling methodology needs to be capable of continuous flow production systems because certain RFB components are produced using continuous web converting processes (Carlson et al., 2005; James and Kalinoski, 2009; Orest Adrianowycz et al., 2010). Web converting production methods typically produce parts continuously, which are then rolled and cut up. Thus, instead of adding extra pieces of equipment, as is typical for discrete part manufacturing, additional production lines (duplicates) would be needed to meet high annual production volume requirements when demand exceeds the capability of a single production line for web converting methods. The cost modeling methodology must be capable of handling discrete production capabilities, however, in order to accommodate RFB components manufactured using discrete part production systems. The cost models assume that continuous production lines are both balanced and leveled based on typical lean system setups (Tapping, 2002). Balanced production lines have the same rate of production on each line, while leveled lines are assumed to have parts produced at a

constant rate year round. The previous cost equations already assume the production lines are leveled, as a constant throughput is used.

If continuous flow production lines are used, then the number of lines needs to be calculated. This is done by dividing the expected annual production demand (accounting for cumulative yield) by the annual demand capacity to determine the number of lines needed, and rounding up to the nearest integer value. If more than one line is needed, then they need to be balanced. The annual production demand (demand per line) is set equal to the production line capacity divided by the number of production lines.

3.2.8 Production and Design Input Selection

Production and design worksheet inputs are determined based on prior bottom-up process-based cost modeling research (Paul, 2013). These inputs represent various production requirements, operation costs, raw material costs, facility construction/procurement costs, facility area required per tool, tool installation cost, tool life, and building life. These input categories are defined to increase the flexibility of the cost models, to allow users to interact with the models, and to enable the models to be built in a modular method with global variables. Values for the specific inputs should be justified from published literature or supplier sources. Individual cost models in a system may have common input variables, along with unique inputs for each model's respective raw material needs. A detailed list of common production and design input parameters is shown in Table 3.1.

Table 3.1: Common Production and Design Inputs

	Input Item	Description
Prod. Req'ts.	Annual production volume	Parts required per year. User defined.
Operation Costs	Labor hour rate	User defined.
	Laborers per line	User defined.
	Labor loading	Total laborers per line. User defined.
	Maintenance cost	Scalar that accounts for labor direct-overhead costs. User defined.
	Natural gas cost	$/kg. User defined.
	Electricity cost	$/kwh. User defined.
	Cumulative yield	This accounts for the scrap generated during production. User defined.
	Working days per year	User defined.
	Working hours per day	User defined.
Raw Material Cost	Raw material cost	Raw material cost per part or weight (as needed in equations)
Facility Construction / Procurement Cost	Cleanroom cost_m^2	Cost of functional cleanroom space (class 10,000) required for production. Cost is in $ per square meter of the functional area. User defined.
	Lab. cost_m^2	Cost of functional laboratory space required for production and/or support. Cost is in $ per square meter of the functional area. User defined.
	Manufacturing cost_m^2	Cost of manufacturing space required for production. Assume light industrial facilities. Cost is in $ per square meter of the functional area. User defined.
	Semi-clean cost_m^2	Cost of semi-clean space. Assume activities such as packaging, QA, inspection, etc. Cost is in $ per square meter of the functional area. User defined.
Facility Area	Gross area ratio	Scalar that allows for space to operate around tool floor space requirements. User defined.
Tool Install Cost	Tool install	Tool installation cost as a % of tool capital cost. User defined. (Note: Some values override this one)
Depreciation	Tool depreciation_yrs	Tool Depreciation in years. Assumes straight line. User defined. (Note: Some values override this one)
	Bldg depreciation_yrs	Building Depreciation in years. Assumes straight line. User defined.

3.2.8.1 Production and Design Inputs: User Interaction

The following describes user interaction with a completed cost model. For production requirements, required parts per year are input by the user. For the operation cost inputs, the labor hourly pay rate, laborers per line, labor loading (scalar that accounts for direct overhead), maintenance cost, natural gas cost, electricity cost, cumulative yield (defined by summation of step yields), working days per year, and working hours per year are defined. For the raw material cost input, the required raw materials prices are selected by the user. For the facility construction and procurement cost inputs, cleanroom, laboratory, manufacturing, and semi-clean room costs are defined. For the facility area required per tool, the gross area ratio is selected (this is a scalar that accounts for additional tool space required for isles and tool storage). For tool installation inputs, the tool-life installation costs are defined as a percentage of tool capital cost (some values within the spreadsheet model override this global input). For depreciation input, the tool and building life in years are defined.

3.2.9 Process Flow Inputs

The process flow worksheet provides a process flow map for each cost model, the baseline production line speed, critical dwell times used for thermal processing, and any scaled-up capital equipment costs. These input categories are provided to increase the flexibility of the cost models, to allow users interact with the models, and to enable the models to be built in a more sequential manner. These inputs can be easily modified on this worksheet, but the model does not currently account for these items to change; thus certain assumptions and design criteria in the model may be violated if the user changes

these inputs. Equipment may need to be scaled from information obtained from literature sources or equipment supplier contacts, which may not provide the adequate size of equipment needed. Additionally, including equations for all of the thermal processing steps, which are assumed to be typical limiting factors for mass production of components in energy storage systems, allows the user to modify the line speed capabilities of each cost model. The equipment costs are scaled-up in two different ways. First, if the piece of equipment to be scaled-up is for thermal processing, such as infrared-dryers and ovens, then the equipment is scaled-up using Equation 3.9 (geometric ratio equation) with α=1.0. Second, for any other equipment, a geometric ratio for the scale-up equation is α=0.6 in Equation 3.9 (Dickey, 2005).

3.2.9.1 Process Flow Geometric Ratio and Exponential Scaling Equations

The geometric and exponential scaling equation cost equation (Dickey, 2005) is shown in Equation 3.9.

$$C_D = C_C \cdot (\frac{F_D}{F_C})^{\alpha} \tag{3.9}$$

where C_D is the cost of the desired (scaled-up or scaled-down) equipment, C_C is cost of the currently available equipment, F_D is the functional unit of the desired equipment, and F_C is the functional unit of the current equipment, α is scaling unit, and is 0.6 for exponentially scaled-up equations, while α=1 for geometric ratio equations (Dickey, 2005). This equation is based on accepted equipment scale-up estimation practice and common chemical engineering scale-up methods (Dickey, 2005).

3.3 Application of the Cost Modeling Methodology

The five-phase cost modeling methodology presented above is applied to assess bipolar plates for VRBs. This section provides the detail of each phase for bottom-up cost modeling for the bipolar plates.

3.3.1 Phase 1: Define the Product System

The bill of materials (BOM) developed for this research shows an expected demand of about 2,000,000 bipolar plates based on the optimistic demand for 1 GW/250 MWh of capacity (based on the 1 MW/0.25 MWh system modeled by Viswanathan et al. (Viswanathan et al., 2012). More details concerning the BOM and the modeled VRB system is provided by Southworth et al. (Southworth et al., 2013a). The bipolar plate functions as an electron transfer location (Eckroad, 2007). The bipolar plate is typically the heaviest component in a VRB stack, as a physical structure that contains the electrolyte and blocks proton passage, while also being corrosion resistant (Blanc and Rufer, 2010; Eckroad, 2007; Yuan et al., 2005; Brett, 2005). , Although BPPs often incorporate machined flow channels machined (Brett, 2005; Yuan et al., 2005), the bipolar plate investigated in this work does not have integrated flow channels (SGL Group, 2012). The BPP is modeled after SGL's TF6 fluor polymer naturally expanded graphite bipolar plate (SGL Group, 2012). The selected manufacturing method and operations are described in the Phase 3 discussion.

3.3.2 Phase 2: Investigate Component Literature

One potential manufacturing method for BPPs, with an optimistic demand for 1 GW/2 GWh of capacity puts the component pricing at $\$25/m^2$ (Viswanathan et al., 2012). Other

bipolar plates for similar high-volume projects are found to be \$6.85 per 0.5 m^2 (Orest Adrianowycz et al., 2010), \$10.87 per 0.5 m^2 (Orest Adrianowycz et al., 2010), \$8.2 per 0.5 m^2 (Carlson et al., 2005), \$9 per 0.5 m^2 (Sinha et al., 2009), and \$12.75 per 0.5 m^2 (Viswanathan et al., 2012). Recently developed graphite bipolar plate (BPP) production methods produce flow channels by injection or compression molding (or alternative flow frame structures are used to support the bipolar plates), while traditional methods use the costly approach of machining flow channels into the plates (Orest Adrianowycz et al., 2010; Cunningham and Baird, 2006; Yuan et al., 2005; Müller et al., 2006; Cunningham et al., 2007), while other methods have produced flow channels using a stamping process (James and Kalinoski, 2009; Orest Adrianowycz et al., 2010). Thin bipolar plates are also known as foils, while naturally expanded graphite plates are also known as flexible graphite sheets (Brett, 2005; Mercuri, 2008; Ottinger et al., 2004).

Prior cost modeling research for naturally expanded resin impregnated graphite bipolar plates was undertaken to estimate the cost of transportation and storage systems (Carlson et al., 2005; Sinha et al., 2009; Orest Adrianowycz et al., 2010) that are designed using different configurations, constraints, and assumptions than the system modeled by PNNL (Viswanathan et al., 2012). The bipolar plate cost models reviewed are typically made for smaller web widths (for automotive applications) and different annual production volumes (e.g., 500,000 units for the DOE's fuel cell program (US DOE, 2012)) (Carlson et al., 2005; Sinha et al., 2009; Orest Adrianowycz et al., 2010). Additionally, raw material prices have recently dropped for graphite flakes and the other materials used in bipolar plate production, which limits the applicability of published results from prior

cost models. Thus, a new cost model is needed that aligns the cycle times for each of the components in the VRB cells, including the BPP, since the cell stack components will be assembled once they are produced (instead of being packaged). The currently selected components have lengthy dwell times for thermal processing, thus equipment should be further reviewed to see how they affect the other cost categories, as demonstrated by Southworth et al. (Southworth et al., 2013a).

3.3.3 Phase 3: Define the Production Method

The SGL TF6 (SGL Group, 2012) production method for a 0.7 m x 0.7 m x 0.6 mm bipolar plate is largely selected from SGL patents, literature about current manufacturing processes, and cost models for other PEMFCs (Carlson et al., 2005; Orest Adrianowycz et al., 2010; Öttinger et al., 2013). The model is termed Naturally Expanded and Resin Impregnated Graphite Bipolar Plate - No Flow Channels. A continuous web converting method is selected to enable in-line VRB cell assembly (James and Kalinoski, 2009; Mercuri, 2008). For the selected manufacturing method, nine manufacturing operations and two raw materials are identified for the NEG resin impregnated flow-frameless bipolar plate. Raw materials include the raw graphite flake and PTFE resin for impregnation (details are reported by Southworth et al. (Southworth et al., 2013b)). The first process is intercalation at 125 ℃ (oxidization with sulfuric acid), which oxidizes the graphite flakes (Carlson et al., 2005; Orest Adrianowycz et al., 2010; Mercuri, 2008; Norley et al., 2009). The second process is water rinsing or oxidative leaching, which is done to prepare the flakes for exfoliation, and to give them the desired chemical and physical properties (Carlson et al., 2005; Norley et al., 2009; Woods, 2003; Mercuri et

al., 2002). Next is exfoliation of the graphite flakes at 1400 ℃ to expand them in preparation for compression and to provide the desired chemical and physical properties (Carlson et al., 2005; Orest Adrianowycz et al., 2010; Mercuri, 2008). The fourth process is compression using a roller press (Orest Adrianowycz et al., 2010; Mercuri, 2008) at approximately 2000 pounds per linear inch of roll face, based on discussion with an equipment supplier. Next is inline resin impregnation (Orest Adrianowycz et al., 2010; Mercuri, 2008; Ottinger et al., 2004; Norley et al., 2009), followed by heated roll pressing (Carlson et al., 2005; Orest Adrianowycz et al., 2010). In the seventh process, gauging (thickness) inspection with a beta-gauge is undertaken and assumed to be similar to other web converting processes. Next is web shaping or cutting (Orest Adrianowycz et al., 2010; Norley et al., 2009), with the final process being resin curing (Carlson et al., 2005; Orest Adrianowycz et al., 2010; Norley et al., 2009; Woods, 2003). It is assumed that solvent recovery is not needed in the baseline model (Orest Adrianowycz et al., 2010; Ottinger et al., 2004). Figure 3.3 shows a graphical representation of the bipolar plate manufacturing process flow, with additional details and in-depth descriptions of assumptions given by Southworth et al. (Southworth et al., 2013b).

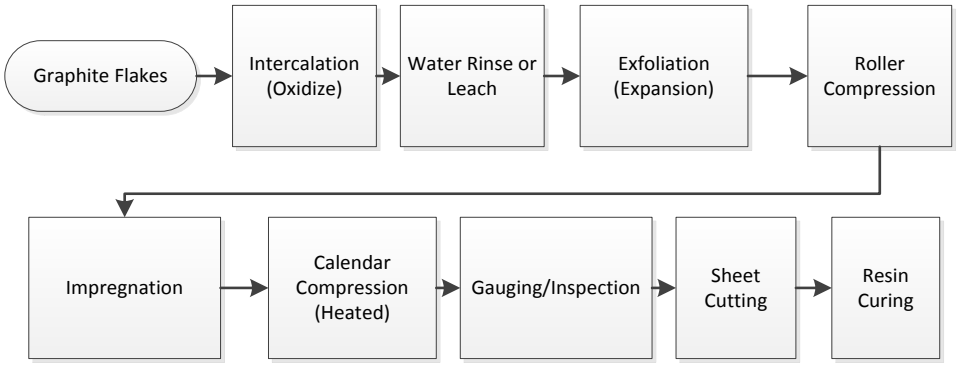

Figure 3.3: Bipolar Plate Manufacturing Process Flow

(Carlson et al., 2005; SGL Group, 2012; Orest Adrianowycz et al., 2010; James and Kalinoski, 2009; Mercuri, 2008; Ottinger et al., 2004; Woods, 2003; Öttinger et al., 2013; Norley et al., 2009; Woods, 2003; Mercuri et al., 2002)

3.3.4 Phase 4: Equipment and Raw Material Supplier Investigations

Equipment and raw material suppliers were investigated in Phase 4 to gather additional information on equipment capabilities. As a result, suppliers provided key information for the seven unit cost categories for the selected bipolar plate. Nearly a dozen budgetary quotes were obtained for capital equipment and two for raw material pricing, while additional discussions with suppliers and budgetary quotes for similar pieces of equipment were also obtained. Additional information was gathered under Phase 3 and from technical supplier literature to supplement the information provided by the suppliers.

3.3.5 Phase 5: Cost Model Spreadsheet Creation and Results

Next, in Phase 5, MS-Excel spreadsheet software was used to create and implement cost modeling calculations. Global design and production inputs were selected for the BPP.

The process flow input worksheet provides the flow map created in Phase 3, along with a suggested (baseline) production line speed, dwell times for thermal processes, and the scaled-up capital equipment costs (see Equation 3.9). The detailed process flow inputs for this cost model are described by Southworth et al. (Southworth et al., 2013b).

For the bipolar plate modeled in this research, the baseline production speed capability is determined based on GrafTech's 2009 DOE-funded PEMFC NEG bipolar plate research at a maximum realistic line speed of 3 meters/minute (Orest Adrianowycz et al., 2010). Thinner bipolar plates are assumed to be produced at 6 meters/minute (Carlson et al., 2005; Sinha et al., 2009). The mass of the bipolar plate is determined to be 0.50 kg/part based on the bulk density given for SGL TF6 (SGL Group, 2012). The resin curing conditions are 120 ℃ for 10 minutes (Orest Adrianowycz et al., 2010; Norley et al., 2009). Per a discussion with an equipment supplier, a curing oven at 0.95 m long has a capital cost of $75,000, and scaling up this equipment to 30 m, based on curing time and line speed, puts the capital equipment cost at $2.4 million (Eq. 3.9). The intercalation equipment is estimated to need a 150 kg/hr capability, based on the properties of the selected bipolar plate (SGL Group, 2012). This equipment is priced $300,000 in a previous cost model for 200 kg/hr processed at 125 ℃ (Carlson et al., 2005). Scaling this equipment down to 150 kg/hr puts the capital equipment cost at $225,000. Lastly, previous cost models reported equipment for exfoliation of approximately 200 kg/hr at the 1400 ℃ is $2 million (Carlson et al., 2005), scaling this equipment down to 150 kg/hr puts the capital equipment cost at $1.7 million.

The unit cost output by the bipolar plate cost model is \$4.93 per 0.5 m^2. The resulting graphical outputs include the unit cost breakdown by category (Figure 3.4) and by process (Figure 3.5) for an annual production volume demand of 2 million parts. Additional graphical results could be generated to report annual production volume, capital costs, scrap costs, and raw material costs. Furthermore, a detailed description of the assumptions should be developed for this cost model; an exhaustive list of input data and assumptions is reported by Southworth et al. (Southworth et al., 2013b).

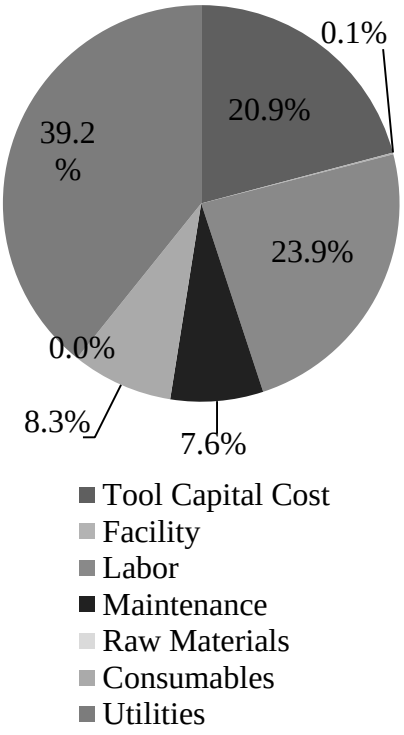

Figure 3.4: Bipolar Plate Costs Category

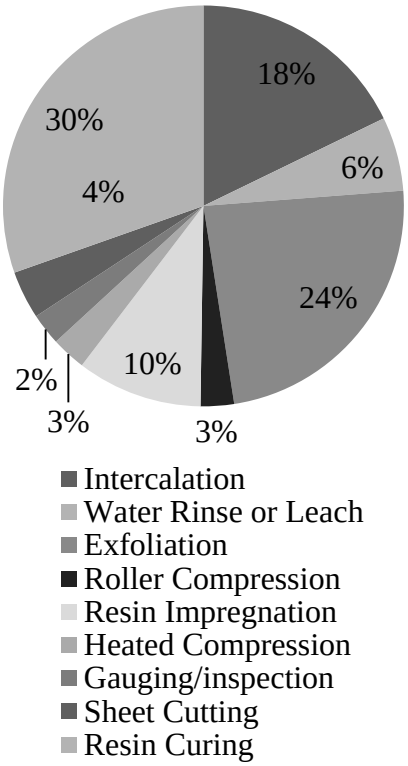

Figure 3.5: Bipolar Plate Costs by Process (Raw Materials Included)

3.4 Discussion

The cost modeling methodology to produce the models that are developed in this research, and the cost models that have been created for three VRB components, have a variety of uses and implications. The primary purpose of developing the methodology is to provide an approach that can repeatedly create bottom-up cost models to estimate unit component costs and elucidate cost drivers for large-scale energy storage systems (modular systems), such as RFBs. The resulting cost models are designed so that the component design, production processes, and process inputs can be easily modified by changing global variables on the Production and Design Inputs and Process Flow Input worksheets. The cost models produced by this methodology can now be used to analyze

cost drivers, cost trends, effects of various cost inputs and interactions, and effects of various design parameter changes.

There are four critical aspects of the cost modeling methodology developed and applied in this research. The first is to accurately create a full BOM for a desired system. The second is to select proper equipment and raw materials with input from potential suppliers. The third is to obtain budgetary quotes for each piece of equipment along with gathering specifications. Finally, the bottom-up cost model can be created solely based on a review of publications and supplier literature, if the annual product demands are known, and if machine equipment and raw material budgetary quotes are obtained with their respective specifications.

The manipulation of the design and process inputs in the cost models developed by this methodology can be used to show cost trends and to simulate similar production systems for varying types of components. Other outputs can show what drives process step costs at a range of production demands. These outputs will reveal an estimate of when the economies of scale no longer warrant larger production volumes, that is, the point where there is a significantly diminished reduction of cost when demand is still increasing exponentially.

For the specific VRB network to which this cost modeling methodology was applied, there is assumed to be an annual demand of two million bipolar plates. This volume accounts for a 1 GW power-scale VRB system that utilizes a cross-sectional electrode surface area of 0.5 m^2 (Viswanathan et al., 2012). The resulting unit costs are validated

by reviewing similar components from existing cost models, as seen Table 3.3. The average projected bipolar plate cost was found to be $9.50 per unit, which is almost double the estimated unit cost ($4.93) found using the model developed here. This result indicates that the cost models created in this research can create results similar to cost models developed for similar components by other researchers and organizations. Unit costs from this methodology were expected to be low since they do not include price elements (e.g., indirect overhead and taxes).

Table 3.3: Bipolar Plate Cost Comparison

Annual Prod. Volume per Cross Section	Model Component Detail	Primary Material Used	Material Price ($/kg)	Unit Cost ($/0.5 m^2)	Reference
2 million, 0.5 m^2	NEG resin impreg. BPP	‘ ‘	2.00	4.93	This work
19 million, ~0.5 m^2	NEG resin impreg. BPP	‘ ‘	5.51	6.85	(Orest Adrianowycz et al., 2010)
19 million, ~0.5 m^2	NEG resin impreg. BPP	‘ ‘	6.84	10.87	(Orest Adrianowycz et al., 2010)
Over 0.5 million, ~323 cm^2	Flexible foil	‘ ‘	4.40	8.20	(Carlson et al., 2005)
231 million, ~277 cm^2	Expanded graphite foil	‘ ‘	0.54	9.00	(Sinha et al., 2009)
Not specified	Not specified	-	-	12.75	(Viswanathan et al., 2012)

3.5 Conclusions

Government programs are assisting with the implementation and technological development of products and systems needed to facilitate the use of renewable resources (US DOE, 2011a; US DOE, 2012; Parfomak, 2012). PEMFCs, RFBs, and VRBs each

have specific technological and practical challenges that need to be overcome so they can be used to help promote the use of renewable energy resources (Weber et al., 2011). Currently, PEMFCs, RFBs, and VRBs are too expensive, according to the U.S. DOE (US DOE, 2011a; Houchins et al., 2012; Nexight Group, 2010), to effectively compete with alternative technologies (Greene et al., 2011;US DOE, 2011b).

There is a need for a simplified estimation tool to create and apply cost models for various RFB components. Thus, a cost modeling tool for continuous part processing was developed as a part of this research based on a discrete part cost modeling method developed under prior work. This methodology and the bipolar plate cost model can be evaluated to assist with the production of VRB components, and to compare technologies and manufacturing methods for emerging energy storage systems. Cost modeling results for the bipolar plate indicate that a competitive advantage can be gained if a company has access to affordable raw materials and utilities. Bottom-up cost models can help new companies enter into the market, help researchers and manufacturers focus on what cost drivers to pursue, and show trends and predictions of when these technologies will be usable.

The cost model methodology developed in this research focuses on identifying unit equipment and manufacturing process costs that comprise the overall production cost of VRB components. Discussions with equipment and raw material suppliers, equipment supplier budgetary quotes and literature, and research and product literature were successfully used as the foundation for cost models created by applying the five phase modeling methodology. The bottom-up cost model methodology developed in this

research successfully determined the costs associated with each manufacturing process and cost category, independent of profit and general administrative costs. Further, it was shown that the resulting outputs can be used to drive competitive strategies for different companies or economies in the development of redox flow battery systems.

Acknowledgements

The authors from Oregon State University (OSU) gratefully thank the support of the Pacific Northwest National Laboratory (PNNL) for their support of this research. The authors express appreciation to Ms. Qi Gao and Mr. Babak Lajevardi from OSU for their insights into bottom-up process-based methodologies. Also, gratitude is extended to the many unnamed suppliers and their representatives who were extremely helpful in offering insights into their industries, equipment, and materials.

Chapter 4: Cost Analysis of Gigawatt-Scale Vanadium Redox Flow Battery Component Manufacturing using Bottom-up Cost Models

by
Zachary J. Southworth, Karl R. Haapala, Brian K. Paul, and Scott A. Whalen

To be submitted to the Journal of Power Sources

http://www.elsevier.com/journals/journal-of-power-sources/

Chapter 4: Cost Analysis of Gigawatt-Scale Vanadium Redox Flow Battery Component Manufacturing Using Bottom-up Cost Models

Abstract

Increasing energy demands in the United States and around the world have stimulated a need for new utility grid-scale energy sources. Specifically, sporadic renewable energy sources are being incorporated into utility energy portfolios. Thus, supporting stationary energy storage technologies are needed to make these renewable sources reliable and feasible for grid-scale use. Large-scale redox flow battery systems, such as the vanadium redox flow battery (VRB) system, are being investigated to determine if they are capable of meeting these energy storage needs. The U.S. Department of Energy (DOE) Office of Electricity (OE) has released capital cost targets for 2015 of $150/kWh for energy capacity and $1,250/kW for power capacity for stationary energy storage technologies. These targets are 30% lower than energy storage costs in 2011. Baseline bottom-up cost models are created to assess the feasibility of these cost targets, to identify major cost drivers for three major VRB stack components, and to identify cost reduction opportunities. The components modeled herein are the porous graphite felt electrode and the Nafion® perfluorosuflonic acid (PFSA) proton exchange membrane (PEM). A cost model developed in prior research for the naturally expanded graphite (NEG) bipolar plate is also assessed. It is shown that these components can meet the OE cost targets when state-of-the-art manufacturing methods are used to evaluate costs of a theoretical 1 GW power-scale and 250 MWh energy-scale VRB network. The cost drivers are revealed to be the raw materials and the resin curing manufacturing process, utilities costs

and the continuous graphitization manufacturing process, and raw materials and the drying and cooling manufacturing process, for the bipolar plate, felt electrode, and membrane, respectively. These results indicate that a company or economy will have a competitive advantage if it has access to affordable raw materials, utilities, and state-of-the-art thermal processing equipment.

4.1 Introduction

There is an increasing need for the use of renewable energy resources worldwide, as well as in the U.S. (Li et al., 2011; Kear et al., 2011). Technologies are in development to assist with the integration of renewable energy sources in a variety of applications, ranging from large-scale utility grids, i.e., GW power capacity and GWh energy capacity (Viswanathan et al., 2012), to small-scale vehicle transportation applications (Parasuraman et al., 2013; Weber et al., 2011). The U.S. DOE has a strategic plan that is funding the research, demonstration, and commercialization of energy storage technologies for applications in both automotive and non-automotive industries, including regenerative PEMFCs for grid-scale energy storage (US DOE, 2011a; Greene et al., 2011; US DOE, 2011b). The U.S. DOE Office of Electricity and Energy Reliability (OE) is planning to provide funds of $200 million between 2011 and 2015 for such projects (US DOE, 2011a). The U.S. Congress appropriated another $136 million in 2012 for the development of hydrogen and fuel cell technologies (US DOE, 2012). There has been much recent research and development activity investigating fuel cells and their related technologies, as seen by commercial product availability and patent developments (Hamrock and Yandrasits, 2006; US DOE, 2012; Wee, 2007). Proton exchange

membranes (PEMs), for example, have selective ion transportation properties that have been pushing their application in commercial fuel cell technologies, particularly DuPont's Nafion® PEMs (Peighambardoust et al., 2010; Wu et al., 2013). Proton exchange membrane fuel cells (PEMFCs) were first used in the U.S. by NASA (developed by General Electric) in the 1960s for the Gemini Space Flights (Litster and McLean, 2004; Scott, 2009; Paola Costamagna, 2001). A significant amount of commercial and research activities are currently underway for the use of proton exchange membrane fuel cells (PEMFCs) as power sources for small-scale transportation and energy generation solutions (US DOE, 2011a; Houchins et al., 2012; Wee, 2007).

The U.S. DOE is actively funding and promoting research for PEMFCs in the range of 500,000 fuel cell units, which is the anticipated annual production volume for automobiles (Houchins et al., 2012; Carlson et al., 2005; US DOE, 2011b). There is a need for energy storage systems that have adequate energy capabilities, power capabilities, durability, and efficiencies for use in utility grid systems (Weber et al., 2011). The redox flow battery (RFB) is a potential solution to meet the needs of these large scale operations (Li et al., 2011). Flow battery technology was first patented in Germany in 1954 (Kangro, 1954; Shigematsu, 2011). VRBs have been identified as a promising energy storage technology by EPRI (Eckroad, 2007) and other literature sources (Blanc and Rufer, 2010). A number of large scale VRB facilities have already been developed and are under development in Japan, Australia, Thailand, and the U.S. (Eckroad, 2007).

There is a need for MW to GW and MWh to GWh scale battery systems to meet growing power capacity and energy demands (Viswanathan et al., 2012; Parasuraman et al., 2013; (Kear et al., 2011). The U.S. Department of Energy (DOE) has released capital energy storage 2015 (performance) cost targets for energy at $150/kWh and for power at $1,250/kW for stationary energy storage capacity (US DOE, 2011a), these targets can be applied to the costs of large scale battery systems (Johnson, 2012). Additional grid storage energy cost targets of $500/kWh were released by Sandia National Laboratory (Nexight Group, 2010) and $100/kWh by Advanced Research Projects Agency-Energy (Zhang et al., 2012). The 2015 cost targets from the OE are approximately 30% below energy storage cost capabilities in 2011; and it is posited that this reduction should make the use of more viable renewable resources than in current use (US DOE, 2011a; Houchins et al., 2012). The OE cost targets are not met by current production methods nor when considering predictions of component raw material prices (US DOE, 2011a; Houchins et al., 2012). Capital cost targets have been released to drive development of renewable energy technologies, stationary electrochemical battery storage systems, and fuel cell technologies (US DOE, 2011a; Houchins et al., 2012).

The benefits of incorporating new energy storage methods into the U.S. electricity grid have been recognized by companies and governmental agencies, who are now promoting the technological development and implementation of these storage methods. The U.S. DOE created the Hydrogen and Fuel Cells Program to increase the use of hydrogen and fuel cells throughout the U.S., for which $136 million dollars was appropriated for 2012 (US DOE, 2012). Specific applications that will benefit from reduced energy storage

costs are residential, commercial, and industrial backup power systems (US DOE, 2011a; Tokuda et al., 2011; Tang et al., 2011), solar powered homes, hydrogen fuel cells for automobiles, wind energy conversion, and remote area power systems (RAPs) (Skyllas-Kazacos et al., 2011; Weber et al., 2011; Kear et al., 2011). Additionally, electrical energy storage (EES) technologies can also be used as portable power systems and secondary power systems, and to make it more practical for the industrial use of sustainable resources (US DOE, 2011b). RFBs are one type of EES technology being researched as a utility grid-scale solution to these challenges (Weber et al., 2011).

Two of the major challenges with using renewable resources are that they sporadically supply energy (Parasuraman et al., 2013; Turker et al., 2013; Weber et al., 2011) and that current mass production technology incorporation in manufacturing settings are still in the early stages for their production and commercialization (Kear et al., 2011; Mohamed, 2012; Harris et al., 2010). An increase in renewable resources will likely have positive social, economic, and political impacts both in the U.S. and worldwide (Kear et al., 2011). The increased use of renewable resources will potentially lower the cost of living, reduce the reliance on other countries for energy resources, reduce pollution, and promote future energy research and development efforts worldwide (US DOE, 2011a; Kear et al., 2011). There is also a national benefit from the use of renewable energy systems as critical power sources in disasters (BTI, 2013).

In this research, a vanadium redox flow battery (VRB) stack is referring to a group of cells, a group of stacks is called a system, and a group of systems is called a network (a VRB network is typically referring to the VRB systems used throughout the U.S.). The

VRB is being investigated because it is an effective technology that has already been incorporated in a large number of facilities around the world (Li et al., 2011; Skyllas-Kazacos et al., 2011; Parasuraman et al., 2013; Kear et al., 2011; Prudent, 2012; IPHE, 2010; You et al., 2009). The purpose of the research reported herein is to understand and identify cost drivers, cost trends, design parameter interactions, and component design selection for the selected VRB stack components. This research applies a previously developed cost modeling method to major VRB components by determining how they are produced, and by reviewing the variability of the results.

4.1.1 Redox Flow Battery Technology

Redox flow batteries (RFBs) are electrochemical systems that function by transferring energy between charged and uncharged electrolytes through reduction and oxidation reactions (Weber et al., 2011). Grid-scale applications typically use high volume tanks for storing the electrolytes in order to provide adequate energy capacity (Parasuraman et al., 2013; Weber et al., 2011; Kear et al., 2011). RFBs are typically composed of a felt electrode, ion exchange membrane, bipolar plate, frame, electrolytes, tanks, pumps, a power system, and other components (Tokuda et al., 2011; Weber et al., 2011). In RFBs, a series of stacks is called a system, while a group of cells is called a stack (Blanc and Rufer, 2010). PEMs are a primary component in RFB technologies (Eckroad, 2007; Parfomak, 2012). PEMs serve as the cation exchange component in these batteries, and enable the transfer of protons between the half cells (Kear et al., 2011; Carlson et al., 2005). Vanadium redox flow batteries (VRBs) are a specific type of flow battery. Generation one (G1) VRBs use only one electrolyte mixture, while other RFBs

(bromine/polysulfide, zinc/bromine, zinc/cerium, iron/chromium (Skyllas-Kazacos et al., 2011; Weber et al., 2011; Eckroad, 2007)) typically use two. For these G1 VRBs, the electrolyte liquid has vanadium dissolved with sulfuric acid, and other compounds (Parasuraman et al., 2013; Eckroad, 2007; Ma et al., 2012). Flow battery (a type of PEMFC) research has been conducted since the 1970s by NASA, while VRB-related research was initiated at the University of New South Wales in 1984 (Weber et al., 2011; Kear et al., 2011; Blanc and Rufer, 2010).

4.1.2 Redox Flow Battery Challenges and Benefits

RFBs have several unique benefits, especially when compared to traditional battery storage technologies. In particular, power and energy storage capacities are independent from each other, allowing for more flexible system design (Eckroad, 2007; Ma et al., 2012). RFBs have several other advantages over other EESs, including lengthy lifetimes and relatively high performance parameters (efficiencies and component life) (Viswanathan et al., 2012; Li et al., 2011; Parasuraman et al., 2013; Eckroad, 2007; Blanc and Rufer, 2010; Li et al., 2012).

Typical challenges with RFBs are associated with the large amount of electrolyte transfer occurring between the tanks and stacks, the degradation of the components, side reactions, cross contamination, and the periodic need to remix the electrolyte (Kear et al., 2011; Eckroad, 2007; Tang et al., 2011; Ma et al., 2012). In addition, poisonous and explosive gasses can sometimes be produced by RFBs (Blanc and Rufer, 2010; Eckroad, 2007).

Recently, proton exchange membrane fuel cells (PEMFC) and other proton exchange membrane (PEM) applications have been heavily used in various industries as electrical energy storage (EES) systems (Li et al., 2011). PEMFCs work by transferring energy from a fuel, commonly hydrogen (BTI, 2012), into various media through chemical reactions by utilizing a membrane that restricts fluid transfer, while still transferring protons between charged and uncharged electrolytes (Blanc and Rufer, 2010; Eckroad, 2007). Redox flow batteries use PEMs to transfer protons between electrolytic compounds to transfer energy through reduction and oxidation chemical reactions (Skyllas-Kazacos et al., 2011; Parasuraman et al., 2013; Weber et al., 2011). RFBs are less commonly known as regenerative fuel cells (Brandon et al., 2012; Skyllas-Kazacos et al., 2011 Li et al., 2011), electrochemical energy storage systems (Li et al., 2011; Parasuraman et al., 2013), polymer electrolyte membrane fuel cells (Li and Sabir, 2005), and as a type of PEMFC (EG&G, 2005). These RFBs typically use a Nafion ® PEM, which is a challenge due to its high cost.

Nafion® PEMs are typically used due to their commercial availability and stability (10-40 ℃) (Houchins et al., 2012; Parasuraman et al., 2013; Weber et al., 2011; Eckroad, 2007). The use of Nafion® is prevalent in PEMs for VRBs due to its conductive properties, stability, and efficiencies (Weber et al., 2011). The Nafion® raw material typically accounts for most of the cost in an RFB cell (Skyllas-Kazacos et al., 2011; Chen et al., 2013). Nafion® PEM cost is driven by the manufacturing process and the raw material pricing at low volumes; the Nafion® ionomer is priced at about $1000/kg (Eckroad, 2007; James and Spisak, 2012). Nafion® PFSA PEMs are challenged with

high amounts of active ion crossover (Weber et al., 2011). Despite the widespread use of Nafion® membranes, it is theorized that alternatives to the current membranes would be beneficial to VRBs (Parasuraman et al., 2013). Research is being conducted into various new high temperature PEMs that do not rely on Nafion® (Houchins et al., 2012; Harris et al., 2010; DuPont, 2009), while additional research is underway to investigate modifications to the current Nafion® membranes to improve performance (Weber et al., 2011; Mauritz and Moore, 2004). VRBs are able to overcome some of the major problems that exist with other RFB technologies.

4.1.3 Vanadium Redox Flow Battery Challenges and Benefits

The VRB has similar challenges and benefits as most of the other major RFBs (Zhao et al., 2006). The VRB, however, has the significant benefit of not suffering from electrolyte cross contamination, and it can operate at 80% up to 90% efficiency (Skyllas-Kazacos et al., 2011; Kear et al., 2011). Additional benefits of VRBs include electrolyte recyclability and reduced component corrosion (Kear et al., 2011; Tang et al., 2011; Ma et al., 2012). Aside from the potential cost benefits, another major benefit of using VRBs is the comparatively small environmental impact than more toxic batteries, such as lead-acid batteries, although there are toxic elements in VRBs (Kear et al., 2011). Additionally, the VRB electrolytes in each half cell do not cause contamination due to electrolyte leakage through the PEM when the VRB is in the uncharged state (Eckroad, 2007). The VRB is also promising because it has already been used to provide high power capacity (kW to MW scale) in multiple facilities, including Sumitomo Densetsu (3 MW, 800 kWh in Osaka, Japan) (Skyllas-Kazacos et al., 2011; Doughty et al., 2010),

VRB Power Systems Inc. (10 MWh in Canada) (Kear et al., 2011), Pacificorp Castle Valley (250 kW, 2 MWh in Utah) (Kear et al., 2011) (Doughty et al., 2010), Prudent Energy VRB Systems (600 kW, 3.6 MWh in Oxnard, California) (Prudent, 2012), Chinese National Grid (Zhangbei, Hebei, China) (Skyllas-Kazacos et al., 2011), Painesville Municipal Power Station (1 MW, 8 MWh in Ohio) (Skyllas-Kazacos et al., 2011), Pinnacle VRB (250 kW, 1 MWh in Australia) (Skyllas-Kazacos et al., 2011). Due to industrial and academic research efforts to produce large scale VRBs, it is likely that recent technological advances will enable U.S. DOE energy storage cost targets to be met.

The VRB is a promising RFB EES system, as it does not exhibit cross contamination between the electrolytes in each half cell and associated problems (including corrosion), because each half cell only has a vanadium-based electrolyte (Viswanathan et al., 2012; Skyllas-Kazacos et al., 2011; Parasuraman et al., 2013; Liu et al., 2012). The storage capacity of the VRB is determined by the overall amount of vanadium used in the electrolyte (Yamamura et al., 2011), while the power is determined by the overall electrode reactive area in the VRB system (Viswanathan et al., 2012; Skyllas-Kazacos et al., 2011). VRBs can be produced with a variety of components, but often they use similar components: felt electrodes, bipolar plates, flow channels, proton exchange membranes, pump systems, PVC frames, tank systems, and electrolytes (Blanc and Rufer, 2010; Eckroad, 2007).

Major challenges with the use of Nafion® PFSA PEMs are the limited operating temperature of the current technology – typically 10-40 ℃ for a 2 molar vanadium

electrolyte solution (Skyllas-Kazacos et al., 2011; Parasuraman et al., 2013; Eckroad, 2007). Current research is developing high temperature PEMs with improved efficiencies, with an operational target of 120 ℃ or higher proposed by the U.S. DOE (Houchins et al., 2012; Harris, 2006). An additional challenge is the high Nafion® membrane cost (it is the most expensive structural component in typical VRB stacks) (Skyllas-Kazacos et al., 2011; Chen et al., 2013). VRBs suffer from their reliance on vanadium in the electrolyte, which is the other cost-prohibitive element in the stack (Eckroad, 2007; Kear et al., 2011). Vanadium is not available in high volume quantities, and primarily mined in South Africa, Russia, and China (half of all vanadium is produced in China) (Eckroad, 2007; Perles, 2012).

4.1.4 Need for Cost Modeling

Due to the high and uncertain costs of VRB components and systems, research is needed to better understand the key contributors to manufacturing costs. To assist in this effort, a five-phase bottom-up process-based cost modeling methodology was developed and demonstrated for bipolar plate manufacturing by Southworth et al. (Southworth et al., 2013c). Cost models developed using this methodology can be used to assist with the reduction of the component costs in VRBs. This methodology provides a repeatable approach to devise cost models that can be used for components produced using a continuous flow or discrete processing methods.

Bottom-up process-based models are built by investigating unit process costs (for profit, indirect overhead, research and development, taxes / regulatory fees are not included in these costs). The manufacturing operations used to create individual components as these

process models are able to show cost drivers for individual components. Top-down cost models are similar to bottom-up cost models, except they focus on market and economy-wide values (McFarland et al., 2004). For energy technologies, top-down cost models have been constructed from available component prices, rather than costs, that reflect purchases of one or more component types in large volumes from component suppliers, or reflect costs from an even higher level economy-wide or marketing point of view (McFarland et al., 2004; Böhringer and Rutherford, 2008).

Additional research is needed to assist with the commercialization of VRB and other RFB systems, since existing processing methods and material technologies are largely proprietary and limited to a small number of producers, while supply chains do not exist for several key materials and components. Cost models, as developed and applied in this research, will contribute towards the determination of the viability of VRB system components using various manufacturing technologies. These models can also be used to identify cost drivers and other key manufacturing information for VRB cell stack components.

4.1.5 Research Objective

There are two objectives of this research. The first is to create cost models for a graphite felt electrode and Nafion® PEM using the previously developed bottom-up process-based cost modeling methodology. The second is to determine the feasibility of producing these components relative to cost targets, the cost drivers, the capital costs, the cost trends, and the cost reduction opportunities, along with the graphite bipolar plate

modeled by Southworth et al. (Southworth et al., 2013c). This research will provide a framework for future RFB component and technology cost evaluations.

4.1.6 Research Summary

The three VRB stack components modeled and discussed in this research are the naturally expanded graphite bipolar plate injected with resin, nonwoven graphite felt injected with resin, and the PFSA PEM Nafion® membrane. These components are selected because they are known to work in vanadium redox flow batteries and other flow battery systems, and they have been found to be the most costly stack components (Skyllas-Kazacos et al., 2011; Parasuraman et al., 2013; Eckroad, 2007; SGL Group, 2012; DuPont, 2009). DuPont Nafion® membranes have been successfully used in VRBs are commonly used in other applications (Eckroad, 2007; Chen et al., 2013). Graphite bipolar plates impregnated with resins have been used in recent VRB systems (Eckroad, 2007), and have been made using an impregnation method by POCO Graphite and SGL Carbon (Brett, 2005).

Uncertainties and fluctuations in raw material pricing posed challenges for the information gathering phase of the cost model development. Also, long dwell times are needed for various heating operations, which posed a challenge in modeling the targeted state-of-the-art line speed capabilities, as very long dryers and ovens are required. Furthermore, there are challenges in selecting certain manufacturing process steps and with determining what equipment is needed for each step, as some of these components use new materials and processing technology.

4.2 Cost Modeling Methodology

A bottom-up process-based cost modeling methodology (Southworth et al., 2013c) is used to create three bottom-up cost models for each of the three stack components introduced above. The cost modeling methodology is based on a modified methodology to analyze discrete part manufacturing (Lajevardi et al., 2011; Paul, 2013; Lieth et al., 2010). The methodology is a step-by-step approach designed to create cost models for a sequence of independent manufacturing operations to produce modular, stationary energy storage systems.

This methodology consists of five main phases. Phase 1 includes the identification of energy storage system details along with selection of the specific component to be evaluated. Phase 2 is a detailed review of the desired component to determine current state-of-the-art mass production methods. Phase 3 is comprised of the selection of methods and operations for modeling component manufacturing. Phase 4 consists of discussions with machine equipment suppliers to obtain more detailed information about production processes and equipment capabilities, and to obtain budgetary quotes for capital equipment. Equipment suppliers should be queried for the specifications for the equipment that is quoted. Phase 5 consists of the creation of the bottom-up cost model in spreadsheet software. Information that cannot be obtained directly from an equipment supplier can be supplemented by consulting product or technical literature. Next, this method is described for the development of bottom-up cost models for the three selected VRB components.

4.2.1 Phase 1: Define the Product System

First, a bill of materials (BOM) for the entire VRB system must be defined, as well as describing the function and form of each component and selecting the components that will be modeled. To assist with defining the system and its components, a high-level, schematic view of the operation of a single VRB cell is illustrated in Figure 4.1. The BOM is based on a theoretical 1 GW power-scale VRB system based on a system previously described (Viswanathan et al., 2012) and is summarized in Table 4.1. A complete BOM has been detailed by Southworth et al. (Southworth et al., 2013b). In this system, the 1.5 molar vanadium electrolyte has a 5 molar sulfuric acid content (Viswanathan et al., 2012). A VRB cell is composed of two half cells, with each side having the electrolyte at a different charged state, whereas other RFBs use different electrolyte solutions in each half cell (Blanc and Rufer, 2010; Eckroad, 2007). The basic components of a cell are a proton exchange membrane, an electrode (felt) on each side of the membrane, and a bipolar plate on the outside of each electrode; flow channels are either in a frame around the bipolar plates or on the surface of the bipolar plates (Blanc and Rufer, 2010; Liu et al., 2012).

Electrochemical reactions occur in each cell as the charged or discharged electrolytes are pumped through the system, which then cause energy to be released or stored, respectively (Blanc and Rufer, 2010). These electrochemical reactions change the vanadium electrolytes to one of four charged states, with the charged (V^{5+} oxidation state) vanadium electrolytes stored in large tank reservoirs (Blanc and Rufer, 2010; You et al., 2009; Hiroshige et al., 2012). In Figure 4.1, the different oxidation states of the

vanadium electrolyte compound are described in a simplified manner as V^{2+} (purple), V^{3+}(green), V^{4+} (blue) and V^{5+} (charged state, yellow) (Yamamura et al., 2011; Blanc and Rufer, 2010; You et al., 2009; Eckroad, 2007). The figure illustrates four cells, or eight half cells, and supporting equipment including 1: Tank, 2: Pump, 3: Pipe, 4: Frame, 5: Bipolar Plate, 6: Current Conductor, 7: End Frame, 8: Felt Electrode, and 9: Proton Exchange Membrane.

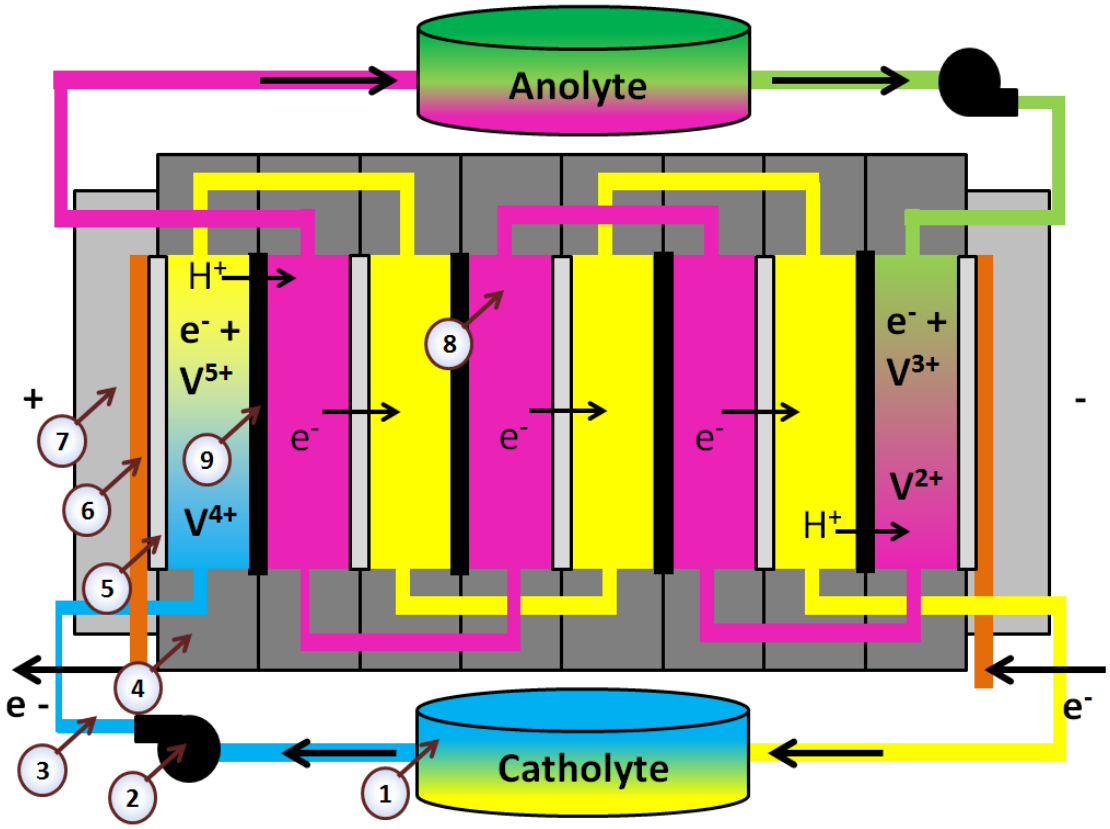

Figure 4.1: VRB Charging Schematic Diagram

(Li et al., 2011; Eckroad, 2007; Weber et al., 2011; Blanc and Rufer, 2010; You et al., 2009)

In the stack charging scenario above, the valence states of the electrolyte are represented by the colors that they will roughly look like when the stack is running. While a simplified explanation of the charging electrochemical reaction is discussed here, the actual set of reactions is complex with side reactions and interactions with the non-vanadium compounds in the electrolyte. During charging, valence state 2 electrolytes (with electrons) are pumped to the anode side of the stack (shown with a "-"). Meanwhile, valence state 3 electrolyte is pumped to the other end of the stack. As the valence state 2 and state 3 electrolytes are flowed into each half cell, oxidation and reduction reactions occur. As reactions occur, the protons are passed through the proton exchange membrane, enabling the redox reaction to occur in the adjacent half-cell. As the electrolytes are flowed through the system in this charging schematic, electrons pass through the bipolar plate from the anode tank electrolyte to the cathode tank electrolyte. As the charging occurs, valence state 4 electrolytes in the cathode tank is replaced by the valence state 5 electrolyte (Li et al., 2011; Eckroad, 2007; Weber et al., 2011; Blanc and Rufer, 2010; You et al., 2009; Skyllas-Kazacos et al., 2011). A summarized bill of materials is shown in Table 4.1 below.

Table 4.1: Summarized Vanadium Redox Flow Battery Bill of Materials

Lvl.	Name	Qty.	Material	Descr.	Dim.	Function	Reference
0	VRB network	1	-	Group of VRB systems	16353 k Liters	1 GW, 250 MWh	
1	VRB system (machine)	1k	-	Group of stacks	16353 Liters	1 MW, 0.25 MWh	(Viswanathan et al., 2012)
2	VRB stack	36	-	Groups of Cells	454 Liters	Charges and uncharges electrolytes	(Viswanathan et al., 2012)
3	VRB cell	60	-	2 Half-cells	0.8 x 0.8 x 0.006 m	Location of electrolyte charge / discharge	(Viswanathan et al., 2012)
4	BPP	1*	Fluor polymer resin impregnated naturally expanded graphite	Bipolar Plate with No Flow Channels	0.7 x 0.7 x 0.0006 m	Separate electrolyte and transfer electrons	Modeled after SGL TF6 Fluor Polymer (SGL Group, 2012)
4	Felt electrode	2	Epoxy resin impregnated PANOX polymer precursor porous graphite felt	Porous Graphite Felt Electrode	0.7 x 0.7 x .0046 m	Conductive transfer of electrons between electrolyte and BPP	Modeled after SGL GFD4.6 Polymer Precursor (SGL Group, 2012)
4	PEM	1	Nafion® PFSA PEM, 1100 EW	Nafion® Perfluorosulfonic Acid Proton Exchange Membranes	0.7 m x 0.7 m x 5 mil	Transfer protons between half cells	Modeled after DuPont Nafion® 115 (DuPont, 2009)

4.2.1.1 Selected VRB Component Detail

Cell stack components are selected for the cost modeling investigation in this research. The size and amount of cells in a stack (stacks combine to form a system) determines the power rating of a VRB (Blanc and Rufer, 2010). The stack components modeled are the nonwoven graphite felt injected with resin, modeled after SGL's GFD4.6 polymer precursor graphite felt (SGL Group, 2012)), and the Nafion® PFSA PEM, modeled after DuPont's Nafion® 115 (DuPont, 2009). Additionally, analysis is performed for the bipolar plate modeled by Southworth et al. (Southworth et al., 2013c). These specific components are selected because they are known to work in vanadium redox flow batteries and other flow battery systems, and they are the most costly components in the stack (Skyllas-Kazacos et al., 2011; Parasuraman et al., 2013; Eckroad, 2007; SGL Group, 2012; DuPont, 2009). These specific components are selected for modeling because they are the proven and most costly components of the cell stacks in VRB Systems and other flow battery systems (Houchins et al., 2012; Weber et al., 2011; SGL Group, 2012; DuPont, 2009; Brett, 2005), and they are currently a focus of VRB development at PNNL.

The Nafion® membranes by DuPont are commonly used in RFBs and have been successfully used in VRBs (Eckroad, 2007; Chen et al., 2013). The Nafion® PFSA PEM is selected because it successfully transfers protons between the half-cells, while keeping the electrolyte from mixing (Weber et al., 2011). This material is desirable in RFBs because of its good sodium conductivity, proton conductivity, and stability; it also has been shown to have high current efficiencies in VRBs (Weber et al., 2011). Graphite

bipolar plates impregnated with resins have been used in recent VRB systems (Eckroad, 2007), and these plates have traditionally been made using a resin impregnation method by POCO Graphite and SGL Carbon (Brett, 2005). These BPPs are well suited for RFBs as they have good conductivity, electrochemical stability, and low permeability (SGL Group, 2012). Additionally, graphite felts have recently been used in VRBs in place of other electrode materials (Parasuraman et al., 2013), particularly soft porous graphite felts manufactured by SGL (SGL Group, 2011). These SGL porous graphite felt electrodes are selected as they have good conductivity, electrochemical stability, porosity, and elasticity (SGL Group, 2012).

4.2.1.2 Bipolar Plate Detail

The naturally expanded graphite (NEG) bipolar plate information analyzed here is from prior work by Southworth et al. (Southworth et al., 2013c). The annual demand for VRB applications is assumed to be 1,000,000 (2,000,000 m^2) based on optimistic annual growth of 1 GW/250 MWh of capacity. Material quantities herein are scaled up from information provided for a prior cost and performance model of a 1 MW/0.25 MWh VRB system (Viswanathan et al., 2012).

4.2.1.3 Felt Electrode Detail

Similarly, an annual demand of about 2,000,000 (4,000,000 m^2) felt electrode components is expected, also based on the optimistic annual growth of 1 GW / 250 MWh of VRB capacity. Graphite felt electrodes are used in a variety of high temperature battery applications, including the VRB (Parasuraman et al., 2013; Weber et al., 2011; Liu et al., 2012), as well as furnaces, electrodes, and other high temperature applications

(SGL Group, 2013a). For VRB applications, the porous graphite felts function as electrochemical reaction sites (Skyllas-Kazacos et al., 2011). The graphite felt selected will not dissolve in vanadium sulfuric electrolytes and is porous enough to facilitate the reactions. The selected system configuration has the graphite felt unattached (it is placed in between the bipolar plate and membrane without any adhesive) in the VRB systems. The selected manufacturing method and operations are shown in the discussion for Phase 3.

4.2.1.4 Membrane Detail

Annually, a demand of about 1,000,000 (2,000,000 m^2) PEMs is expected based on the optimistic annual growth of 1 GW/250 MWh of VRB capacity. The Nafion® membranes selected are 1100 equivalent weight (EW), where EW is a measure of the mass (grams) of dry Nafion® per mole of sulfonic acid group (Mauritz and Moore, 2004) at a 5 mil thickness (DuPont, 2009). Nafion® is the standard membrane product used in the PEMFC industry (Carlson et al., 2005). DuPont originally produced Nafion® membranes using an extrusion casting technique, but recently solution-casting (dispersion) techniques have been employed to create membranes for RFBs (Harris et al., 2010; Carlson et al., 2005). The membrane selected for modeling was the Nafion® PFSA ionomer dispersion at approximately 30% water and isopropanol content and 40% solid weight (Carlson et al., 2005; DuPont, 2009). For every 0.5 m^2 of 1 mil Nafion® PFSA PEM produced, there is an estimated 0.125 kg of Nafion® required for production (DuPont, 2009; James and Kalinoski, 2009; DuPont, 2008). The selected manufacturing

method and operations are detailed in the discussion for Phase 3 of the cost modeling methodology.

Nafion® PEMs are currently used in a variety of applications. These include medical filtration devices, automobiles, flow batteries, hydrogen fuel cells, and proton passage components in VRBs (US DOE, 2011a; BTI, 2012; Houchins et al., 2012). In the all-vanadium redox flow battery, the PFSA PEM Nafion® membrane acts as a separator between the electrolytes, it keeps water permeability low, it provides resistance to prevent shorts in the cell, and it allows protons to pass between the half cells (Houchins et al., 2012). If the Nafion® membrane used is too thin, the quality may significantly decrease due an increased chance of pinholes and tears (Harris et al., 2010; Grot, 2003). A film backing is thus used to assist with the subsequent assembly operation (DuPont, 2008)

4.2.2 Phase 2: Investigate Component Literature

Phase 2 in the cost modeling methodology is to review publications for details on the selected components, review theoretical and current production methods, and review production methods for similar components.

4.2.2.1 Current Component Research

As mentioned above the three components investigated in this research are the graphite felt electrodes, NEG bipolar plates, and PFSA Nafion® proton exchange membranes. A brief discussion follows on current research and production methods for these components. Current suppliers have the capability to produce large volumes of felt electrodes and graphite bipolar plates, however, there have been shortages of these felts

for other products (Eckroad, 2007). Existing systems are typically set up for narrow web widths, and for components that may not be ideal for large scale stationary energy storage technologies, as the majority of the current research demand for these components comes from non-stationary fuel cell technologies (Houchins et al., 2012). PFSA PEMs for VRBs typically use DuPont's Nafion®, and they are not being produced at high volumes (Eckroad, 2007; Carlson et al., 2005; Chen et al., 2013). There is a considerable amount of research being done by researchers and commercial entities to improve Nafion® membranes, as well as to find alternatives that have similar or improved functionality (Houchins et al., 2012; Chen et al., 2013). DuPont currently has two production methods for Nafion® membranes: extrusion casting and dispersion casting (DuPont, 2009; DuPont, 2008). Membranes made with the extrusion casting method are made with a Nafion® mixture melted through a slot or die onto rolls (Harris, 2006). Membranes made with the dispersion casting method have Nafion® dispersions cast onto a polymer belt (Carlson et al., 2005; Curtin and Howard, 2003). Other methods have been theorized for large-scale production, which are similar to the dispersion casting method (Carlson et al., 2005; Harris et al., 2010). Naturally expanded graphite plates for VRBs can be made in a variety of methods, as discussed by Southworth et al. (Southworth et al., 2013c). Porous graphite felts in VRBs can be made from woven or nonwoven fiber precursors utilizing commonly available production methods (Carlson et al., 2005; Trapp et al., 2003; SGL Group, 2013b).

4.2.2.2 Current State of Manufacturing Methods for VRB Components

Industry currently uses emerging commercial technologies, scaled-up laboratory production processes, prototype systems, and production systems that are not designed for high volume output systems for the production of VRB components (Weber et al., 2011; Kear et al., 2011; Mohamed, 2012; Harris et al., 2010). Automotive fuel cell components are being mass produced (Harris et al., 2010; Carlson et al., 2005; James and Spisak, 2012; Sinha et al., 2009), and are in the same family of components as the selected VRB components considered herein. Some companies are producing the needed VRB components, while others are assembling entire VRB systems. Companies creating entire VRB systems include VRB Power Systems, Sumitomo Electric Industries, and Cellenium (Skyllas-Kazacos et al., 2011; Eckroad, 2007). Major companies that produce components for VRBs include GrafTech, DuPont, and SGL (SGL Group, 2012; DuPont, 2009; Orest Adrianowycz et al., 2010). Other suppliers create similar components for alternative solutions and traditional batteries, for instance, Asahi makes PFSA membranes for other PEMFCs (Hamrock and Yandrasits, 2006). Additionally, it is assumed that the individual cells are assembled directly after completion of the continuous web converting process; these are production processes where products are created in continuous widths and thicknesses, and then often rolled up and transported for subsequent processing (James and Kalinoski, 2009; Mercuri, 2008).

One potential manufacturing method for BPPs, with an optimistic demand of 1 GW/2 GWh capacity estimates the component pricing as $\$25/m^2$ (Viswanathan et al., 2012). One potential manufacturing method for BPPs, with an optimistic demand of 1 GW / 2

GWh puts and maximum current density of 300 mA cm^2, puts the component pricing at \$200 per m^2 (Viswanathan et al., 2012). Other typical costs are also described in the analysis and discussion portion of this work.

Limitations, some similar as those for BPP cost modeling exist for graphite felt electrodes. Prior cost models for transportation and storage systems are designed with different assumptions than the models reported herein. Woven carbon fiber precursors, for example, are produced with a hydrophobic treatment process (Carlson et al., 2005; Sinha et al., 2009). The graphite felt electrodes reviewed are for varying web widths and production volumes. Felt electrodes should be produced at cycle times equivalent to those for the other stack components and the primary VRB components to facilitate continuous manufacturing and assembly, while minimizing work in process inventory. One potential felt electrode manufacturing method, with an optimistic demand of 1 GW/2 GWh capacity estimates the component pricing as \$20/m^2 (Viswanathan et al., 2012). Other typical costs are discussed below.

Similarly, PEM cost modeling research is attendant with several limitations. Each of the seven cost categories (i.e., tool, facility, labor, maintenance, raw materials, consumables, and utilities costs) used in this research are not individually broken down in prior cost models for VRB and PEMFC component manufacturing. This reduced the ability of past work to identify certain cost drivers. Additionally, prior research did not investigate Nafion® membranes at a 0.5 m^2 surface area (typically much smaller areas are investigated and calculated for a scaled-up 1 m^2 surface area). Furthermore, the origins

of all cost value estimates are not clear, as well as what costs are from real equipment and what manufacturing methods are selected.

4.2.2.3 Current State of Component Costs

Current storage systems operate under a range of energy storage costs, energy transfer costs, and capabilities (Skyllas-Kazacos et al., 2011; Kear et al., 2011). The all-vanadium redox flow battery energy capital costs exceed U.S. DOE energy storage cost targets (US DOE, 2011a; Viswanathan et al., 2012).

4.2.3 Phase 3: Define the Production Method

Phase 3 of the cost modeling methodology is to select manufacturing methods, operations, and machine equipment to produce each component (Southworth et al., 2013b). Production methods are selected for each of the components based on an extensive literature review of publications and patents from the specific suppliers for each of the components. Next, the details of each manufacturing operation are determined based on current literature, with a focus on literature from manufacturers who supply the components used as a basis for the cost models. Once the manufacturing details are determined, cost model variable inputs are determined and the cost models are input into the spreadsheet model.

The naturally expanded graphite bipolar plate analyzed and discussed was selected from the same group of materials as the SGL graphite felt modeled in this research (SGL Group, 2012). It was modeled by Southworth et al. (Southworth et al., 2013c).

The spunlaced production method for impregnated nonwoven graphite felt, using GL GFD4.6 Polymer Precursor (SGL Group, 2012), of a size of 0.7 m x 0.7 m x 4.6 mm largely from SGL patents (Trapp et al., 2003), product literature (SGL Group, 2012; SGL Group, 2013c), and other sources for nonwoven felt production (James and Kalinoski, 2009; Mercuri, 2008; AUTEFA, ND; SGL Group, 2013d; Stry, 2013; McConnell, 2008; Dahiya et al., 2004; Kishio et al., 1989; Jonouchi et al., 1994; 2010; Calitzler, 2013; Lorenz et al., 2003). A continuous web converting method is selected to provide material to the cell assembly process (James and Kalinoski, 2009; Mercuri, 2008). Ten manufacturing processes, including four pieces of tension and feed equipment, are identified, as well as five raw materials, i.e., PANOX (oxidized PAN fiber) (Trapp et al., 2003; SGL Group, 2013d), PTFE prepreg agent, epoxy/resin prepreg agent, carbon powder prepreg agent, and distilled water. The first operation is fiber processing to open and handle the PANOX fiber, followed by continuous graphitization at 2300 ℃ (Trapp et al., 2003; Stry, 2013; McConnell, 2008). This converts the PANOX fiber into graphite fiber. Third is the airlay process, the web formation step (Dahiya et al., 2004; Kishio et al., 1989). Next, edge trimming is performed with a slitting machine (James and Kalinoski, 2009), followed by needle punching to felt the fibers with a pre-needler (Trapp et al., 2003; Jonouchi et al., 1994; AUTEFA). Next is a second edge trimming operation, followed by prepreg impregnation to B-stage (Trapp et al., 2003; Kishio et al., 1989; 2010; Calitzler, 2013; SGL Group, 2012). Nest is resin curing with infrared equipment at 160 ℃ (Lorenz et al., 2003), and then inline inspection for pinhole and thickness

detection is assumed. The last process is sheet cutting the webs to length. The process flow for the bipolar plate manufacturing method is shown in Figure 4.2.

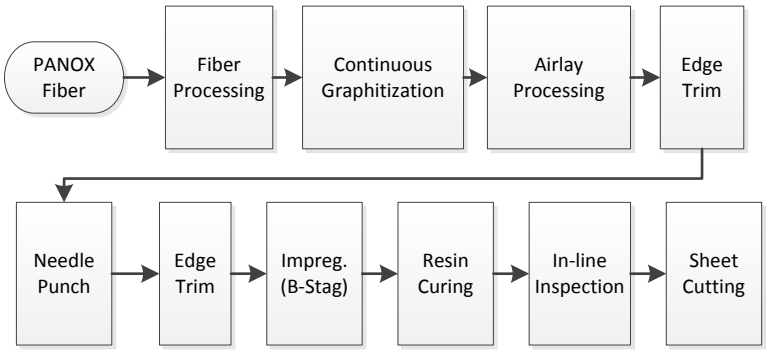

Figure 4.2: Felt Electrode Manufacturing Process Flow

(SGL Group, 2012; James and Kalinoski, 2009; Mercuri, 2008; Trapp et al., 2003; SGL Group, 2012; AUTEFA; SGL Group, 2013d; Stry, 2013; McConnell, 2008; Dahiya et al., 2004; Kishio et al., 1989; Jonouchi et al., 1994; 2010; Calitzler, 2013; Lorenz et al., 2003)

4.2.3.3 Membrane Production Method Selection

The PEM production method is largely selected from DuPont patents (Grot, 2003; Curtin and Howard, 2003) for 5 mil Nafion® PFSA, literature about DuPont's Nafion® membranes (Grot, 2003; Curtin, 2002; Ion-power, 2003), and cost model literature (Carlson et al., 2005; Sinha et al., 2009). A continuous web converting process is selected process to model costs (James and Kalinoski, 2009; Mercuri, 2008). For the selected manufacturing method, eight unique manufacturing processes, of which seven are repeated three times, and two raw materials are identified. The materials are the Nafion® PFSA ionomer dispersion at approximately 30% water and isopropanol and

40% solid weight (Carlson et al., 2005; DuPont, 2009), and a 2 mil silicone-coated PET backing film. The first process is film handling of the silicone-treated PET backing film (Carlson et al., 2005; Sinha et al., 2009; Grot, 2003; Curtin, 2002). Second is thickness measurement using a betagauge (Carlson et al., 2005; Curtin, 2002). Next is the dispersion layer coating on the PET backing film using a knife-over-edge roll coater; this process applies wet layers of the Nafion® ionomer that result in a final 1 mil dry thickness per pass (Carlson et al., 2005; Curtin, 2002). This is followed by a second thickness gauging step (Carlson et al., 2005; Curtin, 2002). Next is drying using infrared equipment (flash and full dry) and air cooling at 50, 110, and 20 ℃, respectively (Carlson et al., 2005; Grot, 2003; Kim et al., 2006; Ion-power, 2003). Next is moisture gauging to check the moisture (Carlson et al., 2005), and inspection for pinholes and thickness gauging (Carlson et al., 2005; Curtin, 2002; DuPont, 2012). Last is a sheet cutting step with a blade to cut the membranes to length (Ion-power, 1993). The process flow for the felt manufacturing is shown in Figure 4.3.

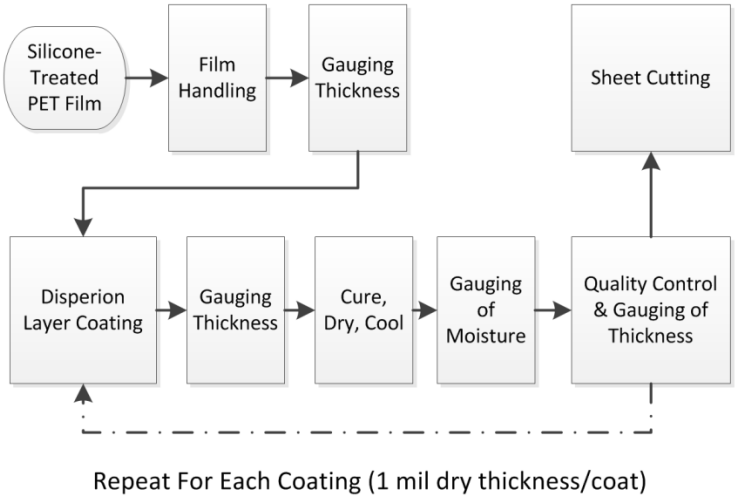

Figure 4.3: Membrane Manufacturing Process Flow

(Carlson et al., 2005; DuPont, 2009; Harris, 2006; Sinha et al., 2009; James and Kalinoski, 2009; Mercuri, 2008; Grot, 2003; Curtin and Howard, 2003; Curtin, 2002; DuPont, 2012; Ion-power, 1993; Kim et al., 2006; Ion-power, 2003)

4.2.4 Phase 4: Equipment and Raw Material Supplier Investigations

Phase 4 in this methodology is to contact suppliers to determine machine capabilities, capital costs, and specifications for each piece of equipment as needed for input parameters and cost category equations (Southworth et al., 2013a; Paul, 2013). Information was obtained from more than 50 equipment suppliers for the three cost models discussed in this work, including those for the bipolar plate reported in previous work (Southworth et al., 2013c). Other data from literature are used for the capital equipment and material costs (Carlson et al., 2005; Sinha et al., 2009; Trapp et al., 2003; Ottinger et al., 2004; James and Spisak, 2012; Ernst, 2009). Nafion® ionomer prices are reported in Table 4.2. Additional information gathered from supplier discussions and budgetary quotes are described in more detail by Southworth et al. (Southworth et al., 2013b).

The bipolar plate and felt electrode raw material prices are determined based on current pricing, while the membrane raw material cost is based on projected pricing. A summary of Nafion® cost estimates for high volume production of one million component (5 mil) membrane equivalents (0.125 kg) are reported in Table 4.2. The price reported in most

recent literature ($92/kg) is selected as the most likely future cost at the volume desired for this baseline cost model (James and Spisak, 2012; Ernst, 2009; Mathias et al., 2004).

Table 4.2: Nafion® Ionomer Price Projections

Projected Price ($/kg)	Year	Source	References
400	2002	DuPont	(Curtin, 2002)
~100	2004	GM	(Mathias et al., 2004)
80	2005	Tiax	(Carlson et al., 2005)
~75	2007	DuPont	(Eckroad, 2007)
75/92	2010	GM	(James and Spisak, 2012; Ernst, 2009)

4.2.5 Phase 5: Cost Model Spreadsheet Creation and Results

Phase 5 in this methodology is to develop a spreadsheet model that combines production and design inputs, process flow inputs, calculations, and results. A grouping of these spreadsheets is made for each of the cost models for the bipolar plate, felt electrode, and proton exchange membrane.

Model mathematical relationships calculate the cost for each category in detail for the VRB cell components. The unit costs can be compared in pie charts and bar charts to illustrate the cost drivers according to cost categories and manufacturing operations. The cost model can be used to explore the effect of changes of production volume on unit costs and cost drivers.

Production and design input criteria are selected as inputs to the baseline bottom-up cost model for each component. These inputs represent various production requirements, operation costs, raw material costs, facility construction/procurement costs, facility area

required per tool, tool installation costs, and tool costs. Common production and design inputs were reported by Southworth et al. (Southworth et al., 2013c). A detailed description of the production and design inputs used in these cost models were reported by Southworth et al. (Southworth et al., 2013b).

4.2.5.1 Process Flow Inputs

The process flow inputs worksheet provides a process flow map for each component, the baseline production line speed, critical dwell times used for thermal processing, and any scaled-up capital equipment costs. It can be noted that thermal processing equipment lengths are determined by multiplying dwell times by the line speed capability.

4.2.5.2 Bipolar Plate Process Flow Inputs

For the bipolar plate, the process flow inputs are selected and defined from the previous work (Southworth et al., 2013c). The baseline production line speed is 3 m/min., and an estimated $525,000 worth of equipment is found by scaling-up, or scaling down if necessary, equipment budgetary quotes provided by suppliers.

4.2.5.3 Felt Electrode Process Flow Inputs

For the felt electrode, the baseline production speed capability is assumed to be 10 m/min. based on a literature review of nonwoven felt production line capabilities (Cai et al., 2012; Harper, 2012; Stry, 2012). The felt electrode mass is determined to be 0.2125 kg/part (SGL Group, 2012). The inline graphitization furnace had baseline inputs of 2300 ℃ and a 1 minute dwell time (Stry, 2013; McConnell, 2008). Infrared resin curing occurs at 160 ℃, with a 10 minute dwell time selected (Lorenz et al., 2003). Scaled-up

capital equipment costs are calculated for the inline graphitization furnace and the infrared curing oven based on discussions with equipment suppliers. An inline graphitization furnace with 0.028 m^3 of working volume is $1.1 million. Scaling up the furnace to 0.044 m^3 of working volume using a scaling rule (Equation 3.9 in Southworth et al. (Southworth et al., 2013c)) results in a capital equipment cost at $1.7 million. An infrared curing oven at 1.22 m in length (at about a 0.7 width) is at $50,000. Scaling up this equipment to the needed 100 m length, results in a capital equipment cost of $4.1 million.

4.2.5.4 Membrane Process Flow Inputs

For the membrane, the baseline production speed of 6 m/min. is determined based on an estimation of line speed capability in 2006 (Harris, 2006). Another estimate of the likely capabilities for PFSA Nafion® membranes placed the line speed at 6 m/min. (Carlson et al., 2005), while other literature suggests line speed capability could range between 35 m/min. (James and Kalinoski, 2009) and 0.25 m/min. (Grot, 2003). The baseline infrared flash drying dwell time input of 30 minutes and full dry time input of 15 minutes are determined based on product literature (Ion-power, 2003). The baseline air dry time input of 5 minutes is determined from a previous cost model (Carlson et al., 2005). Per supplier literature, a curing oven of 1.2 by 3.1 meters is priced at $100,000 (Noblelight, ND), which scales up to a capital equipment cost of $5.1 million for a curing oven at 300 meter web length equivalent.

4.3 Results

Graphical results are output by the bottom-up cost models to illustrate the cost drivers for the various cost categories and manufacturing operations. Results reveal production trends, factory capital costs, scrap unit costs by process, and a unit cost comparison. The graphite bipolar plate, graphite felt electrode, and Nafion® PFSA PEM unit costs are estimated to be $4.93, $2.85, and $29.85, respectively.

4.3.1 Bipolar Plate Costs by Production Volumes

The estimated bipolar plate unit cost by annual production volume reveals diminishing unit cost reductions, and once a demand of 500,000 m^2 is reached, there is no reduction through 1,000,000 m^2 annual demand (see Figure 4.4 and Figure 4.5). An observable "knee" in the unit cost curve is observed when demand increases exponentially. This knee is assumed to occur when unit cost decreases by 4% or less with an increase in production volume at a logarithmic rate. This knee exists due to the law of diminishing returns, as applied to the unit costs of these components, when the components are needed at increasing volumes (Anderton, 2000).

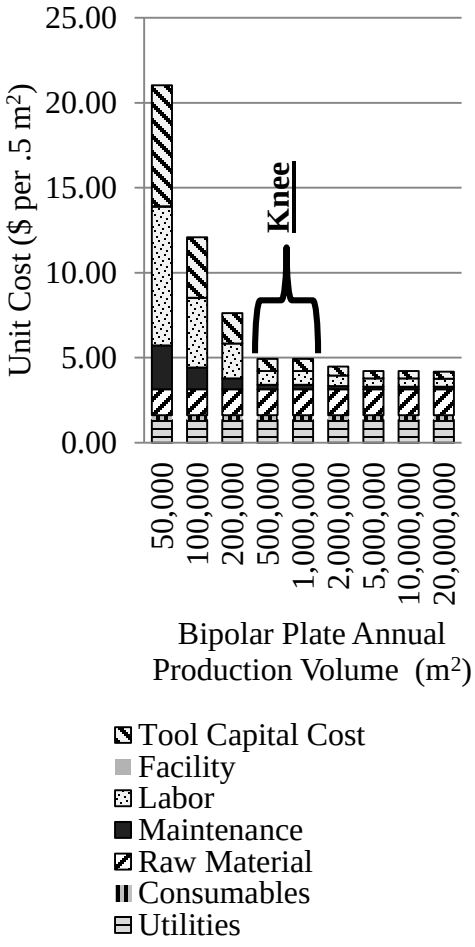

Figure 4.4 Bipolar Plate Unit Costs by Category, with Varied Annual Demand

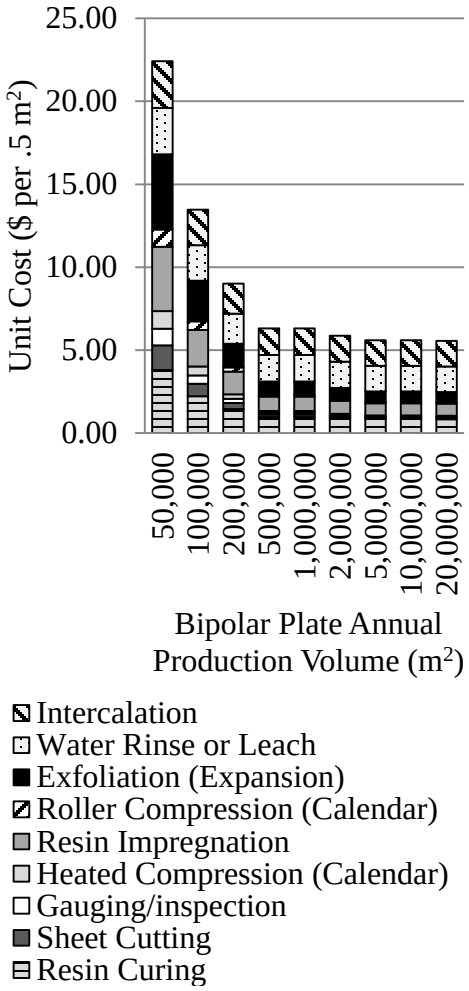

Figure 4.5: Bipolar Plate Unit Costs by Process, with Varied Annual Demand

The total capital cost to create a bipolar plate factory that can meet a 1,000,000 m^2 annual production volume demand, with a 3 m/min. production line rate and two production lines, is $13.87 million ($13.65 million capital tool and $0.22 million capital facility costs), as shown in Figure 4.6. When only one production line is needed, for lower annual production demand, the total capital cost is $6.93 million. At 2, 5, 10, and 20 million m^2 annual production demand, 3, 6, 12, and 23 duplicate production lines are needed, respectively.

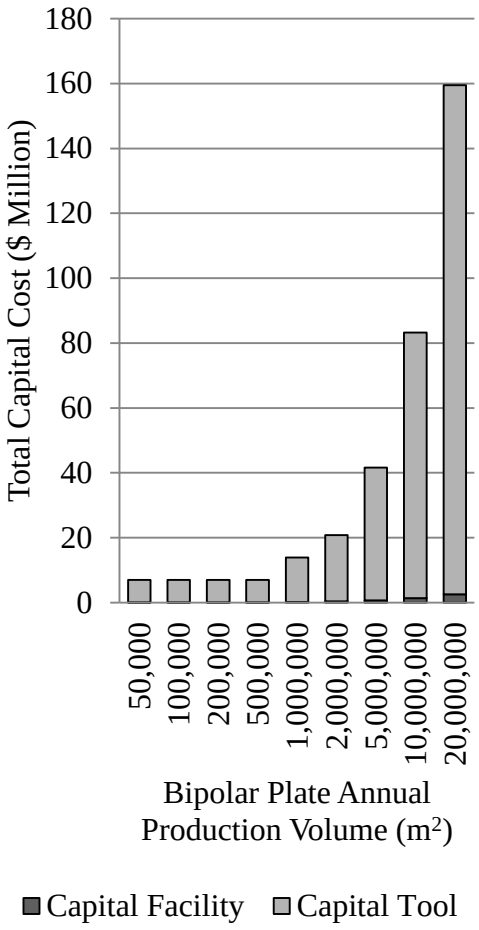

Figure 4.6: Bipolar Plate Capital Costs, 1 Plant, 3 m/min. Production Rate Capability

4.3.2 Felt Electrode Costs by Production Volumes

The estimated felt electrode unit cost by annual production volume reveals diminishing unit cost reductions once a demand of 2,000,000 m^2 is reached, there is a resulting knee (4% reduction) in unit cost between 2,000,000 and 5,000,000 m^2 annual demand (see Figure 4.7 and Figure 4.8).

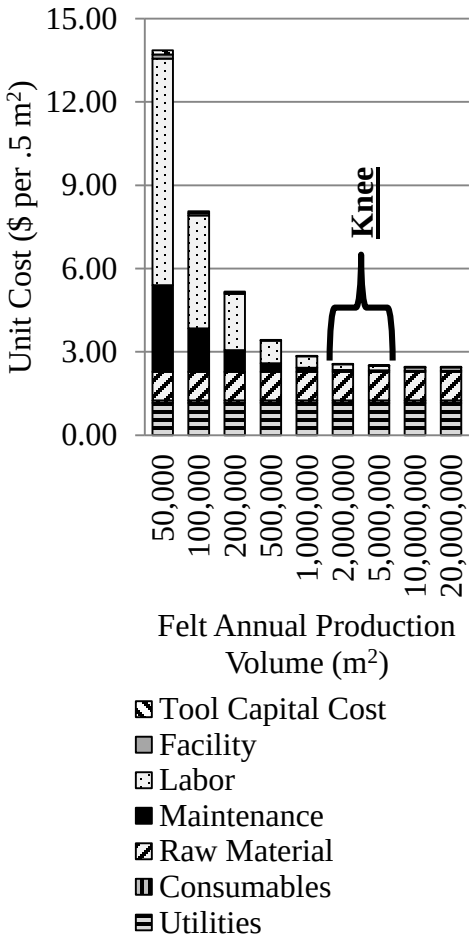

Figure 4.7: Felt Electrode Unit Costs by Category, with Varied Annual Demand

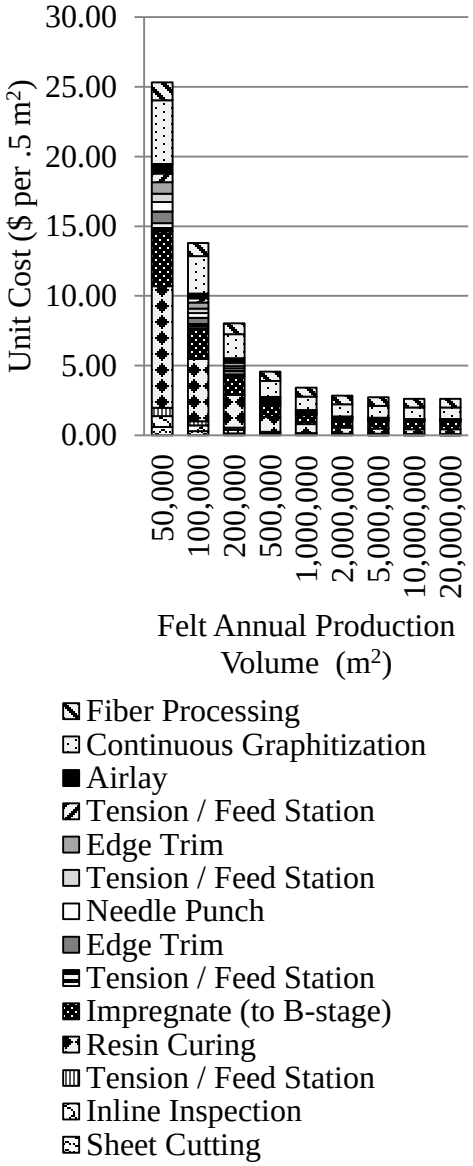

Figure 4.8: Felt Electrode Unit Costs by Process, with Varied Annual Demand

The total capital cost to create a felt electrode facility that can meet a 2,000,000 m^2 annual production volume demand, with a 10 m/min. line rate, using a single production line, is $8.70 million ($8.31 million capital tool and $0.39 million capital facility costs), as shown in Figure 4.9. Each additional production line would cost $8.60 million. There

are two, three, and six duplicate production lines are needed for 5, 10, and 20 million m^2 annual production volume demands, respectively.

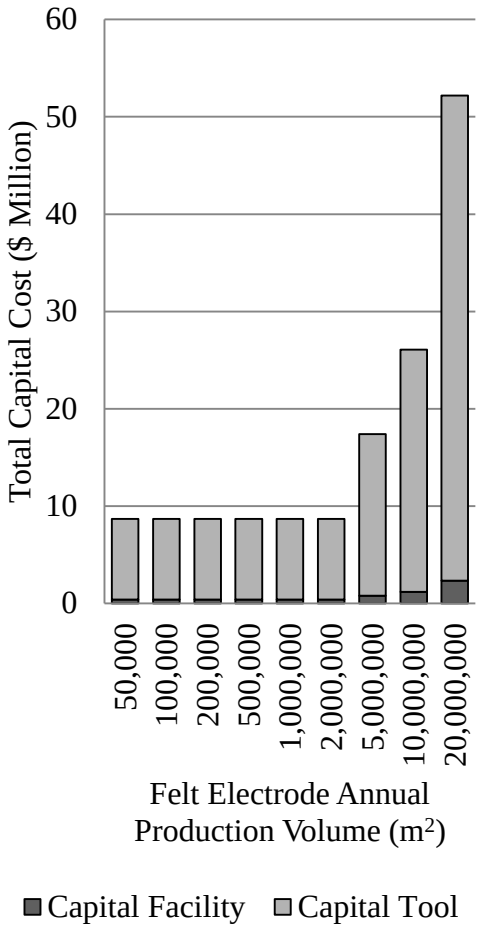

Figure 4.9: Felt Electrode Capital Costs, 1 Plant, 10 m/min Production Rate

4.3.3 Membrane Costs by Production Volumes

The estimated membrane unit cost by annual production volume demand reveals diminishing unit cost reductions once a demand of 2,000,000 m^2 is reached, there is a minimal reduction in unit cost between 2,000,000 and 5,000,000 m^2 annual demand (see Figure 4.10 and Figure 4.11).

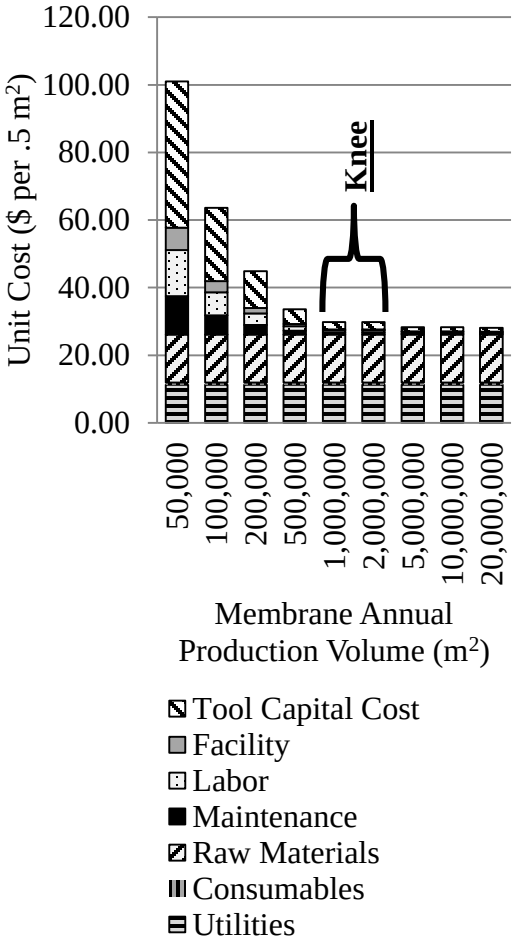

Figure 4.10: Membrane Unit Costs by Category, with Varied Annual Demand

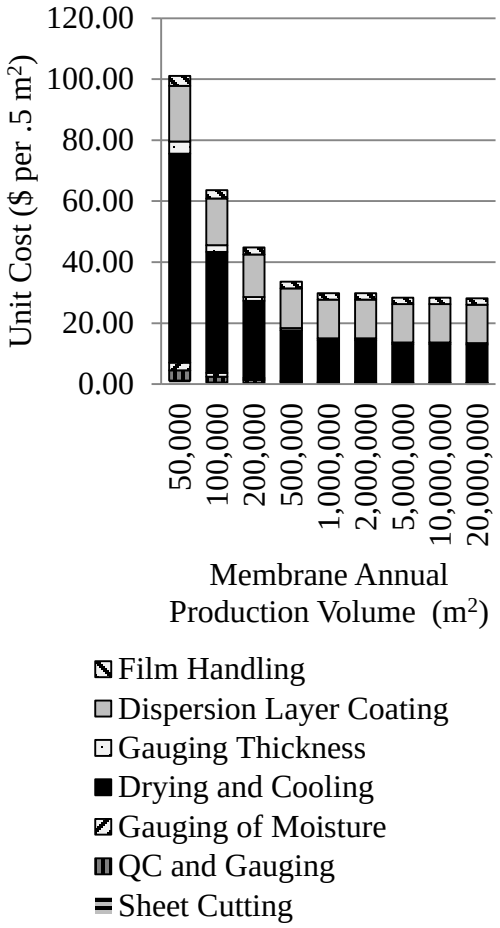

Figure 4.11: Membrane Unit Costs by Process, with Varied Annual Demand

The total capital cost to create a membrane production facility that can meet a 1,000,000 m^2 annual demand, using a 6 m/min. production line rate and one production line, is $47.75 million ($19.16 million capital tool and $28.59 million capital facility costs), as shown in Figure 4.12. Each additional production line costs another $47.75 million. Two, three, six, and eleven duplicate production lines are needed for 2, 5, 10, and 20 million m^2 annual production volume demands, respectively.

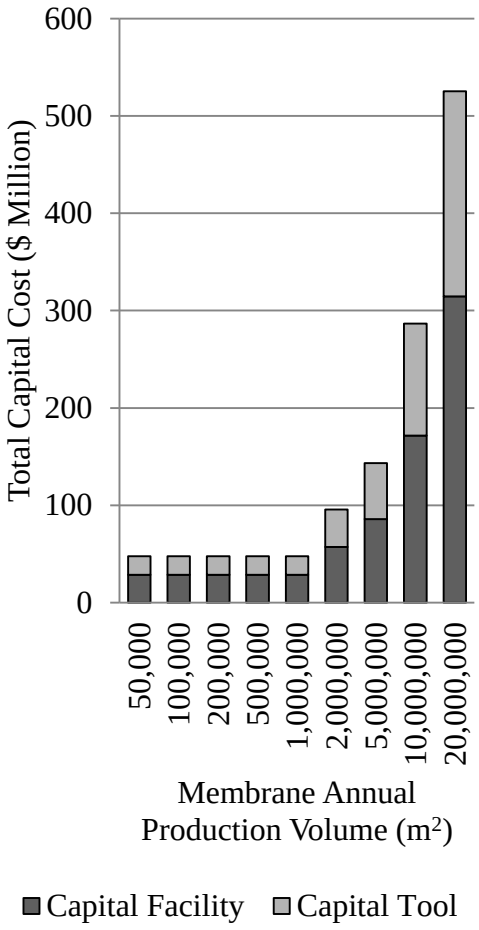

Figure 4.12: Membrane Capital Costs, 1 Plant, 6 m/min. Production Rate

4.3.4 Bipolar Plate Costs at 1 Million m^2 per Year

In addition to assessing the effect of production volume, the key cost drivers can be examined for the seven cost categories and various manufacturing operations. Model results reveal the cost drivers for the bipolar plate at a 1 million m^2 annual production volume, which are reported in more detail by Southworth et al. (Southworth et al., 2013c). By considering manufacturing process costs, without including raw material

costs, the cost drivers are continuous graphitization at 47.85% ($0.87/unit) and resin curing at 23.6% ($0.43/unit), as shown in Figure 4.13.

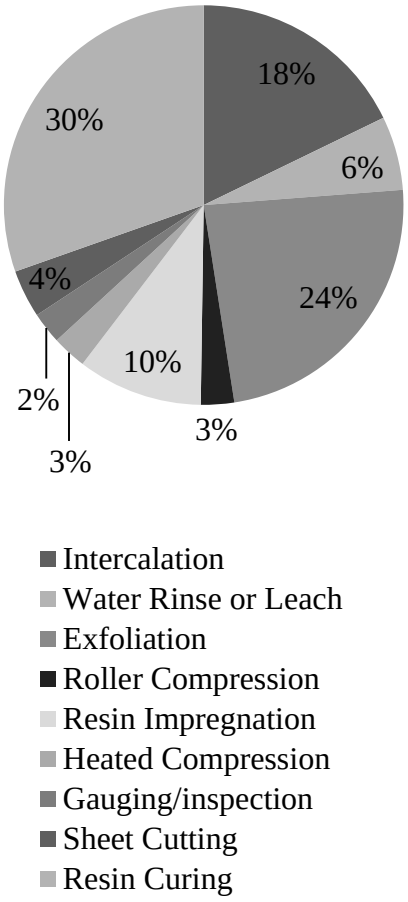

Figure 4.13: Bipolar Plate Cost Drivers by Process, No Raw Material

4.3.5 Felt Electrode Unit at 2 Million m^2 per Year

Similarly, graphical results for felt electrode manufacturing reveal the cost drivers at a 2 million m^2 annual production volume. As seen in 4.14, the key category cost drivers are utilities, at 40.7% ($1.16/unit), and raw material, at 35.9% ($1.02/unit). The manufacturing operation cost drivers are continuous graphitization, at 30.7% ($0.87/unit),

and fiber processing, at 21.8% ($0.62), as seen in Figure 4.15. If raw materials are separated from the manufacturing process costs, the cost drivers are continuous graphitization, at 47.85% ($0.87/unit), and resin curing, at 23.6% ($0.43/unit) (Figure 4.16).

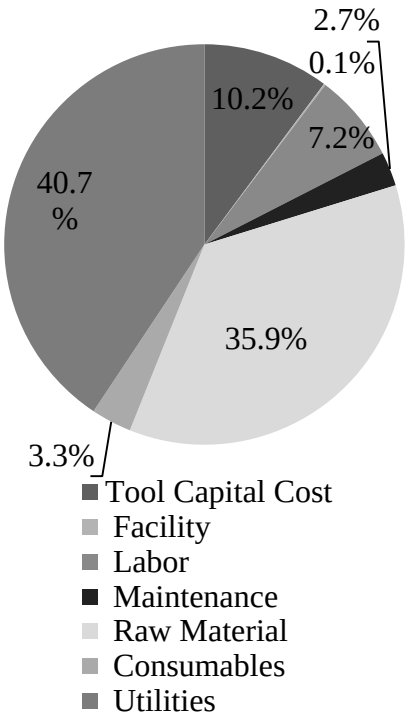

Figure 4.14: Felt Cost Drivers by Category

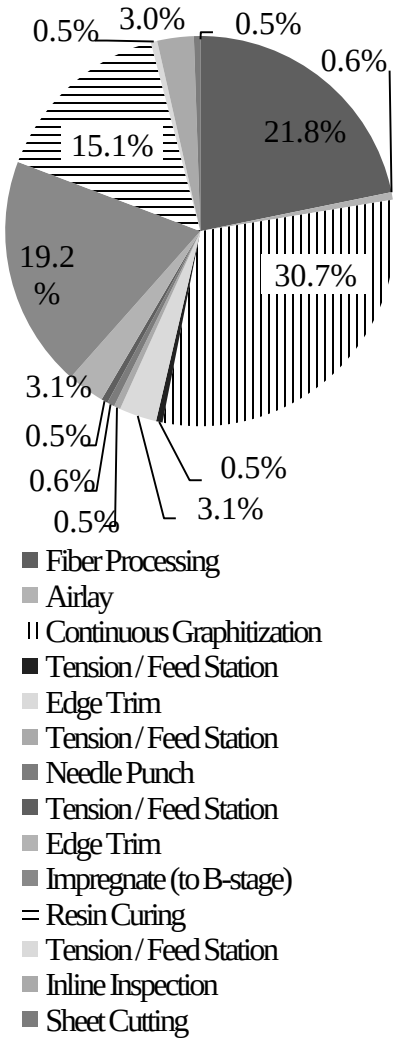

Figure 4.15: Felt Cost Drivers by Process, Raw Material Included

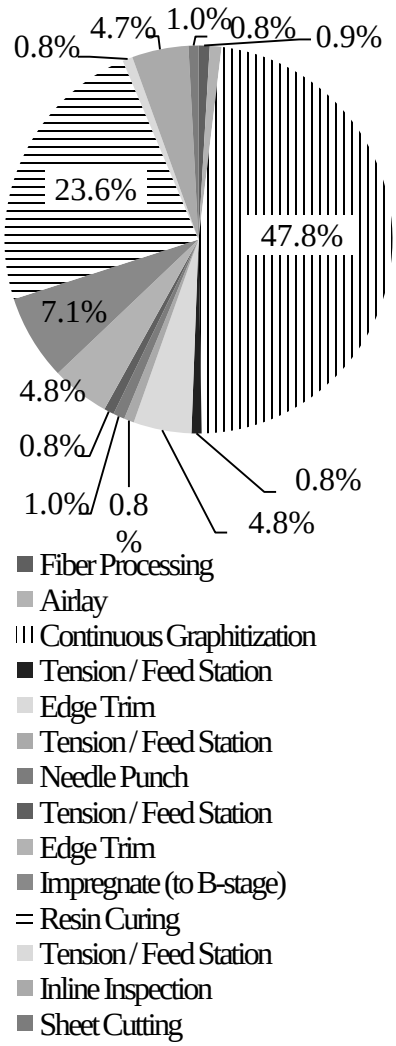

Figure 4.16: Felt Cost Drivers by Process, No Raw Material

4.3.6 Membrane Unit at 1 Million m^2 per Year

Modeling results reveal the cost drivers by category for the membrane at a 1 million m^2 annual production volume are the raw materials, at 47.5% ($14.18/unit), and utilities, at 37.8% ($11.29/unit), as seen in Figure 4.17. The manufacturing operation cost drivers are drying and cooling steps, at 45.9% ($13.69/unit), and fiber processing, at 42.7% ($12.75/unit), as seen in Figure 4.18. If raw materials are separated from the

manufacturing process costs, the cost drivers are the drying and cooling steps, at 87.4% ($13.69/unit), and gauging thickness steps, at 3.8% ($0.59/unit), as seen in Figure 4.19.

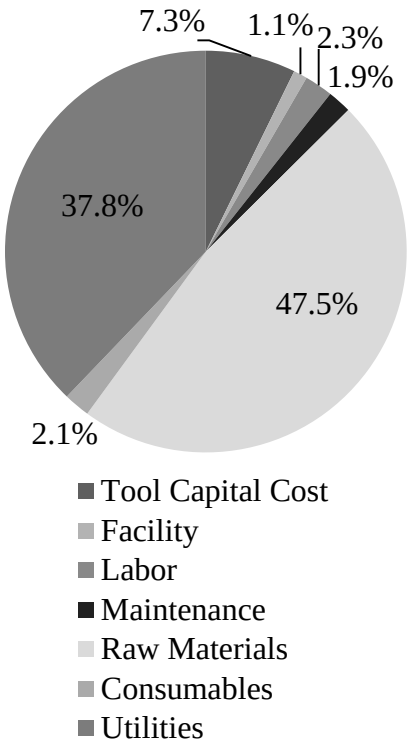

Figure 4.17: Membrane Cost Drivers by Category

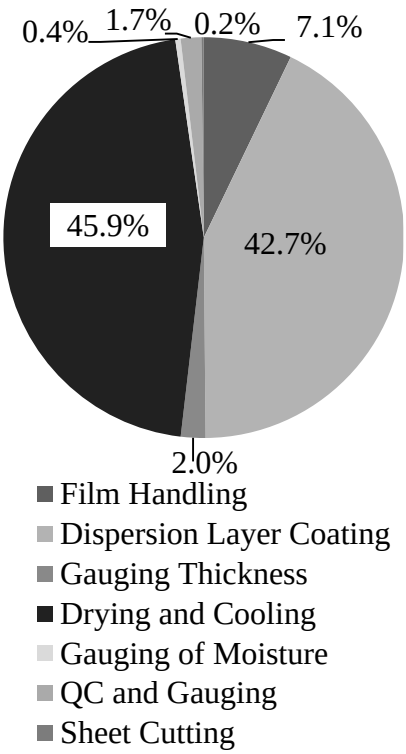

Figure 4.18: Membrane Cost Drivers by Process, Raw Material Included

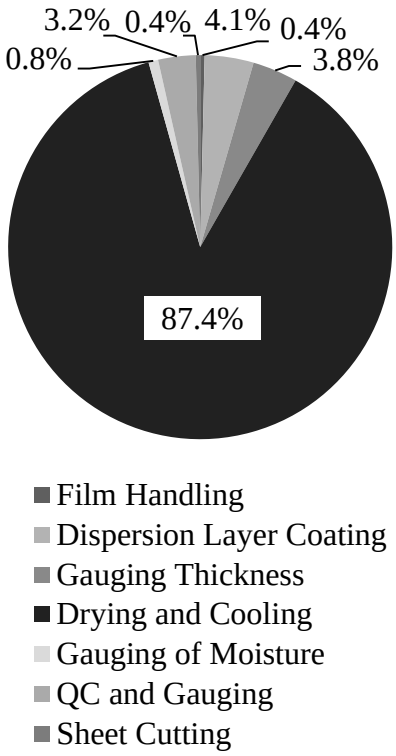

Figure 4.19: Membrane Cost Drivers by Process, No Raw Material

4.3.7 Cost Target Comparisons

The feasibility of producing the components is examined by reviewing three scenarios to calculate desired unit costs, as shown in Figure 4.20, Figure 4.21, and Figure 4.22. In Scenario 1, a VRB component cost breakdown based on the cost and performance model reported by PNNL (for a similar VRB system as specified here) is applied to OE's cost target (Viswanathan et al., 2012; US DOE, 2011a). In Scenario 2, the same component cost breakdown is used to compare the unit costs found in this research with Viswanathan et al.'s top-down model with equivalent demand. Scenario 3 shows the results from the cost models created in this research.

Specifically, Scenario 1 applies the Viswanathan et al.'s price breakdown to Viswanathan et al.'s optimistic performance target. In the Viswanathan et al.'s cost and performance model, one membrane is 44%, one bipolar plate is 6%, and two felt electrodes are 6% of total VRB system costs. The OE cost target (VRB performance target) of $1,250/kW (US DOE, 2011a) is then applied to the VRB system modeled in this research, resulting in a desired membrane price of $550, bipolar plate price of $75, and felt price of $37.5 per half-cell. Scenario 2 has the Viswanathan et al.'s price breakdown applied to the OE's cost performance target. This scenario represents Viswanathan et al.'s Gen. 1 VRB with 1 GW/2 GWh network performance (best case at $458/kW) applied to Viswanathan et al.'s Gen. 2 all-vanadium redox flow battery (VRB 1 MW/0.25 MWh component breakdown , 44%, 6%, 3% cost breakdown) (Viswanathan et al., 2012). The Gen. 2 VRB uses an improved electrolyte mixture, which results in a VRB unit membrane cost of $201.5, bipolar plate cost of $27.5, and felt cost of $13.7 (Viswanathan et al., 2012). Scenario 3 captures the results of the bottom-up cost models created in this research, which revealed costs of $2.85 , $29.85, $4.93, per part (per 0.5 m^2) for the bipolar plate, membrane, and felt electrode, respectively. It is important to note that scenario 3 does not include profit, indirect overhead, research and development, and other elements. These costs are considered optimistically low, as a high product demand is assumed.

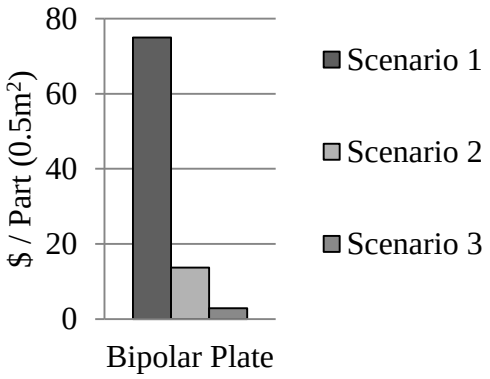

Figure 4.20: Bipolar Plate Cost Comparison

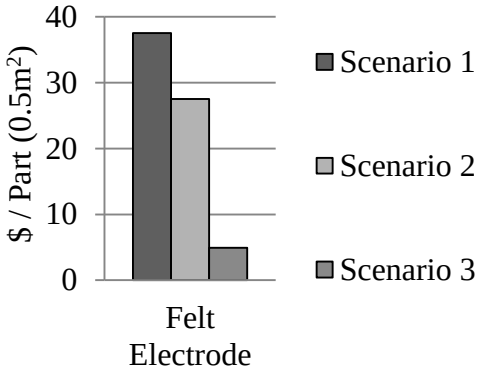

Figure 4.21: Felt Electrode Cost Comparison

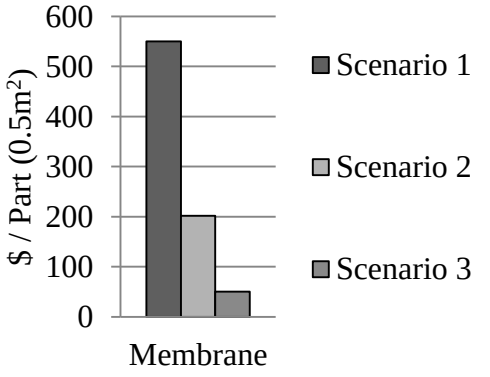

Figure 4.22: Membrane Cost Comparison

4.4 Analysis and Discussion

VRB cost modeling results can be analyzed for unit cost comparisons, cost drivers, cost reduction opportunities, cost trends, and process improvement opportunities. The cost model for each component has its unique strengths, weaknesses, and assumptions.

4.4.1 Category Cost Drivers

The top category cost drivers for each of the components are the raw materials and utilities. Specifically, the bipolar plate raw materials and utilities costs were 30.9% and 27.1% of total cost, respectively, when producing 2 million parts per year (Southworth et al., 2013c). The felt raw materials and utilities costs were 35.9% and 40.7%, respectively, at 4 million parts per year (Figure 4.14). The membrane raw materials and utilities costs were 47.5% and 37.8%, respectively, at 2 million parts per year (Figure 4.17). Thus, raw material and utility costs should be investigated for potential cost reduction opportunities. Alternative types of equipment should be investigated for thermal processing operations. For example, hybrid gas and electric ovens could significantly reduce electricity use and associated utility costs, with a marginal increase in energy costs due to natural gas (based on discussions with equipment suppliers).

4.4.2 Process Cost Drivers

Process cost drivers are identified with the cost models. Each component had independent manufacturing lines. Raw materials are found to be the largest contributor to component manufacturing costs. Specifically, the top process cost drivers for bipolar plate production are intercalation and exfoliation at 35% and 20%, respectively (Southworth et al., 2013c). The top process cost drivers for felt production are continuous

graphitization and needle punch at 30.7% and 21.8%, respectively (Figure 4.15). The top process cost drivers for membrane production are drying/cooling and dispersion layer coating at 45.9% and 42.7%, respectively (Figure 4.18). It can be concluded that operations related to thermal processing are the key drivers of manufacturing cost for all three components. This shows that further research is needed to investigate the advantages and disadvantages of using various production equipment and component designs for VRBs.

4.4.3 Unit Cost Comparisons

The unit costs for the bipolar plate, felt, and membrane are found to be $4.93, $2.85, and $29.85 per part respectively. The membrane is clearly the most expensive of these components, followed by the bipolar plate and felt. The results show unit prices based on PNNL top-down cost model are roughly five times higher than the unit costs calculated using the baseline bottom-up cost model. It is predicted that component costs can meet the DOE/OE cost targets for 2015 (US DOE, 2011a) when applying the PNNL cost and performance model (Viswanathan et al., 2012) and when applying the baseline cost model developed in this research. It was found that when the raw material input price for the membrane, the most expensive component, varied from current pricing to the best realistic case for the projected future high volume pricing, a 49% reduction in the combined cost of these stack components is seen, including a 75% reduction in the membrane cost.

To validate the accuracy of the cost model results, calculated component costs are compared to those using other top-down and bottom-up cost modeling methods. The

average projected bipolar plate cost was found to be $9.50 per unit (Southworth et al., 2013c), which is almost double the estimated unit cost ($4.93) found using the model developed here. The average felt/cloth reviewed had a cost of $8.00 per unit (Table 4.3), which is about two and a half times higher than the estimated unit cost ($2.85) found using the model developed here. The average equivalent (adjusted for thickness) Nafion® PFSA PEM reviewed had a cost of $31.40 per unit (Table 4.4), which is slightly higher than the estimated unit cost ($29.85) found using the model developed here. These results indicate that the cost models created in this research are able to generate results that are similar to cost models developed by other researchers for similar components. The unit costs predicted using the model developed in this research were expected to be lower, since they consider costs from the unit process level and do not include other costs, e.g., indirect overhead and taxes, as some of the other models. The membrane costs are likely similar due to the reliance of these models on the same Nafion® price projections (Nafion ® is the major contributor to cost).

Table 4.3: Felt Electrode Cost Comparison

Annual Prod. Volume per Cross Section	Model Component Detail	Primary Material Used	Material Price ($/kg)	Unit Cost ($ / 0.5 m^2)	Ref.
4 million, 0.5 m^2	Impreg. nonwoven graphite felt	PANOX	2	2.85	This work
(over 1 million) ~323 cm^2	Woven carbon	Woven carbon fiber	30	9.7	(Carlson et al., 2005)
370 million, ~335 cm^2	-	-	-	5.5	(James and Spisak, 2012)
(High volume)	-	Woven graphite fiber	-	7.75	(Ernst, 2009)
219 million, ~277 cm^2	Woven carbon	Woven carbon fiber	20	6.74	(Sinha et al., 2009)
Not specified	-	-	-	10	(Viswanathan et al., 2012)

Table 4.4: Membrane Cost Comparison

Annual Prod. Volume per Cross Section	Model Component Detail	Primary Material Used	Material Price ($/kg)	Unit Cost ($ / 0.5 m^2)	Ref.
2 million, 0.5 m^2	5 mil thick	Nafion® ionomer	92	29.85	This work
(over .5 million), ~323 cm^2	2 mil thick	Nafion® ionomer	80	11.69	(Carlson et al., 2005)
370 million, ~335 cm^2	1 mil thick	Nafion® ionomer	75	9.09	(James and Spisak, 2012)
108 million, ~277 cm^2	2 mil thick	Nafion® ionomer	25	7.84	(Sinha et al., 2009)
Not specified	-	Nafion® ionomer	-	100	(Viswanathan et al., 2012)

4.4.4 Cost Trends

The predicted effect of increasing annual production demand reveals when production volume increases there is a diminishing cost reduction benefit (Figure 4.23, Figure 4.24, and Figure 4.25). The presence of this "knee" shows when economies of scale effects are no longer beneficial. Thus, annual demand has implications for the cost drivers related to the technological and production capabilities of the selected manufacturing system. If product demand is below the knee in the curve, then adding more capital equipment to a manufacturing system should result in a significant reduction in the unit cost (Anderton, 2000).

Investigating the predicted level of demand is significant because it will indicate the best likely type of cost reduction strategy. If the demand is greater than where the knee in the curve is positioned, then a capital cost improvement is expected to have an insignificant cost reduction. For the membrane, Figure 4.24 shows that a decreasing reduction in the unit cost is projected as the raw material pricing inputs are reduced; a 63% and 76% reduction in Nafion® ionomer pricing results in a 41% and 49% price reduction. Thus, the nonlinear benefit of reducing raw material price shows that it is important to investigate process-related cost reduction opportunities.

4.4.5 Cost Reduction Opportunities

The analysis of results reveals several cost reduction opportunities. The primary opportunities are related to raw material pricing, raw material selection, equipment utility sources, and manufacturing operations that use thermal operations as shown by the variable inputs and process cost drivers. Raw material prices may be reduced if larger

volumes of materials are ordered for the silicone-coated PET film (Carlson et al., 2005; DuPont, 2008; Grot, 2003), for the resins in the electrode and bipolar plate, and for Nafion® ionomer. Alternatives to high cost materials, such as Nafion®, PET film, and resins could significantly reduce the VRB system costs. Thermal processes have been identified as the bottleneck for each of the production flows. If larger pieces of equipment are used, or methods of producing the components with shorter dwell times are found, the unit cost would be significantly reduced for each component. Also, the knee in the annual production volume curves are near the annual demands, which means equipment capabilities and designs should be reviewed for potential cost reductions. Specifically, doubling web width is projected to reduce bipolar plate cost significantly (11%). Finally, high capital costs for each of the manufacturing lines in the baseline cost models are primarily driven by the thermal processing steps. Specifically, 66%, 73%, and 93%, respectively, of bipolar plate, felt, and membrane capital costs result from thermal processing equipment.

4.4.6 Strengths of Results

The cost model results are strengthened by the research methodology, justification found for each model input, supporting ranges of values found, and selection of real-world values of cost-effective manufacturing methods and inputs. Varying sources are found for each cost category and piece of equipment, when possible. A detailed justification is provided for each cost characteristic and data point that is used. The equations and cost categories selected have been verified here and in prior MBI research. Other literature sources and supplier component costs are reviewed to validate the results. As discussed,

these bipolar plate, felt electrode, and membrane unit costs calculated are roughly two times, 2.5 times, and the same as those found from similar cost models, respectively, which strengthens the results. Sensitivity analysis is conducted below to further validate the findings in this research.

4.4.7 Assumptions

Assumptions are made for each of the baseline cost models to resolve ambiguous information, account for information gaps, or simplify the cost models. When possible, correlations are made and detailed justifications are identified for each assumption. One major assumption is that the manufacturing methods modeled represent mature systems, and second is that a new, prototyped Nafion® PFSA proton exchange membrane is used (Carlson et al., 2005). In addition, floor space for raw materials, automated component handling steps, and the assembly operation following component production were not accounted for. Assumptions are discussed in detail by Southworth et al. (Southworth et al., 2013b).

4.4.8 Sensitivity, Validation, and Statistical Analysis

Tornado charts and Monte Carlo simulations are conducted to demonstrate the utility and relevance of the cost models as estimation tools. They show the sensitivity of the selected product, design, and process inputs. Additionally, various other literature sources have identified unit costs for similar types of components at large quantities. The baseline unit cost found in this research is in range of what prior literature found for similar components at similar volumes.

4.4.8.1 Tornado Chart

Tornado charts, which graphically depict the significance of various cost contributors, are made for each of the baseline cost models to assist with the parameter sensitivity analysis. The product, design, and process inputs are modified one at a time to find the unit cost values. The bipolar plate cost is by far the most sensitive to graphite flake price (Figure 4.23). The felt electrode cost is most sensitive to the web width (Figure 4.24). The membrane is by far the most sensitive to the Nafion® ionomer price (Figure 4.25). In producing the tornado charts, the size and cost of the thermal processing equipment was adjusted according to production line parameters. Second, when the web widths are increased, Equation 3.9 is used to adjust capital equipment costs.

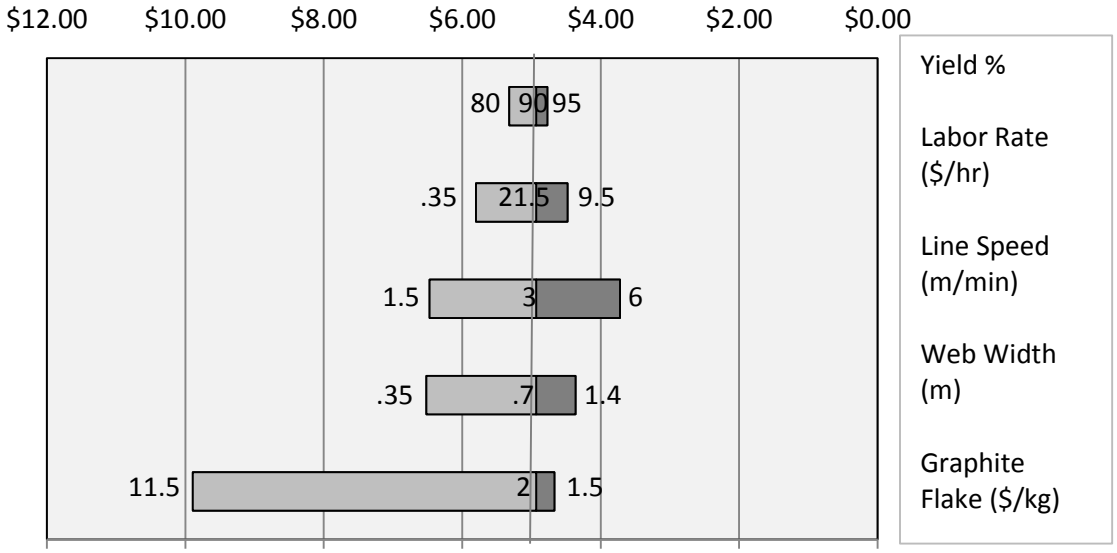

Figure 4.23: Bipolar Plate Unit Cost Tornado Chart, at 2 million m^2 Annual Demand

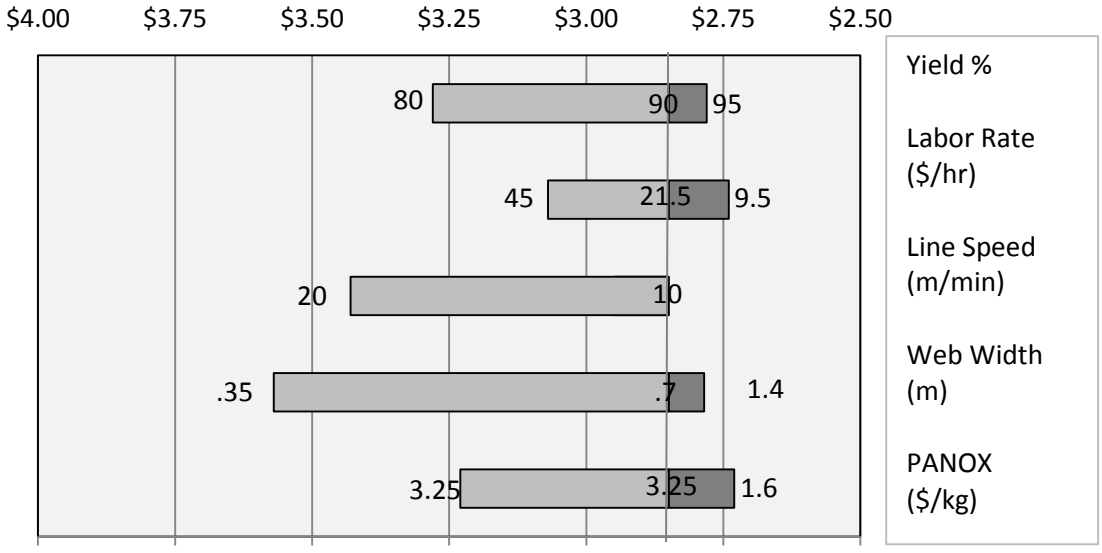

Figure 4.24: Felt Electrode Unit Cost Tornado Chart, at 4 million m^2 Annual Demand

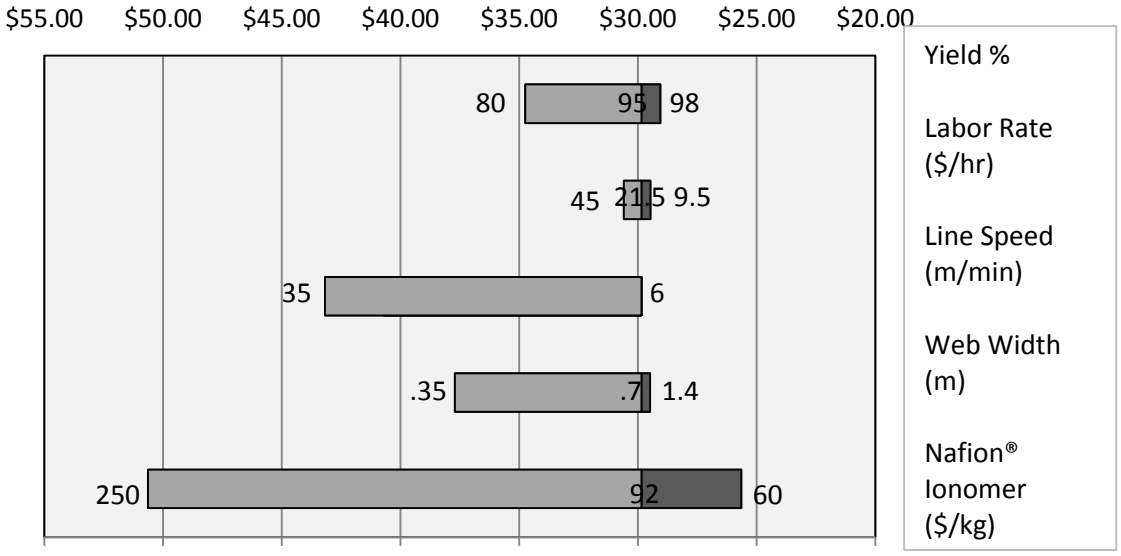

Figure 4.25: Membrane Unit Cost Tornado Chart, at 2 million m^2 Annual Demand (0.25 kg Nafion® / Part)

4.4.9.2 Monte Carlo Simulation

Monte Carlo simulations (5,000 trials) were performed assuming a triangular probability distribution for the major input parameters in each of the three cost models, as described by Southworth et al. (Southworth et al., 2013b). Simulations were produced using MS-Excel, and the primary raw material, days per year, hours per day, line speed, labor rate, and percent yield were the selected parameters explored for each of the models. The bipolar plate analysis shows with a 95% certainty that the unit cost would not exceed $6.24 per part, given the range of components used. The bipolar plate results form a bimodal distribution, the left peak represents the situation where one production line is used, while the right is for two production lines. The felt electrode simulation shows with a 95% certainty that the unit cost would not exceed $3.68 per part. The membrane cost results are skewed to the left, likely because of the large discrepancies between the

probable high and low line speeds. The membrane results show with a 95% certainty that the unit costs would not exceed $35.69 per part.

4.4.9.3 Sensitivity, Validation, and Statistical Analysis Summary

The tornado charts reveal that the raw material, line speed, and web width are the most sensitive parameters for these three cost models. The Monte Carlo simulation shows that all three components can meet the DOE cost targets, even at the low-probability high-cost values, and the results show the number of manufacturing lines has a significant impact on the sensitivity of the unit costs.

For further validation of the accuracy of the cost models, the paper by Viswanathan et al. suggests the OE cost targets can be met with current G1 VRB capabilities (Viswanathan et al., 2012). If the best G1 VRB case presented by Viswanathan et al. of $458/kW has the same cost breakdown applied, then, a bipolar plate price of $27.50, a felt price of $13.70, and a membrane price of $201.50 are found. The prices in the work by Viswanathan et al. are about five times higher than the bottom-down process-based model results done in this research. This confirms the accuracy of the results in this research, as a component price should be at least several times higher than its cost (as the cost does not include profit, overhead, taxes, and other costs that are included in the component prices).

The membrane raw material costs are the most sensitive cost category, and Nafion® raw material is the most sensitive parameter for the membrane, the most expensive component reviewed in the cell stacks. The membrane unit cost fluctuates between

$25.64, $29.85, and $50.64 when Nafion® costs is modified, as shown in Figure 4.26 (Southworth et al., 2013b). Monte Carlo simulation (Southworth et al., 2013b) also shows that the membrane unit costs vary between $16.10 and $35.69 (with $23.46 as the most likely value), when seven of the major parameters are changed. This shows that if the current Nafion® ionomer costs of $250/kg does not decrease, it may still be possible to reduce PEM costs to $50 or lower per 0.5 m^2.

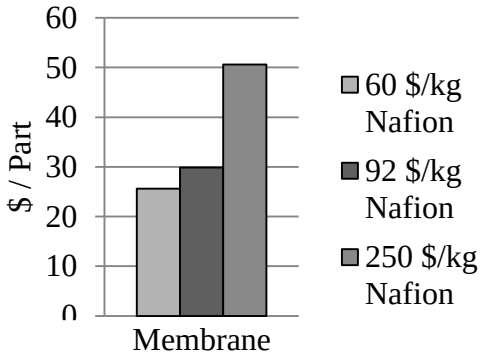

Figure 4.26: Membrane Unit Costs at Various Raw Material Prices

4.5 Conclusion

The analysis of cost modeling results reveals that OE 2015 cost targets (US DOE, 2011a) can theoretically be met for the graphite impregnated bipolar plate, soft graphite felt electrode, and PFSA proton exchange membrane. The bottom-up process-based cost model results show unit costs (0.5 m^2/part) of $4.93, $2.85, $29.85, for the bipolar plate, felt electrode, and membrane, respectively. These costs are considered optimistic, as a high product demand is assumed, using a 1 GW/250 MWh VRB network based on a performance model development at PNNL for a current density of 300 mA/cm^2

(Viswanathan et al., 2012). This work confirms that it is feasible to meet DOE cost performance targets for the three components when targets are applied to prior performance and cost model values (Viswanathan et al., 2012). The estimated process-based costs do not include profit, indirect overhead, taxes/regulatory fees, and research and development costs. Thus, predicted costs are over ten times lower than DOE component cost targets when the component cost breakdown from prior work for a similar Gen 2 VRB system (Viswanathan et al., 2012) is applied to the OE cost target of $1,250/kw (US DOE, 2011a). The work by Viswanathan et al. also suggests DOE cost targets can be met with current G1 VRB capabilities (Viswanathan et al., 2012).

Although recent work has suggested that the PEM cannot see a large decrease in costs, the results and sensitivity analysis show that a 40% reduction in costs may be possible, even if the Nafion® cost does not decrease. This decrease in cost can only be seen if a new manufacturing method is used, however, such as one suggested by Carlson et al. (Carlson et al., 2005). Predicted unit cost results can change depending on the level of optimism used for each cost characteristic input, as most of the data and input values used in the cost models occur over a range. The top cost drivers for the bipolar plate, felt electrode, and proton exchange membrane are found to be raw material costs, utility costs, and thermal processing.

These cost drivers give different regions, countries, and businesses varying competitive advantages for the production of these components. A country that produces lower cost materials (the primary cost driver), such as raw graphite flakes, PTFE, sulfuric acid, and acrylonitrile would have an advantage over other countries. A country that has low

utility costs (the secondary cost driver), such as electricity, natural gas, compressed air, would also have an advantage. Additionally, a business or country that has greater access to capital for investments would have an advantage in construction of the facilities and purchasing of the equipment needed. This advantage would be particularly true for meeting demands over 5 million m^2 for these components, since the knee in the cost curve is well below this level for each component. Competitive advantages for the production of these components could be achieved by investing in methods to produce lower cost raw materials and utilities, and providing capital for facility investment and investment into technologies to decrease energy requirements for large-scale thermal processing operations.

Cost reduction opportunities include investigating new and alternative manufacturing methods that are connected to cost drivers, and optimizing the most sensitive cost model parameters. The most sensitive production, design, and process inputs for the bipolar plate, felt electrode, and PEM are the graphite flakes, web width, and Nafion® ionomer costs, respectively. The bottom-up cost model analysis reveals that increasing equipment capabilities could result in a greater cost reduction than by increasing the capital and facility expenditures to purchase more equipment for the bipolar plate, due to the knee in the production curves occurring well before annual production demand. This knee exists due to the law of diminishing returns, as applied to the unit costs of these components, where the components are needed at increasing volumes (Anderton, 2000). Sensitivity analysis found yields of 95%, 98%, and 98% decrease the unit costs by 3.2%, 2.5%, and 2.7% for the bipolar plate, felt electrode, and membrane, respectively. This research also

identifies areas of potential manufacturing technology limitations, which are primarily thermal processing bottlenecks and manufacturing line speed capabilities.

The cost model analysis suggests that implementing alternative manufacturing operations and manufacturing methods could reduce costs. For the bipolar plate, a stamping operation could be used to create flow channels (Orest Adrianowycz et al., 2010). Felts could be created by hydrolyzing woven fiber (Carlson et al., 2005). Membranes could be produced by alternative dispersion methods or with an alternative to Nafion®. The major limitations of the three cost models stem from the assumptions made, with a lack of real world validation, due to the developmental nature of VRB technology. Future research should investigate and validate the assumptions made, validate cost model results from actual prototypes, or compare results to supplier costs for the actual components modeled.

Acknowledgements

The authors from Oregon State University (OSU) gratefully thank the support of the Pacific Northwest National Laboratory (PNNL) for their support of this research. The authors express appreciation to Ms. Qi Gao and Mr. Babak Lajevardi from OSU for their insights into bottom-up process-based methodologies. Also, gratitude is extended to the many unnamed suppliers and their representatives who were extremely helpful in offering insights into their industries, equipment, and materials.

Chapter 5: Conclusions

5.1 Summary

Energy demands are continuously increasing worldwide. Governments and private companies see the need for renewable and sustainable energy development. Programs and money are being used to assist with the implementation and technological development of products and systems that are needed to facilitate the use of these resources (US DOE, 2011a). Proton exchange membrane systems, redox flow batteries, and vanadium redox flow batteries each have specific technological and practical challenges that need to be overcome so they can be used to help promote the use of renewable energy resources (Weber et al., 2011). Currently, PEMFCs, RFBs, and VRBs are too expensive, according to the DOE (US DOE, 2011a; (Houchins et al., 2012; Nexight Group, 2010), to be used effectively to compete with alternative technologies (Greene et al., 2011; US DOE, 2011b). There is a need for a simplified estimation tool to compare technologies and manufacturing methods for these emerging energy storage systems. Specifically, the cost modeling methodology developed in this work is demonstrated to support the development of such a tool for analyzing the component manufacturing costs for RFB systems. Cost models can assist companies entering into the market by demonstrating the impacts of various competitive strategies, and their advantages, help researchers identify cost drivers to investigate, and reveal trends and predictions of when these technologies will be usable.

Managers and other decisions makers can incorporate the bottom-up cost models into their decisions and analysis. One tool that could be integrated with the cost models to

assist decision making is the balanced score card (BSC). The BSC is a management tool that generally analyzes metrics in four perspectives: customer, business, learning and growth, and financial. The BSC communicates targets from each of these perspectives with numerical measurements to show the status and improvements that are undertaken in a company. (Niven, 2006)

If these models are used along with the BSC, managers can link categories and scores in each of the four perspectives to estimated costs and profits for their products. Potential paths forward can be determined by manipulating the design and process input parameters in the cost model to determine what is the most beneficial for the company. These decisions may include internal business targets and capabilities, as well as financial considerations, such as needed capital, cost of raw materials, cost of maintenance, and cost of utilities. Furthermore, the cost models can strengthen the results in a balance scorecard, as learning and growth factors, such as efficiencies (linked to cycle times), machine maintenance (preventing downtime), and product yields can be shown to each directly affect an estimated product unit cost in a wide variety of situations. (Niven, 2006)

Finally, the annual production volume, driven by market (customer) demand, and target selling price can be directly tied to estimated component unit costs and profits, from the manipulation of model input parameters. With the assistance of the cost models, managers can better communicate a direct link between various strategic and employee driven activities to the short and long term costs. This improved communication can be used to motivate people from each of the BSC's perspectives to take actions to improve

the performance of a company and to incorporate cost reduction tasks, as actions and performance targets can be linked directly to product costs and profits (Niven, 2006).

The cost models developed in this research focus on finding the bottom-level equipment and manufacturing process costs that compose the overall production cost of vanadium redox flow battery (VRB) components. Discussions with equipment suppliers, obtaining equipment supplier budgetary quotes and literature, and identifying additional literature sources are strategies used to determine the values within each of seven cost categories for the major structural and functional components in a VRB. These values are combined, and unit costs are calculated using a spreadsheet model (MS-Excel) and calculations from typical equations and values reported in prior work (Lajevardi et al., 2011; Paul, 2013; Lieth et al., 2010). The outcome of the research includes three cost models, one each for the graphite bipolar plates that are impregnated with resin, soft porous graphite felt electrodes that are impregnated, and PFSA PEMs. In addition, conclusions are drawn about the utility of the models, cost drivers and trends elucidated from application of the models, and potential for continued improvement of the tool and methodology.

5.1.2 Weaknesses and Improvement Opportunities

Weaknesses and improvement opportunities exist throughout each cost model because they are designed to be baseline cost models for use as estimation tools. For the purposes of this research, the estimations and assumptions provide reasonable values. There is a need to reduce some of the major assumptions, and to further verify the accuracy of results by comparing them to production systems already operational for these types of

components. Additionally, certain manufacturing operations are simplified in this research, and, in some cases, only literature sources are used for equipment capital information. For this research, existing calculations are incorporated into continuous production line cost models; the equations could be improved by modifying them for this application. The raw material price projections for Nafion® could be improved by validating them with the material suppliers. The other raw material prices are likely high, as some quotes are for low volumes. Manufacturing methods could be improved if alternative technology, component supplier patents, and literature are reviewed. Current manufacturing methods are based on finding mass production equipment for the manufacturing methods that could be identified by current component suppliers. Specifically, scaled-up (estimation) values are used for key thermal processing steps; budgetary quotes should be obtained for each size of thermal processing equipment needed. Also, the cost models could be designed to accurately incorporate user input changes in line speed and web width into each cost model. The previously mentioned weaknesses and improvement opportunities are expected, as VRB system production and development are still using emerging technologies and production systems.

5.2 Conclusions

Bottom-up cost models can help new RFB companies enter into the market, help researchers and manufacturers focus on what cost drivers to investigate, and show trends and predictions of when these technologies will be usable. The cost model methodology developed in this research focuses on finding the bottom level equipment and manufacturing process costs that compose the overall production cost of RFB

components. The discussions with equipment and raw material suppliers, equipment supplier budgetary quotes and literature, and additional literature were successfully used as the foundation for this cost modeling methodology. The bottom-up cost model method proposed in this research successfully found the costs associated with each manufacturing process and cost category, separate from profit and general administrative costs, using capital equipment information as its foundation.

The analysis of the results reveal that the OE's 2013 (US DOE, 2011a) cost targets for 1,250/kW can theoretically be met by the estimated component unit costs of the graphite impregnated bipolar plate, soft graphite felt electrode, and PFSA PEM membrane. The bottom-up process-based cost model results in this research shows unit costs (each part is .5 m^2) at \$4.93, \$2.85, \$29.85, for the bipolar plate, felt electrode, and membrane, respectively. These costs are considered optimistic, as a high product volume demand is assumed for a 1 GW / 250 MWh VRB network (based on performance model development at PNNL at an current density of 300 mA/cm^2) (Viswanathan et al., 2012) .

The research done in this work confirms that it is feasible to meet the DOE's cost targets because the estimated process-based costs (costs that do not include profit, indirect overhead, taxes / regulatory fees, research and development) from these models are over ten times less than the desired DOE component cost targets when the component cost breakdown from work by Viswanathan et al. (Viswanathan et al., 2012) for a similar generation two, Gen 2, VRB system is applied to the OE cost target of \$1,250/kW (US DOE, 2011a). Work by Viswanathan et al. also suggests OE cost targets can be met with current G1 VRB capabilities (Viswanathan et al., 2012) .

Although recent work has suggested that the PEM cannot see a large decrease in costs, the results and sensitivity analysis show that a 40% reduction in costs may be possible, even if the Nafion® cost does not decrease. This decrease in price is only possible if a new manufacturing method is used, such as the one suggested by Carlson et al. (Carlson et al., 2005). The unit cost results can change depending on the level of optimism for each cost characteristic input, as most of the data and input values used in the cost models are found in ranges. The top cost drivers for the bipolar plate, felt electrode, and proton exchange membrane are found to be raw material costs, utility costs, and thermal processing.

Cost reduction opportunities include investigating new and alternative manufacturing methods that are connected to cost drivers, and optimizing the most sensitive cost model parameters. The most sensitive production, design, and process inputs for the bipolar plate, felt electrode, and PEM are the graphite flakes, web width, and Nafion® ionomer costs, respectively. The bottom-up cost model analysis reveals that increasing equipment capabilities could result in a greater cost reduction than from simply increasing the capital and facility expenditures to purchase more equipment for bipolar plates (relatively less significant benefits for felts and membranes at the annual production demands reviewed in this research); this is due to the knee in the production curves being significantly before the annual production volume demand. This knee exists due to the law of diminishing returns, as applied to the unit costs of these components, where the components are needed at increasing volumes (Anderton, 2000).

Tornado charts are used to explore model sensitivity. The tornado charts also show that increasing the yield to 95%, 98%, and 98% decreases the unit costs by 3.2%, 2.5%, and 2.7% (roughly correlated to the percent increase in yield) for the bipolar plate, felt electrode, and membrane, respectively. This research also identifies areas of potential manufacturing technological limitations, which are primarily thermal processing bottlenecks and manufacturing line speed capabilities.

The cost model analysis suggests that implementing alternative manufacturing operations and manufacturing methods could reduce costs. For the bipolar plate, a stamping operation could be used to create flow channels (Orest Adrianowycz et al., 2010). Felts could be created by hydrolyzing woven fiber (Carlson et al., 2005). Membranes could be produced by alternative dispersion methods or with an alternative to Nafion®. The major limitations of the three cost models stem from the assumptions made, with a lack of real world validation, due to the developmental nature of VRB technology. Future research should investigate and validate the assumptions made, validate cost model results from actual prototypes, or compare results to supplier costs for the actual components modeled.

5.3 Key Contributions

The research reported has resulted in several contributions, as follows:

1.) A bottom-up process-based cost modeling methodology for use with RFBs has been developed. This modeling method is adapted from the bottom-up cost of goods sold method for discrete component manufacturing. The method has been modified to

work with components produced in continuous web converting processes. Products produced in continuous flows do not scale up the same way as products produced by discrete methods. Thus, an approach has been developed and used to account for the need of multiple production lines based on production line speed and capacity.

2.) Baseline bottom-up process-based cost models were created for the following VRB stack components: graphite bipolar plate, nonwoven graphite felt electrode, and Nafion® PFSA PEM. This involved researching manufacturing methods and determining details for 25 state-of-the-art production operations for each of these components. Over 50 equipment and raw material suppliers are investigated to produce this work. Additionally, over 30 budgetary quotes are obtained, along with over 50 equipment and raw material cost values from literature, and 40 supplemental equipment costs posted from company websites.

3.) Cost drivers, cost trends, and cost reduction opportunities are revealed for the modeled VRB stack components. The cost information revealed in this research can assist companies with the development of large-scale production facilities. The cost drivers identify key categories in VRB component development. The trends and reduction opportunities in this research can be used by researchers and companies to know what areas should be investigated in order to further the feasibility of VRB system production.

4.) Factory capital costs for facility and equipment are estimated for the modeled VRB stack components. Researchers and companies can use the capital costs in this

research as a benchmark against their own factory cost projections. This is beneficial as a clear understanding of the capital cost investment in a new facility can assist with the OE's commercialization efforts of grid-scale energy storage components. Companies can use the estimated capital investment costs to understand the profitability or breakeven points of VRB system production, or let businesses know if they need government support to commercialize these VRBs.

5.4 Future Research Opportunities

The first research opportunity to be investigated should involve creating a bottom-up cost modeling methodology that incorporates a performance model for RFB systems. The majority of PEMFC modeling publications reviewed focused on or incorporated energy storage system performance. If a performance model is developed that is robust enough to be used with a variety of RFB systems, an analysis of the emerging RFB technologies could be conducted to determine the best technologies and systems for different energy and power needs.

A second research opportunity exists as a direct result of the cost models developed in this research. Stack components could be investigated to determine component designs that are functional across a variety of energy storage products, both for large stationary systems and transportation systems. Work could be done to find the optimal manufacturing methods for each of these components. If component designs are found that are operational across a variety of products, optimally produced components could be mass produced to reduce costs across energy storage platforms.

Lastly, there is a research opportunity for the thermal processes and equipment investigated in this research. Excessive costs were found for the thermal operations, largely due to expensive equipment and the long dwell times needed for the state-of-the-art production rates identified for the manufacturing methods used to produce the bipolar plate, felt electrodes, and PEM. It is likely that more novel production methods and alternative thermal processesing equipment can be adapted for the production of these components.

APPENDICES

A. Process Flow Inputs

The following tables identify the process flow inputs used for each cost model.

Table A. 1 Bipolar Plate Process Flow Inputs

Description	Values		Values	Units	References
Production flow inputs					
Line speed capability					
	3.0			m/min	(Orest Adrianowycz et al., 2010)
Mass of bipolar plate					
	0.50			kg/part	(SGL Group, 2012)
Curing oven					
Resin curing at 120 ℃	10			min	(Carlson et al., 2005)
Scaled-Up capital equipment costs					
Curing oven					
Original envelope	0.7	x	0.95	m	Supplier discussion
Scaled envelope	0.7	x	30	m	
Original cost/tool			75,000	$	Supplier discussion
Scaled cost/tool			2,368,421	$	
Intercalation (oxidize at 125 ℃)					(Carlson et al., 2005), (Orest Adrianowycz et al., 2010; Norley et al., 2009; Mercuri, 2008)
Original rate			200	kg / hr	(Carlson et al., 2005)
Scaled rate			150	kg / hr	
Original cost/tool			300,000	$	(Carlson et al., 2005)
Scaled cost/tool			225,000	$	
Exfoliation step at 1400 ℃					(Carlson et al., 2005; (Mercuri, 2008)
Original rate			200	Kg / hr	(Carlson et al., 2005)
Scaled rate			150	kg / hr	
Original cost/tool			2,000,000	$	(Carlson et al., 2005)
Scaled cost/tool			1,682,933	$	

Table A. 2 Felt Electrode Process Flow Inputs

Description	Values		Values	Units	References
Production flow inputs					
Line speed capability					
	10.0			m / min	Based on the review of: (Cai et al., 2012; Harper, 2012)
Mass of bipolar plate					
	0.21			kg / part	(SGL Group, 2012)
Inline graphitization furnace					
Resin curing at 2300 ℃	1			min	(Stry, 2013; (McConnell, 2008)
infrared curing					
Resin curing at 160 ℃	10			min	[(Lorenz et al., 2003)
Scaled-Up capital equipment costs					
Inline graphitization furnace					
Original envelope			0.028	m^3	Supplier discussion
Scaled envelope			0.04347	m^3	
Original cost/tool			1,100,000	$	Supplier discussion
Scaled cost/tool			1,681,652	$	
Infrared curing					
Original rate			1.22	meters	Supplier discussion
Scaled rate			100	meters	
Original cost/tool			50,000	$	Supplier discussion
Scaled cost/tool			4,098,361	$	

Table A. 3: Membrane Process Flow Inputs

Description	Values		Values	Units	References
Production flow inputs					
Line speed capability					
	6.0			m / min	(Carlson et al., 2005; Harris, 2006; James and Kalinoski, 2009)
Infrared dryer/curer					
Flash dry 50 ℃	30			min	(Ion-power, 2003; Carlson et al., 2005)
Full dry 110 ℃	15			min	(Ion-power, 2003; Carlson et al., 2005)
Air dry 20 ℃	5			min	(Carlson et al., 2005)
Scaled-Up capital equipment costs					
Curing oven					
Original envelope	1.2	x	3.1	meters	Supplier literature
Scaled envelope	0.7	x	270	meters	
Original cost/tool			100,000	$	Supplier literature
Scaled cost/tool			5,080,645	$	

B. Method Selection

Table B. 1: Bipolar Plate Method Selection

Process	Process Name	Tool / Material	Tool Function
RM1	-	Raw graphite flakes	-
RM2	-	PTFE resin	-
P1	Intercalation (oxidize with sulfuric acid)	Batch furnace	Oxidize
P2	Water rinse or leach	Oxidative leach reactor	Rinse / oxidative leach
P3	Exfoliation step (expansion)	Multiple: batch furnace	Exfoliate
P4	Roller compression (calendar)	Roll press	Compress graphite (2000 PLI - pounds per linear inch of roll face)
P5	Resin impregnation	Impregnation	In-line resin impregnation
P6	Heated compression (calendar)	Heat roll press	Compress graphite and heat graphite (2000 PLI - pounds per linear inch of roll face)
P7	Gauging / inspection	Betagauge	Gauge thickness and inspect
P8	Sheet cutting	Laser cut	Cut graphite plate to size
P9	Resin curing	Curing oven, hold parts/pressurized chamber	Cure resin

Table B. 2: Felt Method Selection

ID	Process Name	Tool / Material	Tool Function
RM1	-	PANOX (oxidized pan fiber) (crimped staple fiber)	-
RM2	-	Prepreg agent - ptfe	-
RM3	-	Prepreg agent - epoxy / resin	-
RM4	-	Prepreg agent - carbon powder	-
RM5	-	Distilled water	-
P1	Fiber processing	Fiber opening and handling equip.	Prepare fiber for use
P2	Continuous graphitization	Graphitization belt furnace	In-line continuous graphitization (2300 ℃)
P3	Airlaid processing	Aerodynamic airlay	Web formation
P4	Tension / feed station	Tensioner	Feed station
P5	Edge trim	Slitting	Edge trim
P6	Tension / feed station	Tensioner	Feed station
P7	Needle punch	Needle punch (with pre-needler)	Needle punching (felting)
P8	Tension / feed station	Tensioner	Feed station
P9	Edge trim	Slitting	Edge trim
P10	Impregnate (to B-stage)	Prepregger	Impregnate (to B-stage) (wet treatment and compress) (hot melt prepreg, bonding by resin)
P11	Resin curing	Infrared curing	Infrared heating (160 ℃)
P12	Tension / feed station	Tensioner	Feed station
P13	In-line inspection	Pinhole and thickness detection	In-line inspection (more adv than gauging=weight reading system)
P14	Sheet cutting	Nonwoven sheet cutting	Cut to length

Table B. 3: Membrane Method Selection

ID	Process Name	Tool / Material	Tool Function
RM1	-	Nafion® (isopropanol, mixed ethers, ethanol, water, polymer)	-
RM2	-	Silicone coated PET backing film (2 mil)	-
P1	Film handling PET film	Single position unwinder (and guiding)	Unwind, splice, guide (edge control and tensioners)
P2	Gauging of thickness	Thickness detection	Check thickness [geometry gauging sensor (beta-gauge)]
P3	Dispersion layer coating	Knife over edge roll coater	Apply dispersion coating layer
P4	Gauging of thickness	Thickness detection	Check thickness [geometry gauging sensor (beta-gauge)]
P5	Drying and cooling	Infrared dry/cure and air cool	Drying and cooling
P6	Gauging of moisture	Moisture detection	Check water moisture
P7	Quality control and gauging of thickness	Pinhole and thickness detection	Check thickness and pin-hole detection / quality control / web insp.
P8	Sheet cutting	Sheet cut with blade	Cut sheets to length

C. Process and Design Inputs

Process and design inputs for common to each cost model are provided in Table C. 1 and Tables C. 2, C. 3, and C. 4 provide inputs for bipolar plates, felt electrodes, and membranes, respectively.

Table C. 1: Common Production and Design Inputs

Input Item	Input Value	Description	References
Operation Costs			
Labor hour rate	$21.50	User defined.	(Orest Adrianowycz et al., 2010),
Laborers per line	3	Total laborers per line. User defined.	(Orest Adrianowycz et al., 2010; Carlson et al., 2005)
Labor loading	1.5	Accounting for low level direct overhead – direct contact with laborers. User defined.	
Maintenance cost	4%	Maintenance cost as a % of tool capital cost. User defined.	
Natural gas cost	0.24	$/kg. User defined.	(EIA, 2013b)
Electricity cost	0.068	$/kwh. User defined.	(EIA, 2012)
Cumulative yield	90-95%	This accounts for the scrap generated during production. User defined.	(Orest Adrianowycz et al., 2010; James and Kalinoski, 2009; Carlson et al., 2005)
Working days per year	351	User defined.	
Working hours per day	24	User defined.	
Facility construction / procurement cost			
Cleanroom cost_m^2	$5,000	Cost of functional cleanroom space (class 10,000) required for production. Cost is in $ per square meter of the functional area. User defined.	
Lab Cost_m^2	$3,000	Cost of functional laboratory space required for production and/or support. Cost is in $ per square meter of the functional area. User defined.	
Manufacturing Cost_m^2	$1,000	Cost of manufacturing space required for production. Assume light industrial facilities. Cost is in $ per square meter of the functional area. User defined.	
Semiclean Cost_m^2	$2,000	Cost of semi-clean space. Assume activities such as packaging, QA, inspection, etc.. Cost is in $ per square meter of the functional area. User defined.	
Facility Area Required per Tool Footprint			
Gross Area Ratio	2	Scalar that allows for space to operate around tool floor space requirements. User defined.	
Tool Installation Cost			
Tool install	6%	Tool installation cost as a % of tool capital cost. User defined. (Note: Some values override this one)	
Depreciation			
Tool depreciation_yrs	7	Tool Depreciation in years. Assumes straight line. User defined. (Note: Some values override this one)	[Or 10 years per: (Sinha et al., 2009; Carlson et al., 2005; Orest Adrianowycz et al., 2010),]
Bldg depreciation_yrs	25	Building depreciation in years. Assumes straight line. User defined.	

Table C. 2: Bipolar Plate Baseline Production and Design Inputs

Input Item	Input Value	Description	References
Parts per Year	2,000,000	Parts required per year. User defined. (Each part is .7 x .7 m)	-
Graphite flake	2.00	$/kg. User defined.	Supplier discussion
Resin (likely TF 5035Z)	20.75	$/kg. User defined.	Supplier discussion

Table C. 3: Felt Baseline Production and Design Inputs

Input Item	Input Value	Description	References
Parts per year	4,000,000	Parts required per year. User defined. (Each part is .7 x .7 m)	
PANOX	2.00	$/kg. User defined.	Supplier discussion
PTFE	20.75	$/kg. User defined.	(Carlson et al., 2005; Sinha et al., 2009; Trapp et al., 2003; Ottinger et al., 2004)
Epoxy	24.26	$/kg. User defined.	(Carlson et al., 2005; Ottinger et al., 2004)
Carbon powder	3.35	$/kg. User defined.	(Carlson et al., 2005)
DI water	0.015	$/kg. User defined.	

Table C. 4: Membrane Baseline Production and Design Inputs

Input Item	Input Value	Description	References
Parts per year	2,000,000	Parts required per year. User defined. (each part is 0.7 x 0.7 m)	
Nafion®	92.00	$/kg. User defined.	(James and Spisak, 2012; Ernst, 2009)
Silicone coated PET backing film (2 mil);	1.97	$/kg. Silicone coated film of biaxially oriented polyetheylene terephthalate. User defined.	Supplier discussion

D. Complete Bill of Materials (BOM)

A complete bill of materials for the entire VRB network is provided in Table D. 1.

Table D. 1: Complete BOM of VRB Network

#	Lvl.	Name	Qty.	Material	Description	Dimension	Function	Reference
0	0	VRB network	1	-	Group of VRB systems	4320000 Gallons	1 GW, 250 MWh	
1	1	VRB system (machine)	1000	-	Group of stacks	4320 Gallons	1 MW, .25 MWh	Viswanathan et al. (Viswanathan et al., 2012)
2	2	VRB stack	36	-	Groups of cells	120 Gallons		Viswanathan et al. (Viswanathan et al., 2012)
3.1	3	VRB cell	60	-	2 Half-cells	.8 x.8 x.006 m	Location of electrolyte charge / discharge	Viswanathan et al. (Viswanathan et al., 2012)
3.1.1	4	Flow frame assy.	1*	-	Structural Component	0.8 x 0.8 x 0.006 m	-	-
3.1.1.1	5	Flow frame	2*	PVC		.8 x.8 x.003 m	-	-
3.1.1.2	4	BPP	1*	Fluor polymer resin impregnated naturally expanded graphite	Bipolar plate with no flow channels	.7 x .7 x .0006 m	Separate electrolyte and transfer electrons	Modeled after SGL TF6 Fluor Polymer (SGL Group, 2012)
3.1.1.3	4	Sealant	NA	-	-	-	Used to attach BPP to Flow Frame	-
3.1.1.4	5	O-ring	2	-	Flow frame assy. component	-	Seal	-
3.1.2	4	MEA	1	-	Membrane electrode assy.	.7 x.7 x .0047 m	-	-

3.1.2.1	5	Felt Electrode	2	Epoxy resin impregnated PANOX polymer precursor porous graphite felt	Porous graphite felt electrode	.7 x.7 x .0046 m	Conductive transfer of electrons between electrolyte and BPP	Modeled after SGL GFD4.6 polymer precursor (SGL Group, 2012)
3.1.2.2	5	PEM	1	Nafion® PFSA PEM, 1100 EW	Nafion® perfluorosul-fonic acid proton exchange membranes	.7m x .7m x 5mil	Transfer protons between half cells	Modeled after DuPont Nafion® 115 (DuPont, 2009)
3.1.3	4	Wire	1	Titanium	-	-	Monitor voltage	-
3.1.4	4	Sealant	NA	-	-	-	-	-
3.2.1	3	Current collector assy.	1	-	-	-	-	-
3.2.2.1	4	Current collector	1	Copper	Copper plate to transfer electricity	.7 x .7 x .0006 m	Transfer electricity	
3.2.2.2	4	Wire	2	Titanium	Current collect wire	-	Transfer electricity	-
3.3.2	3	End plate assy.	2	-	-	-	-	-
3.3.2.1	4	End plate	1	PVC	-	.8 x .8 x .1 m	-	-
3.3.2.2	4	Nuts	20	-	-	-	-	-
3.3.2.3	4	Washer	20	-	-	-	-	-
3.3.2.4	4	Bolts	20	-	-	-	-	-
3.3.2.5	4	Spring	20	-	-	-	-	-
3.2	3	Tank system	1	-	-	120 gallons	-	-
3.2.1	4	Tank	2	-	-	60 gallons	-	Assumed from Viswanathan et al. (Viswanathan et al., 2012)

3.2.2	4	Pipes	5	-	Two pipes are used tank (and they pass through each half cell), a fifth is used for mixing		Electrolyte transfer occurs as the fluid is pumped through the system	-
3.2.3	4	Pump	2	-	-	-	-	-
3.2.4	4	Electronic Control System		-	-	-	-	-

E. Scrap Unit Costs by Processes

The unit scrap costs display the estimated amount of scrap for each process and category. These are determined based on the step and cumulative yields. In the other graphical results, the "cost" of scrap is accounted for by assuming additional production is done to account for the scrap, with a penalty calculated by only accounting for the desired annual production volume (so the costs of the scrap are part of the unit costs). Figures E.1 , E. 2, and E. 3 show the scrap for the bipolar plate, felt electrode, and membrane, respecitively.

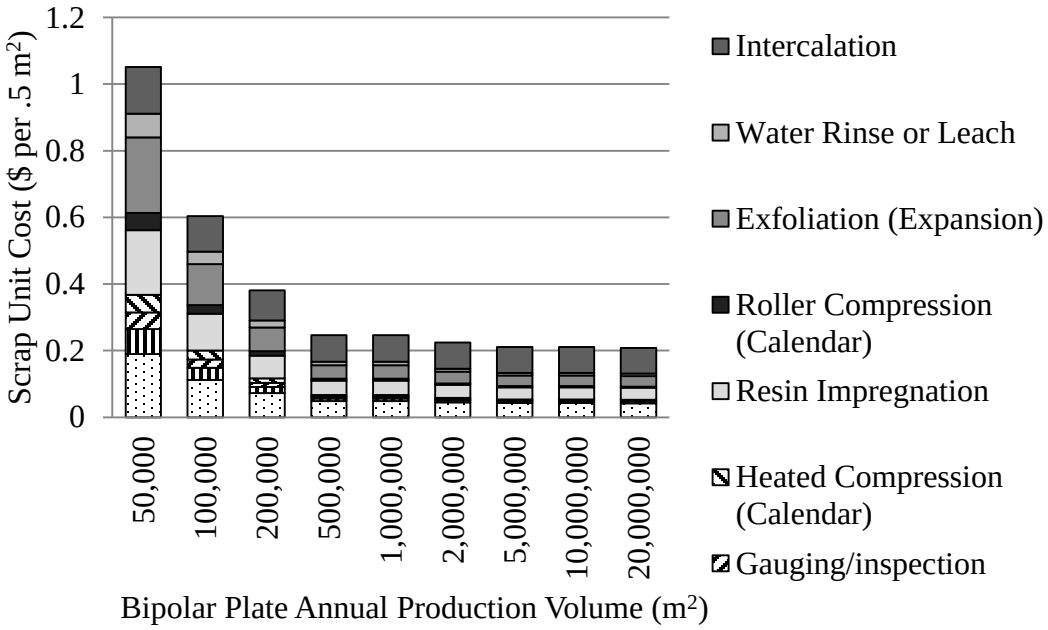

Figure E. 1: Bipolar Plate Scrap Unit Costs by Process

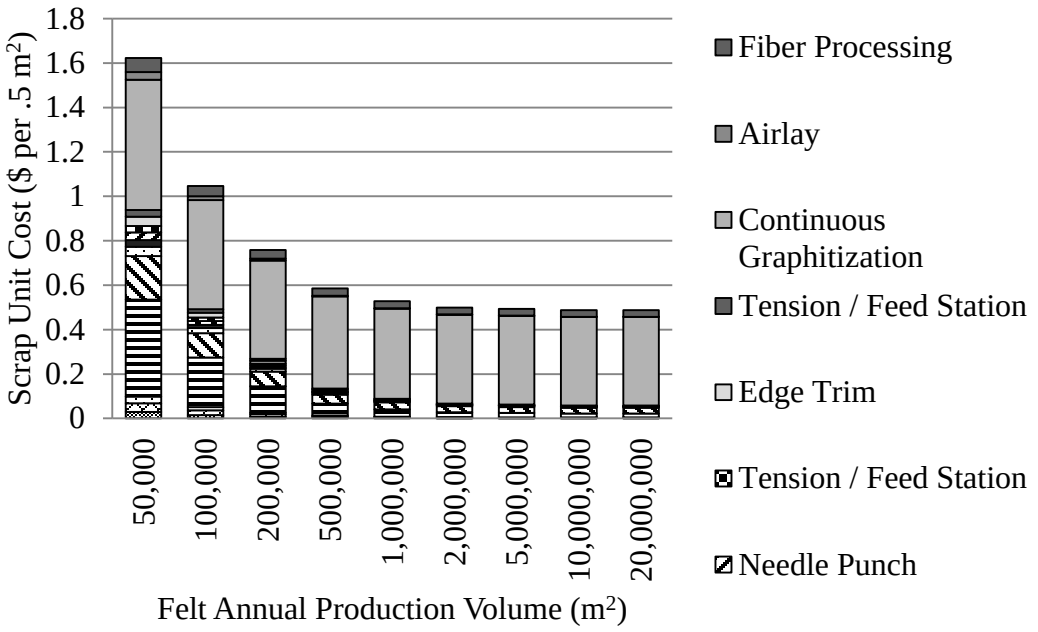

Figure E. 2: Felt Electrode Scrap Unit Costs by Process

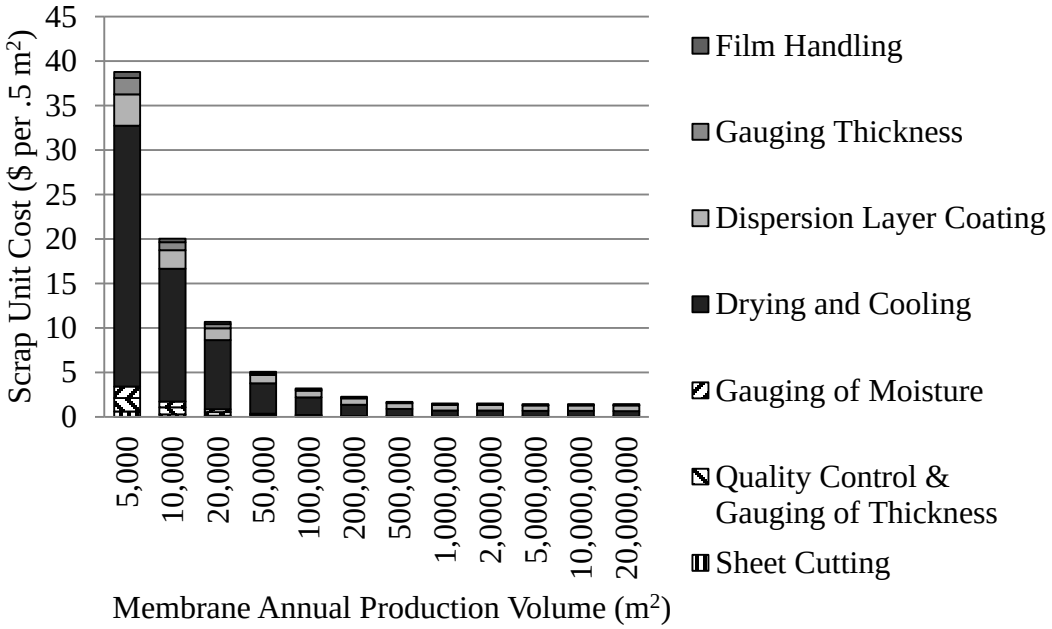

Figure E. 3: Membrane Scrap Unit Costs by Process

F. Monte Carlo Simulation

The following Tables F. 1, F. 2, F. 3 and Figures F. 1, F. 2, and F. 3 show the monte carlo parameter ranges as well as the monte carlo results.

Table F. 1: Bipolar Plate Monte Carlo Parameters

Level	Low	Likely	High	Citation
Graphite flake ($ / kg)	1.5	2	11.5	(Supplier quote)
Days per year	316	351	365	(Assumption)
Hours per day	16	24	24	(Assumption)
Line speed (m / min.)	1.5	3	6	(Carlson et al., 2005; Sinha et al., 2009; Orest Adrianowycz et al., 2010)
Labor rate ($ / hr)	9.5	21.5	45	(Orest Adrianowycz et al., 2010; James and Kalinoski, 2009)
Yield (%)	80	90	95	(Orest Adrianowycz et al., 2010)

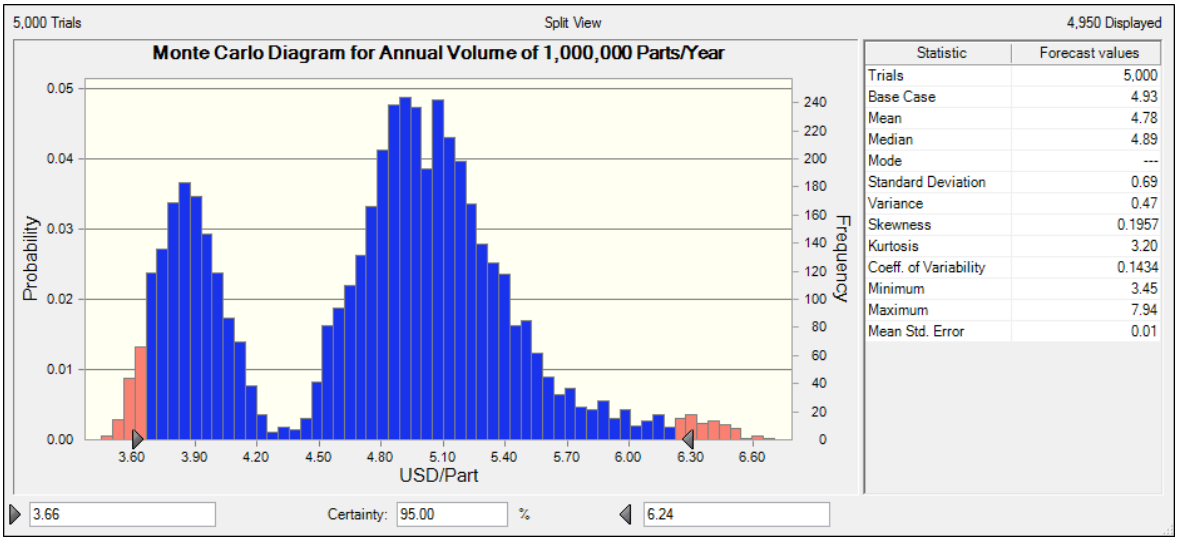

Figure F. 1: Bipolar Plate Monte Carlo Analysis Results at 2 million m^2 Demand per Year

Table F. 2: Felt Electrode Monte Carlo Parameters

Level	Low	Likely	High	Citation
PANOX	1.6	2	3.25	(Supplier Discussion; Eberle, 2012)
Days per Year	316	351	365	(Assumption)
Hours per Day	16	24	24	(Assumption)
Line Speed	5	10	20	(Cai et al., 2012; Harper, 2012; Stry, 2012)
Labor Rate	9.5	21.5	45	(Orest Adrianowycz et al., 2010; James and Kalinoski, 2009)
Yield %	98	95	80	(Carlson et al., 2005; James and Kalinoski, 2009)

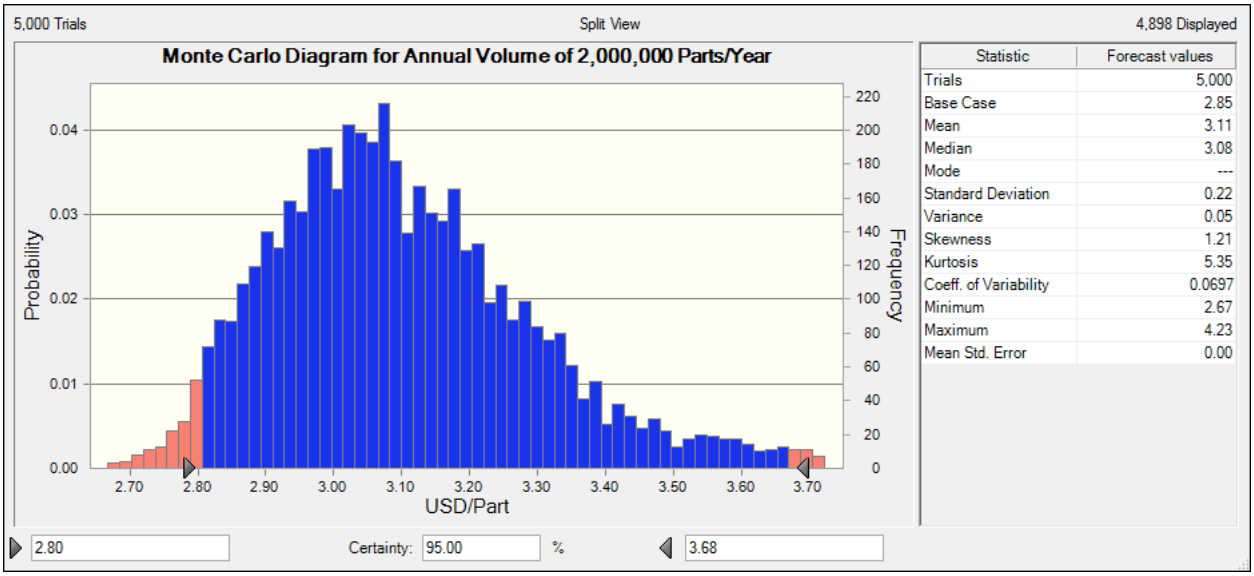

Figure F. 3: Felt Electrode Monte Carlo Analysis Results at 4 million m^2 Demand per Year

Table F. 3: Membrane Monte Carlo Parameters

Level	Low	Likely	High	Citation
Nafion®	60	92	250	(James and Spisak, 2012; Ernst, 2009; Curtin, 2002; Mathias et al., 2004)
Days per year	316	351	365	(Assumption)
Hours per day	16	24	24	(Assumption)
Line speed	35	6	.25	(Carlson et al., 2005; Harris, 2006; James and Kalinoski, 2009)
Labor rate	9.5	21.5	45	(Orest Adrianowycz et al., 2010; James and Kalinoski, 2009)
Cumulative yield %	98	95	80	(Carlson et al., 2005; James and Kalinoski, 2009)

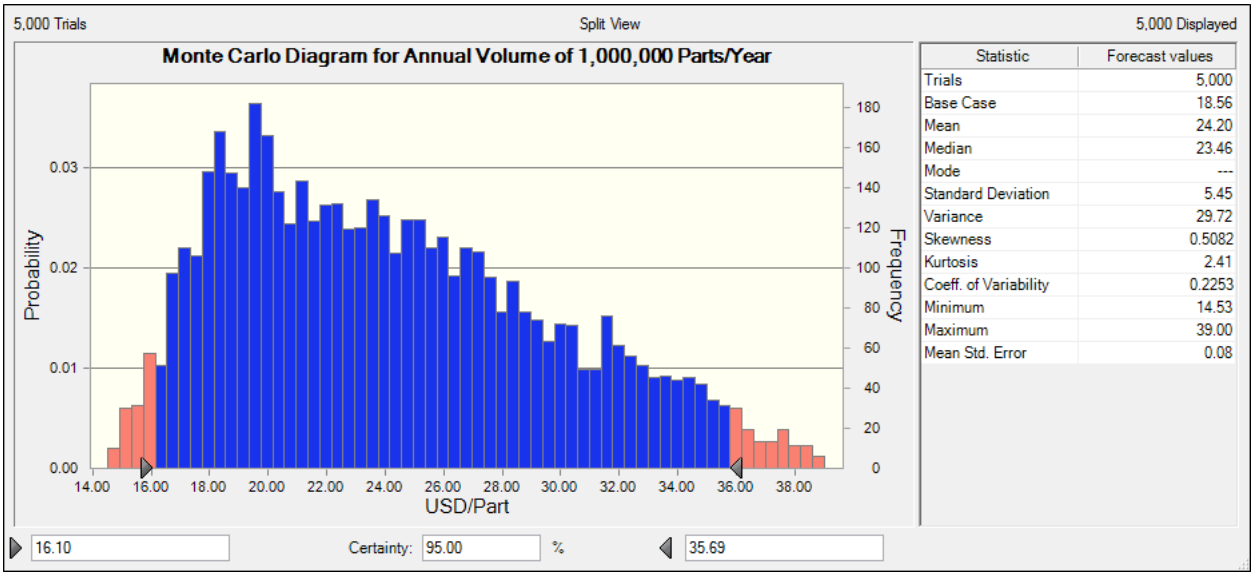

Figure F. 3: Membrane Monte Carlo Analysis Results at 2 million m^2 Demand per Year

G. Assumptions

Common assumptions are used for each model. Each of the manufacturing methods assumed that continuous web converting process should be used, based on the assumption that the next step would be a cell assembly operation (James and Kalinoski, 2009; Mercuri, 2008). The labor hours are set to 24 hours per day, at 351 days per year, to simulate a continuous production system. Laborers per manufacturing line are estimated by placing one laborer per thermal processing step; this results in a similar labor count from reviewed literature (Carlson et al., 2005; Sinha et al., 2009). To simplify the models, no interest payments are added to capital costs. Scrap and waste are not recycled to simplify the models. The scaling-up of thermal processes is done with the assumption that the costs would can be estimated from a geometric ratio of the current verse desired equipment size (see Chapter 3). A large fraction of the equipment tooling footprints are based on approximations of information provided by equipment manufacturers. Each manufacturing method is selected in order to represent a method that is used, or could likely be used, by real manufacturing suppliers of the selected components for mass production. Equipment is selected for mass production based on the identified current production methods. Also, each manufacturing method is designed with the assumption that an assembly operation would immediately follow the production lines. Additionally, all of the infrared thermal processing devices used are assumed to use only electrical energy, in order to simplify the cost models.

A number of major assumptions are made for the bipolar plate cost models. The graphite flakes selected are assumed to be compatible with the required intercalation and

exfoliation steps (Orest Adrianowycz et al., 2010). The target line speed of 3.0 meters/minute is selected in order to best represent what the manufacturer (GrafTech) is currently capable of, per available cost modeling information (Orest Adrianowycz et al., 2010). Also, the bipolar plate manufacturing methods are selected to specifically account for the naturally expanded graphite and absence of flow channels in the plates.

Major assumptions are also made for the graphite felt electrode cost models. PANOX fiber precursor is selected for the starting material, primarily based on SGL's U.S. 6511768 B1 patent (Trapp et al., 2003). Also, the production method selected assumed that a continuous graphitization manufacturing process is done with a continuous furnace, also according to SGL's U.S. 6511768 B1 patent (Trapp et al., 2003). A target production line speed is estimated to be 10.0 meters/minute, based on typical line speed information gathered (Cai et al., 2012; Harper, 2012; Stry, 2012). The felt electrode is also assumed to be nonwoven (SGL Group, 2012; SGL Group, 2013b).

Assumptions for the membrane had the biggest impact of the three cost models developed. For the membrane, a most-likely future Nafion® ionomer pricing is selected for an estimated production volume of 200,000 to 250,000 kg, based on annual production volume determined for this baseline case of a VRB system that uses 2 million PFSA PEMs at 5 mil thickness (DuPont, 2009; James and Kalinoski, 2009; DuPont, 2008). The target line speed is set to 6.0 meters/minute in order to match an estimate of DuPont's line speed capabilities (Harris, 2006) and the likely existing capability of this type of dispersion coating production system (Carlson et al., 2005). Additionally, a new dispersion casting method is selected that lays out coatings onto inert silicone-coated PET

film (Carlson et al., 2005; Grot, 2003). This method is selected because it is similar to the state of the art method that is currently known to be used by DuPont for their newer N21x series of membranes (Carlson et al., 2005; DuPont, 2008). The following tables summarize the assumptions made for each of the components modeled, most of these assumptions had a moderate impact on the model development and results.

Table G. 1: Bipolar Plate Cost Model Assumptions

1	Assume material pricing obtained from suppliers is for approx. the right graphite flake and resin ((Carlson et al., 2005) has older pricing at 5.51, 6.83, 11.57 and 5.43, 24.26, and 38.59 $/kg respectively)
2	Assume line speed capable at going 3 m/min [(Orest Adrianowycz et al., 2010)]; (6 m/min at thinner web widths) [(Carlson et al., 2005; Sinha et al., 2009)]
3	Not accounting for interest payments on capital equipment
4	Assume Load Leveling and Balancing production lines
5	Assume cumulative yield at 95% [(Carlson et al., 2005; James and Kalinoski, 2009)]
6	Not accounting for recycling of waste
7	Assume ventilation/scrubbing/air-treatment equipment is represented in the facility cost
8	Assume 351 days a year and 24 hours a day for baseline values
9	Assume 1 laborer needed per thermal piece of equipment
10	Included inspection, but used equipment that is listed for "films"
11	Did not include winding or packaging
12	Estimate that half the resin used is waste [(Orest Adrianowycz et al., 2010; Jonouchi et al., 1994)] (large amount of ventilation needed for resin VOC for suppliers per EPA permits)
13	Assume solvent-less resin is used [(Orest Adrianowycz et al., 2010; Norley et al., 2009; Ottinger et al., 2004)]
14	Assume web is cut after curing (this requires correct pressure/clamping)
15	Simplification, assume not including potassium compounds in oxidation
16	Assume typical oxidization/exfoliation equipment rates are in 25 kg/hr increments
17	Assume no final inspection step needed

Table G. 2: Felt Cost Model Assumptions

1	Assume material selected is what is used in SGL GFD4.6 (0.7 m x 0.7 m x 4.6 mm) (SGL Group, 2012)
1.1	Select oxidized polyacrylonitrile fiber (PANOX) as the starting point for simplicity (SGL Group, 2013d; Trapp et al., 2003)
1.2	Select prepreg agent PTFE for simplification (Orest Adrianowycz et al., 2010; SGL Group, 2013d; Trapp et al., 2003)] (likely FT 109 (SGL Group, 2012; SGL Group))
1.3	Assume additional prepreg agent is epoxy (SGL Group, 2013d; SGL Group, 2013c)
1.4	Assume additional prepreg agent is carbon powder (Carlson et al., 2005; SGL Group, 2012; SGL Group, 2013d)
1.5	Assume water used with prepreg
2	Assume 10 m/min for baseline line speed - Know similar (carbon fiber) lines are typically 5 m/min (Cai et al., 2012; Klug, 2003; Stry, 2012; Harper, 2012; Calitzler, 2013; Orest Adrianowycz et al., 2010; Stry, 2012; Harper, 2012)
3	Not accounting for interest payments on capital equipment for simplicity
4	Assume Load Leveling and Balancing production lines
5	Assume cumulative yield at 95% [(Carlson et al., 2005; James and Kalinoski, 2009)
6	Not accounting for recycling of waste
7	Assume ventilation/scrubbing equipment is represented in the facility cost
8	Assume 351 days a year and 24 hours a day for baseline values
9	Assume 1 laborer needed per thermal processing piece of equipment
10	Assume 35% PTFE resin waste in impregnation (Jonouchi et al., 1994)
11	Selected inline graphitization equipment; Other methods may be more preferable such as: induction equipment, horizontal slot furnace
11.1	Approximated heat zone for inline graphitization equipment, and assuming the speed can be increased with no cost
12	Assume don't need take-up winder or packaging as the final processes - assume continuous assembly line follows
12	Assume no fiber mixing or cleaning is needed
13	Assume final heat treatment (500 ℃ – 1200 ℃) is not done for simplification (would likely use this step here or at the assembly step (Trapp et al., 2003))
14	Assume air-lay (aerodynamic web formation) is used (Kishio et al., 1989), (Heine and Kompalik, 1998)
15	For simplicity, did not scale converting equipment that was for 1-1.5 m web width (instead of 0.7m)
16	Assume using needle punching for felting (Jonouchi et al., 1994; Trapp et al., 2003)
17	Assume product is nonwoven (SGL Group, 2013b; SGL Group, 2012)
18	Major assumption - graphitization equipment could scale from 4 in./min to 10 m/min at no additional cost

Table G. 3: Membrane Cost Model Assumptions

1	Assume dispersion casting method used (Carlson et al., 2005; Harris, 2006; Grot, 2003; DuPont, 2008)
1.1	Assume knife over roll coating system is used (Carlson et al., 2005; Carlson et al., 2005)
1.2	Assume 0.125 kg of Nafion® ionomer required for the 5 mil thick membranes (James and Spisak, 2012; DuPont, 2009; DuPont, 2008)
1.3	Assume each coating pass should only be 2.5 mil wet thickness (results in 1 mil dry thickness) (Carlson et al., 2005) (and based on the product thicknesses by DuPont) (DuPont, 2008)
2.1	Future Nafion® pricing is speculative and the selected baseline is based on several sources for the most likely price (Ernst, 2009; James and Spisak, 2012)
2.2	Assume silicone coated PET is used (Carlson et al., 2005; Grot, 2003)
3	Line speed at 6 m/min (Carlson et al., 2005; Harris, 2006) (Dupont's current production rate is reported to be 3-6 m/min (Harris, 2006), a similar method puts Nafion® membranes at 5-35 m/min (James and Kalinoski, 2009))
4	Not accounting for interest payments on capital equipment for simplicity
5	Assume Load Leveling and Balancing production lines
6	Assume cumulative yield at 95% (Carlson et al., 2005; James and Kalinoski, 2009) (would assume higher yield if slitting wider widths into multiple components)
7	Not accounting for recycling of waste
8	Assume ventilation/scrubbing equipment is represented in the facility cost
9	Assume 351 days a year and 24 hours a day for baseline values
10	Assume 1 laborer needed per thermal processing piece of equipment
11	Assume 10,000 clean room is needed (Carlson et al., 2005; Harris, 2006; Sørensen, 2005), and that the applied costs are adequate for the moisture requirements of Nafion®
12	Assume edge trim steps are not required, and that sheet cutting wastes are accounting for with the use of the cumulative yield
13	Assume (reduce cost about $6 at 1 million m^2 req) the following are not needed for packaging as this will be part of a continuous line: Film Handling PP Film, Laminating - Coversheet (PP), Laminating - Winding with Roll Changer (and Trim, or rewinder), Packaging (assuming need), PP (0.7 mil), Metallized Polyester Overwrap (0.076 kg)
14	Assume inspection equipment handles both and quality control and thickness steps at the same time
15	Representing the infrared heating elements as linear pieces of equipment, when in reality they would be shorter in a roller system
16	Assume selected infrared equipment is suitable for cleanroom
17	Assume simplified cut to length step - not including pretreatment expansion steps for this baseline model (Ion-power, 1993), a pretreatment stay may not be needed in the next assembly step, depending on the assembly environment and wetness of the membrane (Ion-power, 2000) (DuPont currently sells these membranes in uncut rolls)
18	Assume no (PP) coversheet (Carlson et al., 2005) is needed, as this baseline model assumes the next step is immediate assembly

H. Unit Cost Literature Validation

Table H. 1 is a summary of all of the components modeled.

Table H. 1: Complete List of Cost Models in Literature for Similar Components

Component	Annual Production Volume / Cross Section	Model Component Detail	Primary Material Used	Material Price ($/kg)	Unit Cost ($ / 0.5 m^2)	Ref.
Bipolar Plate	2 million, 0.5 m^2	NEG resin impreg BPP	Raw graphite flake	2	4.93	This work
Bipolar Plate	19 million, ~.5 m2	NEG resin impreg BPP	Raw graphite flake	5.51	6.85	(Orest Adrianowycz et al., 2010)
Bipolar Plate	19 million, ~.5 m2	NEG resin impreg BPP	Raw graphite flake	6.84	10.87	(Orest Adrianowycz et al., 2010)
Bipolar Plate	(over .5 million) ~323 cm^2	Flexible Foil	Raw graphite flake	4.4	8.2	(Carlson et al., 2005)
Bipolar Plate	231 million, ~277 cm^2	Expanded graphite foil	Raw graphite flake	0.54	9	(Sinha et al., 2009)
Bipolar Plate	(Assume 2 million, .5 m^2)	-	-	-	12.75	(Viswanathan et al., 2012)
Felt Electrode	4 million, 0.5 m^2	Impreg nonwoven graphite felt	PANOX	2	2.85	This work
Cloth Electrode	(over 1 million) ~323 cm^2	Woven carbon	Woven carbon fiber	30	9.7	(Carlson et al., 2005)
Carbon Paper Electrode	370 million, ~335 cm^2	-	-	-	5.5	(James and Spisak, 2012)
Felt Electrode	(High volume)	-	Woven graphite fiber	-	7.75	(Ernst, 2009)
Cloth Electrode	219 million, ~277 cm^2	Woven carbon	Woven carbon fiber	20	6.74	(Sinha et al., 2009)
Felt Electrode	(Assume 4 million, .5 m^2)	-	-	-	10	(Viswanathan et al., 2012)
Membrane	2 million, 0.5 m^2	5 mil thick	Nafion® ionomer	92	29.85	This work
Membrane	(over .5 million), ~323 cm^2	2 mil thick	Nafion® ionomer	80	11.69	(Carlson et al., 2005)
Membrane	370 million, ~335 cm^2	1 mil thick on ePTFE	Nafion® ionomer	75	9.09 $/0.5$m^2$	(James and Spisak, 2012)
Membrane	108 million, ~277 cm^2	2 mil thick	Nafion® ionomer	25	7.84 $/0.5$m^2$	(Sinha et al., 2009)
Membrane	(Assume 2 million, .5 m^2)	-	Nafion® ionomer	-	100 $/0.5$m^2$	(Viswanathan et al., 2012)

BIBLIOGRAPHY

Anderton, A.G. (2000). Economics (Ormskirk: Causeway Press).

AUTEFA (ND). Crosslapping. Web Accessed 9-16-13: "http://www.autefa.com/downloads/crosslapping_sd-p.pdf".

Blanc, C., and Rufer, A. (2010). Understanding the Vanadium Redox Flow Batteries.

Böhringer, C., and Rutherford, T. (2008). Combining Bottom-up and Top-down. Energy Econ. *30*, 574–596.

Brandon, N., Kucernak, A., and Yufit, V. (2012). Regenerative Fuel Cells. Patent WO2013104554 A1.

Brett, B. (2005). Bipolar Plates: The Lungs of the PEM Fuel Cell. Fuel Cell Rev. *2*, 15–23.

BTI (2012). 2011 Fuel Cell Technologies Market Report.

BTI (2013). When the Grid Fails: Fuel Cells Power Critical Infrastructure in Disasters.

Cai, M., Thorpe, D., Adamson, D.H., and Schniepp, H.C. (2012). Methods of Graphite exfoliation. J. Mater. Chem. *22*, 24992.

Calitzler (2013). Hot Melt Prepreg Equipment (WAECO).

Carlson, E., Kopf, P., Sinha, J., Sriramulu, S., and Yang, Y. (2005). Cost Analysis of PEM Fuel Cell NREL/SR-560-39104 Systems for Transportation.

Chen, D., Hickner, M., Agar, E., and Kumbur, E. (2013). Optimizing membrane thickness for vanadium redox flow batteries. J. Membr. Sci. *437*, 108–113.

Cunningham, B., and Baird, D.G. (2006). The Development of Economical Bipolar Plates for Fuel Cells. J. Mater. Chem. *16*, 4385.

Cunningham, B.D., Huang, J., and Baird, D.G. (2007). Development of Bipolar Plates for Fuel Cells from Graphite Filled Wet-Lay Material and a Thermoplastic Laminate Skin Layer. J. Power Sources *165*, 764–773.

Curtin, D. (2002). High Volume, Low Cost Manufacturing Process Nafion Membranes.

Curtin, D., and Howard, E. (2003). Compositions Containing Particles of Highly Fluorinated Ion Exchange Polymer.

Curtin, S., Gangi, J., and Skukowski, R. (2012). The Business Case for Fuel Cells 2012.

BIBLIOGRAPHY (Continued)

Dahiya, D., Kammath, M., and Hegde, R. (2004). Wet-Laid Nonwovens.

Dickey, D. (2005). Don't Get Mixed up by Scale-up.

Divya, K., and Østergaard, J. (2009). Battery Energy Storage Technology for Power Systems—An Overview. Electr. Power Syst. Res. *79*.

Doughty, D., Butler, P., Akhil, A., Clark, N., and Boyes, J. (2010). Batteries for Large-Scale Stationary Electrical Energy Storage. Electrochem. Soc. Interface.

DuPont (2008). DuPont Fuel Cells DuPont Nafion PFSA Membranes NR-211 and NR-212.

DuPont (2009). DuPont Fuel Cells DuPont Nafion PFSA Membranes N115, N117, N1110.

DuPont (2012). DuPont™ Nafion® Membranes R&D update and Product Technology Overview.

Eberle, C. (2012). ORNL Carbon Fiber R&D Update.

Eckroad, S. (2007). Vanadium Redox Flow Batteries An In-Depth Analysis.

EG&G (2005). Fuel Cell Handbook.

EIA (2012). Summary [Electrical] Statistics for the United States, 2001-2011. Web Accessed 10-4-13: "http://www.eia.gov/electricity/annual/html/epa_01_02.html"

EIA (2013a). U.S. Energy Information Administration - EIA - Independent Statistics and Analysis. Web Accessed 10-4-13: "http://www.eia.gov/state/?sid=OR".

EIA (2013b). U.S. Natural Gas Prices. Web Accessed 10-4-13: "http://www.eia.gov/dnav/ng/ng_pri_sum_dcu_nus_m.htm".

Ernst, W. (2009). Fuel Cell System Cost for Transportation - 2008 Cost estimate.

Farooq, M., Kumar, S., and Shrestha, R. (2013). Energy, environmental and economic effects of Renewable Portfolio Standards (RPS) in a Developing Country. Energy Policy *62*, 989–1001.

Greene, D., Duleep, K., and Upreti, G. (2011). Status and Outlook for the U.S. Non-Automotive Fuel Cell Industry: Impacts of Government Policies and Assessment of Future Opportunities.

Grot (2003). Preparation of Fuel Cell Electrode Assemblies. Patent 6641862 B1.

BIBLIOGRAPHY (Continued)

Hamrock, S.J., and Yandrasits, M.A. (2006). Proton Exchange Membranes for Fuel Cell Applications. J. Macromol. Sci. Part C Polym. Rev. *46*, 219–244.

Harper (2012). "So You Want to Build A Carbon Fibre Production Line?" - Workshop Scale, The Road to Success and True Efficiency. (London).

Harris, T. (2006). Design Methodology, Science, and Technology to Manuffacture High Temperature Polymer Electrolyte Membranes for Fuel Cells. Rensselaer Polytechnic Institute.

Harris, T.A.L., Walczyk, D.F., and Weber, M.M. (2010). Manufacturing of High-Temperature Polymer Electrolyte Membranes—Part I: System Design and Modeling. J. Fuel Cell Sci. Technol. *7*, 011007.

Heine, M., and Kompalik, D. (1998). Method for converting multidimensional sheet structures consisting of polyacrylonitrile fibres into the thermally stabilized stage.

Hiroshige, Toshio, and Nobuyuki (2012). Method for Designing Redox Flow Battery System. Patent EP 1536507 B1.

Houchins, C., Kleen, G., Spendelow, J., Kopasz, J., Peterson, D., Garland, N., Ho, D., Marcinkoski, J., Martin, K., Tyler, R., et al. (2012). U.S. DOE Progress Towards Developing Low-Cost, High Performance, Durable Polymer Electrolyte Membranes for Fuel Cell Applications. Membranes *2*, 855–878.

Ion-power (1993). Handling and Storage of Du Pont Nafion ® Perfluorinated Membranes.

Ion-power (2000). Nafion Perfluorinated Membranes User's Guide.

Ion-power (2003). Product Bulletin - Liquion Nafion Containing Solutions.

IPHE (2010). 2010 Hydrogen and Fuel Cell Global Commercialization & Development Update.

James, B., and Kalinoski, J. (2009). Mass Production Cost Estimation for Direct H 2 PEM Fuel Cell Systems for Automotive Applications: 2008 Update.

James, B., and Spisak, A. (2012). Mass Production Cost Estimation of Direct H 2 PEM Fuel Cell Systems for Transportation Applications: 2012 Update.

Johnson, M. (2012). ARPA-E Storage Overview DOE Energy Storage Review.

BIBLIOGRAPHY (Continued)

Jonouchi, K., Nishimura, Y., and Watanabe, M. (1994). Process for Producing Carbon Fiber Felt. Patent US 5283113 A.

Kangro, W. (1954). A Method for Storing Electrical Energy. Patent DE 914264 C.

Kear, G., Shah, A., and Walsh, F. (2011). Development of the All - Vanadium Redox Flow Battery for Energy Storage: a Review of Technological, Financial and Policy Aspects. Int. J. Energy Res.

Kim, M.-H., Glinka, C.J., Grot, S.A., and Grot, W.G. (2006). SANS Study of the Effects of Water Vapor Sorption on the Nanoscale Structure of Perfluorinated Sulfonic Acid (NAFION) Membranes. Macromolecules *39*, 4775–4787.

Kishio, M., Kazuharu, S., and Hiroaki, F. (1989). Electrode Substrate for Fuel Cell and Process for Producing the Same. Patent US 4851304.

Klug, J. (2003). Process for Complex Shape Formation Using Flexible Graphite Sheets. Patent US 6663807.

Lajevardi, B., Leith, S., King, D., and Paul, B. (2011). Arrayed Microchannel Manufacturing Costs for an Auxiliary Power Unit Heat Exchanger. In Proceedings of the 2011 Industrial Engineering Research Conference.

Li, X., and Sabir, I. (2005). Review of bipolar plates in PEM fuel cells: Flow-field designs. Int. J. Hydrog. Energy *30*, 359–371.

Li, L., Kim, S., Wang, W., Vijayakumar, M., Nie, Z., Chen, B., Zhang, J., Xia, G., Hu, J., Graff, G., et al. (2011). A Stable Vanadium Redox-Flow Battery with High Energy Density for Large-Scale Energy Storage. Adv. Energy Mater. *1*, 394–400.

Li, L., Kim, S., Xai, G., Wang, W., and Yang, Z. (2012). Advanced Redox Flow Batteries for Stationary Electrical Energy Storage.

Lieth, S., King, D., Paul, B. (2010). Toward Low Cost Fabrication of Microchannel Process Technologies - Cost Modeling for Manufacturing Development. 2010 AlChE Annual Meeting.

Litster, S., and McLean, G. (2004). PEM Fuel Cell Electrodes. J. Power Sources *130*, 61–76.

Liu, Q.H., Grim, G.M., Papandrew, A.B., Turhan, A., Zawodzinski, T.A., and Mench, M.M. (2012). High Performance Vanadium Redox Flow Batteries with Optimized Electrode Configuration and Membrane Selection. J. Electrochem. Soc. *159*, A1246–A1252.

BIBLIOGRAPHY (Continued)

Lorenz, G., Gebauer, E., Schuster, U., Tschacher, M., and Schonrogge, B. (2003). Fiber-Reinforced Material and Production and use Thereof. Patent US 6524979 B1.

Mohamed (2012). Design and Development of Unit cell and System for Vanadium Redox Flow Batteries (V-RFB). Int. J. Phys. Sci. *7*.

Ma, X., Zhang, H., Sun, C., Zou, Y., and Zhang, T. (2012). An Optimal Strategy of Electrolyte Flow Rate for Vanadium Redox Flow Battery. J. Power Sources *203*, 153–158.

Mathias, M., Gasteiger, H., Makharia, R., Kocha, S., Fuller, T., Xie, T., and Pisco, J. (2004). Can Available Membranes and Catalytes Meet Automotive Polymer Electrolyte Fuel Cell Requirements. *49*, 471–474.

Mauritz, K., and Moore, R. (2004). State of Understanding of Nafion. Chem Rev *104*.

McConnell (2008), Vb. The Making of Carbon Fiber : CompositesWorld.

McFarland, J., Reilly, J., and Herzog, H. (2004). Representing Energy Technologies in Top-down Economic Models Using Bottom-up Information. Energy Econ. *26*, 685–707.

Mercuri, R. (2008). Assembling Bipolar Plates. Patent EP 1531990 A4.

Mercuri, R., Capp, J., Warddrip, M., and Weber, T. (2002). Flexible Graphite Article and Method of Manufacture. Patent US 6432336 B1.

Mouron, E. (2011). The Economic Potential of the All-Vanadium Redox Flow Battery With a Focus on State of Charge.

Müller, A., Kauranen, P., Ganski, A., and Hell, B. (2006). Injection moulding of graphite composite bipolar plates. *154*.

Nexight Group (2010). Electric Power Industry Needs for Grid-Scale Storage Applications.

Niven, P.R. (2006). Balanced Scorecard Step-by-Step Maximizing Performance and Maintaining Results (Hoboken, N.J.: Wiley).

Noblelight Case Study: Infrared (IR) Processing for Metals - Heraeus Noblelight (ND).

Norley, J., Brady, J., Getz, G., and Klug, J. (2009). Resin-Impregnated Flexible Graphite Articles. Patent 7494712 B2.

BIBLIOGRAPHY (Continued)

Orest Adrianowycz, Julian Norley, David J. Stuart, David Flaherty, Ryan Wayne, Warren Williams, Roger Tietze, Yen-Loan H. Nguyen, Tom Zawodzinski, and Patrick Pietrasz (2010). Next Generation Bipolar Plates for Automotive PEM Fuel Cells.

Öttinger, O., Bacher, J., and Langer, W. (2004). Impregnated Bodies Made of Expanded Graphite, Process for Producing Such Bodies and Sealing Elements, Fuel Cell Components and Heat-Conducting Elements Formed of the Bodies. Patent US 6746771 B2.

Öttinger, O., Schmitt, R., Bacher, J., Mechen, S., and Hudler, B. (2013). Graphite-Containing Molded Body and Method for the Production Thereof. Patent US 20130032278 A1.

Paola Costamagna, S.S. (2001). Quantum jumps in the PEMFC science and technology from the 1960s to the year 2000 ☆: Part II. Engineering, technology development and application aspects. J. Power Sources *102*, 253–269.

Parasuraman, A., Lim, T., Menictas, C., and Skyllas-Kazacos, M. (2013). Review of material research and development for vanadium redox flow battery applications. Electrochimica Acta *101*, 27–40.

Parfomak, P. (2012). Energy Storage for Power Grids and Electric Transportation: A Technology Assessment.

Paul, B. (2013). IE531 Mesoscale Manufacturing Lecture.

Peighambardoust, S.J., Rowshanzamir, S., and Amjadi, M. (2010). Review of the proton exchange membranes for fuel cell applications. Int. J. Hydrog. Energy *35*, 9349–9384.

Perles, T. (2012). Vanadium Market Fundamentals and Implications.

Prudent (2012). Gills Onions Project - Fact Sheet.

Scott, J. (2009). Fuel Cell Development for NASA's Human Exploration Program: Benchmarking With "The Hydrogen Economy."J. Fuel Cell Sci. Technol.

SGL Group (2011). SGL Group as a Key Component Supplier for Prudent Energy's 1 MWh VRB® Energy Storage System.

SGL Group (2012). Sigracet and Sigracell Components for Flow Batteries.

SGL Group (2013a). Soft Felts for Thermal Insulation made of SIGRATHERM.

SGL Group (2013b). SIGRATEX ® Semi-Finished Textile Products Non-Wovens.

BIBLIOGRAPHY (Continued)

SGL Group (2013c). Prepregs : SGL Group – The Carbon Company.

SGL Group (2013d). PANOX The Thermally Stabilized Textile Fiber Oxidized Fiber.

Shigematsu, T. (2011). Redox Flow Battery for Energy Storage. SEI Technical Review.

Shimada, R., and Mukai, K. (2007). Load-Leveling and Electric Energy Storage. IEEJ Trans. Electr. Electron. Eng. *2*, 33–38.

Sinha, J., Lasher, S., and Yang, Y. (2009). Direct Hydrogen PEMFC Manufacturing Cost Estimation for Automotive Applications 2009 DOE Hydrogen Program Review.

Skyllas-Kazacos, M., Chakrabarti, M., Hajimolana, S., Mjalli, F., and Saleem, M. (2011). Progress in Flow Battery Research and Development. J. Electrochem. Soc. *158*, R55–R79.

Sørensen, B. (2005). Hydrogen and Fuel Cells: Emerging Technologies and Applications (Amsterdam ; Boston: Elsevier Academic Press).

Southworth, Z., Haapala, K., Paul, B., and Whalen, S. (2013a). Cost Analysis of Gigawatt-Scale Vanadium Redox Flow Battery Component Manufacturing Using Bottom-up Cost Models.

Southworth, Z., Haapala, K., Paul, B., and Whalen, S. (2013b). Bottom-up Cost Modeling for Vanadium Redox Flow Battery Component Manufacturing.

Southworth, Z., Haapala, K., Paul, B., and Whalen, S. (2013c). A Bottom-up Cost Modeling Method for Redox Flow Battery Component Manufacturing.

Stry, B. (2012). Innovations in Oxidation Technology to Enable Market Growth.

Stry, W. (2013). Key Parameters for Consideration in the Development of a Carbon Fiber Research Line.

Tang, A., Bao, J., and Skyllas-Kazacos, M. (2011). Dynamic Modelling of the Effects of Ion Diffusion and Side Reactions on the Capacity Loss for Vanadium Redox Flow Battery. *196*.

Tapping, D. (2002). Value stream management: eight steps to planning, mapping, and sustaining lean improvements (New York, N.Y: Productivity).

BIBLIOGRAPHY (Continued)

Tokuda, N., Kanno, T., Hara, T., Shigematsu, T., Tsutsui, Y., Ikeuchi, A., Itou, T., and Kumamoto, T. (2011). Development of a Redox Flow Battery System. SEI Technical Paper.

Trapp, V., Wilde, P., and Leinfelder, H. (2003). Electrode Substrate for Electrochemical Cells Based on Low-Cost Manufacturing Processes. Patent US 6511768 B1.

Turker, B., Klein, S., Hammer, E.-M., Lenz, B., and Komsiyska, L. (2013). Modeling a Vanadium Redox Flow Battery System for Large Scale Applications. Energy Convers. Manag. *66*, 26–32.

US DOE (2011a). Energy Storage Program Planning Document.

US DOE (2011b). The Department of Energy Hydrogen and Fuel Cells Program Plan An Integrated Strategic Plan for the Research, Development, and Demonstration of Hydrogen and Fuel Cell Technologies

US DOE (2012). 2012 Annual Progress Report DOE Hydrogen and Fuel Cells Program.

Viswanathan, V., Crawford, A., Stephenson, D., Soowhan, K., Wang, W., Li, B., Coffey, G., Thomsen, E., Graff, G., Balducci, P., et al. (2012). Cost and Performance Model for Redox Flow Batteries. Journal of Power Sources. *247*, 1040-1051.

Weber, A., Mench, M., Meyers, J., Ross, P., Gostick, J., and Liu, Q. (2011). Redow Flow Batteries: a Review. J Appl Electrochem.

Wee, J.-H. (2007). Applications of proton exchange membrane fuel cell systems. Renew. Sustain. Energy Rev. *11*, 1720–1738.

Woods, J. (2003). Impregnation of a Graphite Sheet with a Sealant. Patent US 6656580 B2.

Wu, L., Zhang, Z., Ran, J., Zhou, D., Li, C., and Xu, T. (2013). Advances in Proton-Exchange Membranes for Fuel Cells: an Overview on Proton Conductive Channels (PCCs). Phys. Chem. Chem. Phys. *15*, 4870.

Yamamura, T., Wu, X., Sato, I., Sakuraba, H., Shirasaki, K., and Ohta, S. (2011). Vanadium Cell. Patent WO2011049103 A1.

You, D., Zhang, H., and Chen, J. (2009). A Simple Model for the Vanadium Redox Battery. Electrochimica Acta *54*, 6827–6836.

Yuan, X., Wang, H., Zhang, Jiujun, and Wilkinson, D. (2005). Bipolar Plates for PEM Fuel Cells - From Materials to Processing. J. New Mater. Electrochem. Syst. 257–267.

BIBLIOGRAPHY (Continued)

Yufit, V., Hale, B., Matian, M., Mazur, P., and Brandon, N.P. (2013). Development of a Regenerative Hydrogen-Vanadium Fuel Cell for Energy Storage Applications. J. Electrochem. Soc. *160*, A856–A861.

Zhang, M., Moore, M., Watson, J.S., Zawodzinski, T.A., and Counce, R.M. (2012). Capital Cost Sensitivity Analysis of an All-Vanadium Redox-Flow Battery. J. Electrochem. Soc. *159*, A1183–A1188.

Zhao, P., Zhang, H., Zhou, H., Chen, J., Gao, S., and Yi, B. (2006). Characteristics and Performance of 10 kW Class All-Vanadium Redox-Flow Battery Stack. J. Power Sources *162*, 1416–1420.

(2010). Phenolic Resins: a Century of Progress (Heidelberg : New York: Springer).

(2012). 2012 Annual Progress Report DOE Hydrogen and Fuel Cells Program.